AGR-1 Safety Test Predictions Using the PARFUME Code

Blaise Collin

May 2012

INL
Idaho National
Laboratory

AGR-1 Safety Test Predictions Using the PARFUME Code

Blaise Collin

May 2012

Idaho National Laboratory
VHTR Program
Idaho Falls, Idaho 83415

http://www.inl.gov

VHTR Program

AGR-1 Safety Test Predictions Using the PARFUME Code

INL/EXT-12-26014

May 2012

Prepared by:

Blaise Collin   5/17/2012
Blaise P. Collin   Date

Approved by:

D. Petti for J. T. Maki   5/17/12
John T. Maki   Date
VHTR Technical Lead, Fuel Performance Modeling

Jack Simonds   5/17/2012
Jack Simonds   Date
VHTR Program Manager

David Petti   5/17/12
David A. Petti   Date
VHTR TDO Director

Kimberly Armour   5/17/12
Kimberly J. Armour   Date
VHTR Quality Assurance

ABSTRACT

The PARFUME modeling code was used to predict failure probability of TRISO-coated fuel particles and diffusion of fission products through these particles during safety tests following the first irradiation test (AGR-1) of the Advanced Gas Reactor program.

These calculations support AGR-1 Safety Testing, which is part of the post-irradiation examination effort on AGR-1. Modeling of the AGR-1 Safety Test Predictions includes 620 days of irradiation followed by 300 hours of safety testing for selected AGR-1 compacts. Results include fuel failure probability, palladium penetration, and fractional release of fission products.

Results show that no particle failure is predicted during irradiation or safety testing, and that fractional release of fission products is limited during irradiation but that it significantly increases during the safety tests.

CONTENTS

FIGURES

TABLES

ACRONYMS

AGR	Advanced Gas Reactor
ATR	Advanced Test Reactor
AGR-1	first irradiation test of the AGR program
BAF	Bacon Anisotropy Factor
EFPD	Effective Full Power Day
EoI	End of Irradiation
FIMA	Fissions per Initial heavy Metal Atom
FP	Fission Product
IAEA	International Atomic Energy Agency
INL	Idaho National Laboratory
IPyC	Inner Pyrolytic Carbon
NGNP	Next Generation Nuclear Plant
PARFUME	PARticle Fuel ModEl
OPyC	Outer Pyrolytic Carbon
PyC	Pyrolytic Carbon
SiC	Silicon Carbide
TAVA	Time-Average Volume-Average
TMAP	Tritium Migration Analysis Program
TRISO	TRistructural ISOtropic
UCO	Uranium oxycarbide
UO_2	Uranium dioxide

1. INTRODUCTION

This report documents analyses performed to predict failure probability of TRISO-coated fuel particles and diffusion of fission products through these particles during safety tests following the first irradiation test of the Advanced Gas Reactor program (AGR-1). The analyses include calculation of the AGR-1 irradiation that occurred from December 2006 to November 2009 in the Advanced Test Reactor (ATR) and calculation of a safety testing phase currently under way at Oak Ridge National Laboratory and at Idaho National Laboratory (INL) for a selection of AGR-1 compacts. The heat-up of AGR-1 compacts is a critical component of the AGR-1 fuel performance evaluation, and its objectives are to identify the effect of fuel type, accident test temperature, burnup, and irradiation temperature on the performance of the fuel at elevated temperature. Safety testing of compacts will be followed by detailed examinations of the fuel particles to further evaluate fission product retention and behavior of the kernel and coatings.

The analyses were completed using the particle fuel model computer code PARFUME (PARticle FUel ModEl) developed at INL. PARFUME is an advanced gas-cooled reactor fuel performance modeling and analysis code (Miller 2009). It has been developed as an integrated mechanistic code that evaluates the thermal, mechanical, and physico-chemical behavior of fuel particles during irradiation to determine the failure probability of a population of fuel particles given the particle-to-particle statistical variations in physical dimensions and material properties that arise from the fuel fabrication process, accounting for all viable mechanisms that can lead to particle failure. The code accounts for these calculated particle failures in determining the diffusion of fission products from the fuel through the particle coating layers, and through the fuel matrix to the coolant boundary.

The objective of this document is to present results of calculations and analyses made by PARFUME on the subset of compacts selected for post-irradiation examination, taking into account their irradiation and safety testing phases. These results include:

- Fuel failure probability
- Palladium penetration
- Fractional release of fission products

Details associated with completion of these analyses are provided in the remainder of this document: the AGR-1 Safety Testing plan is briefly introduced in Section 2, PARFUME modeling is outlined in Section 3, results are described in Section 4, conclusions are given in Section 5, and references are listed in Section 6.

For Quality Assurance purposes, note that calculations were performed with PARFUME Version 2.22 compiled with Intel FORTRAN Compiler 11.1.073 on an SGI Altix ICE 8200 platform operating under SUSE Linux Enterprise Server 10.

2.   AGR-1 SAFETY TESTING

The objectives of the safety testing campaign are to identify the effects of fuel type, accident test temperature, burnup, and irradiation temperature on the performance of the fuel at elevated temperatures. Because of programmatic funding and time constraints, only one-fourth (18 out of 72) of the AGR-1 compacts will undergo safety tests (Demkowicz 2012).

In order to accomplish the safety testing objectives, a test matrix has been developed to assign specific compacts to safety test conditions in a manner that will optimize the ability to identify the effect of the various independent variables on fuel performance. The specific objectives of the safety test matrix are to estimate the:

- Differences in performance between Variants 1, 3, and Baseline fuel types.
- Effect of accident test temperature on performance.
- Effect of irradiation temperature and burnup on performance.
- Random variation in fuel performance during safety tests.

Figure 1 displays the distribution by burnup and Time-Average Volume-Average (TAVA) temperature of the 72 AGR-1 compacts (red), together with the 18 compacts selected for safety testing (blue). Details of the selection process are given by (Demkowicz 2012).
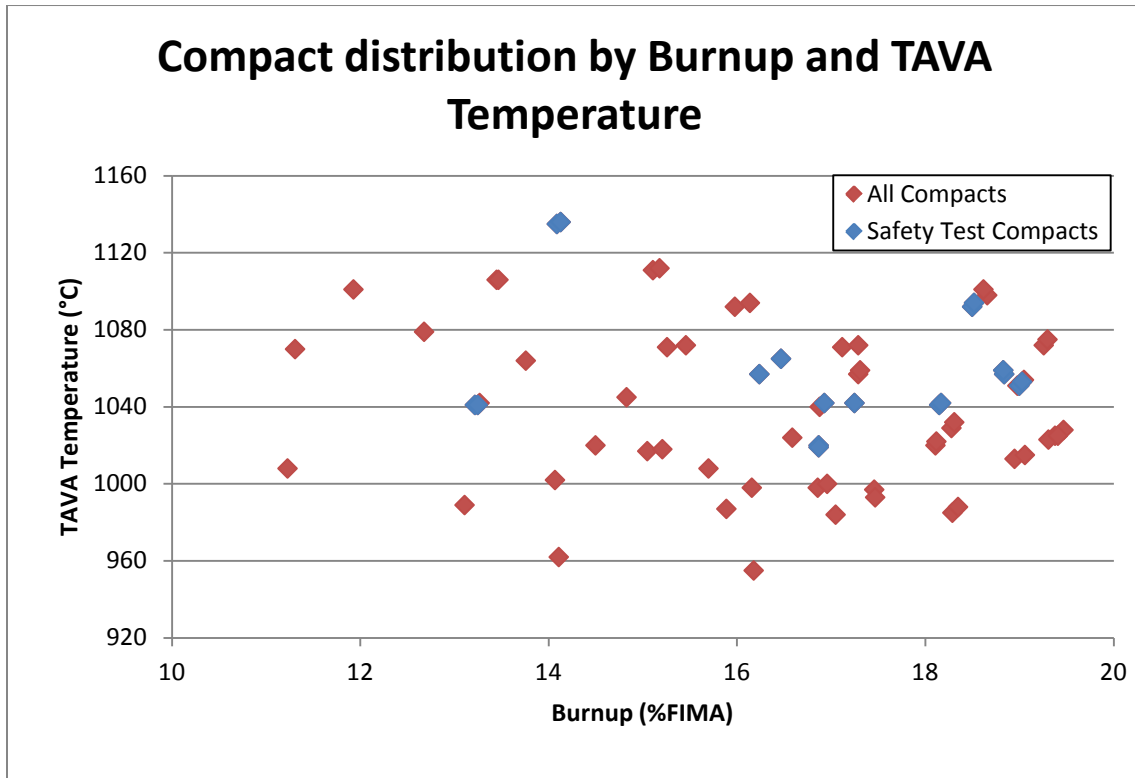

Figure 1. AGR-1 compact distribution by burnup and TAVA temperature.

Safety testing consists of a 300-hour heat-up in a furnace at temperatures ranging from 1600°C to 1800°C. The irradiation and safety test characteristics of the 18 selected compacts are detailed in Table 1 (Collin 2012, Demkowicz 2012). The safety test temperature range was chosen because a temperature difference of 200°C has been shown historically to have a significant effect on fuel performance. In addition, compacts from a specific fuel variant shall be tested at an accident test temperature of 1600°C before proceeding to test another compact at higher temperature in order to verify that the fuel is sufficiently robust at the lower temperature. The temperature profiles for the safety tests are shown in Figure 2 (Demkowicz 2011).

Table 1. End-of-irradiation and safety test characteristics of compacts.

Variant	Capsule	Level	Stack	Burnup (%FIMA)	TAVA Temperature (°C)	Fast Neutron Fluence (10^{25} n.m^{-2} E > 0.18 MeV)	Safety Test Temperature (°C)
Baseline	6	4	1	13.22	1041	2.43	1600
		2		14.09	1135	2.87	1600
		4	3	13.25	1041	2.46	1600
		2		14.13	1136	2.90	1600
1	5	1	1	18.15	1041	3.76	1700
		3	3	16.93	1042	3.65	1600
		1		18.17	1042	3.82	1800
3	4	4	1	18.84	1057	3.99	1800
		3		18.50	1092	4.10	1600
		3	2	16.24	1057	3.68	1800
		2		16.47	1065	3.73	1600
		1		17.25	1042	3.72	1600
		4	3	18.83	1059	4.06	1700
		3		18.52	1094	4.16	1600
Baseline	3	3	1	19.00	1051	4.23	1700
		3	2	16.87	1020	3.80	1600
		2		16.87	1019	3.79	1600
		2	3	19.03	1053	4.28	1800

NB: compacts are labeled C-L-S as in "Capsule – Level – Stack".
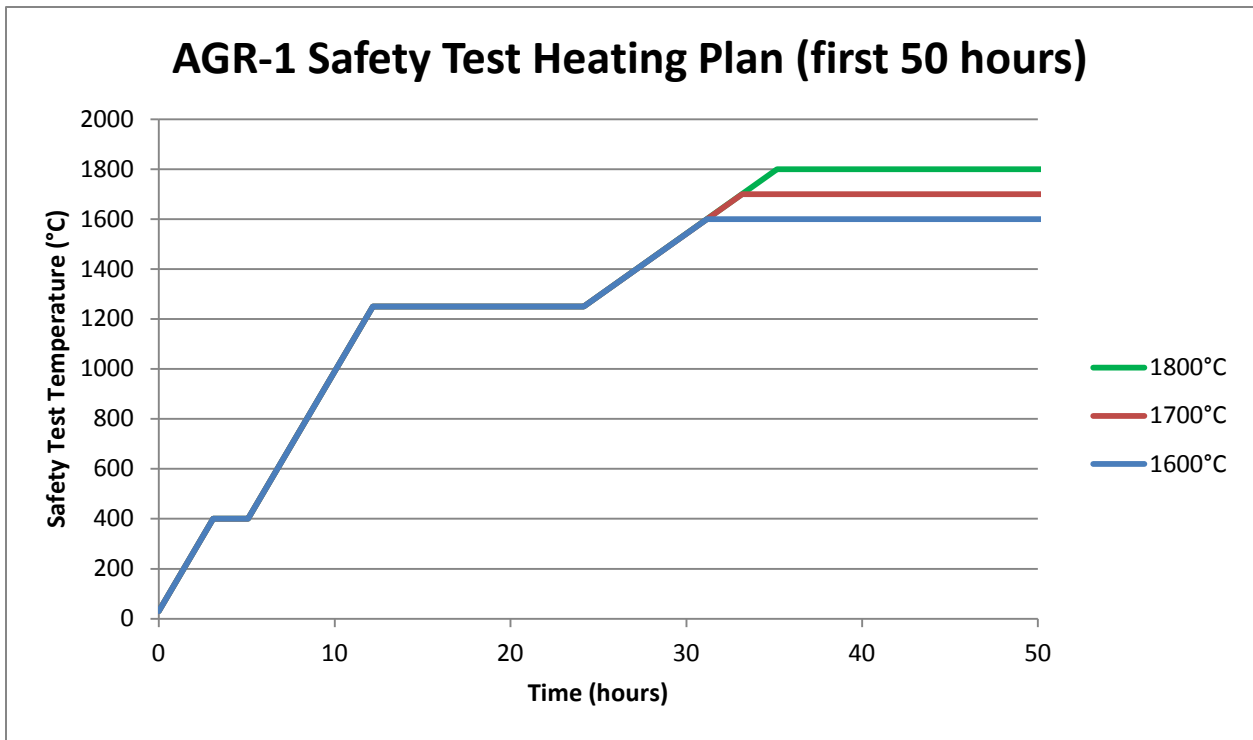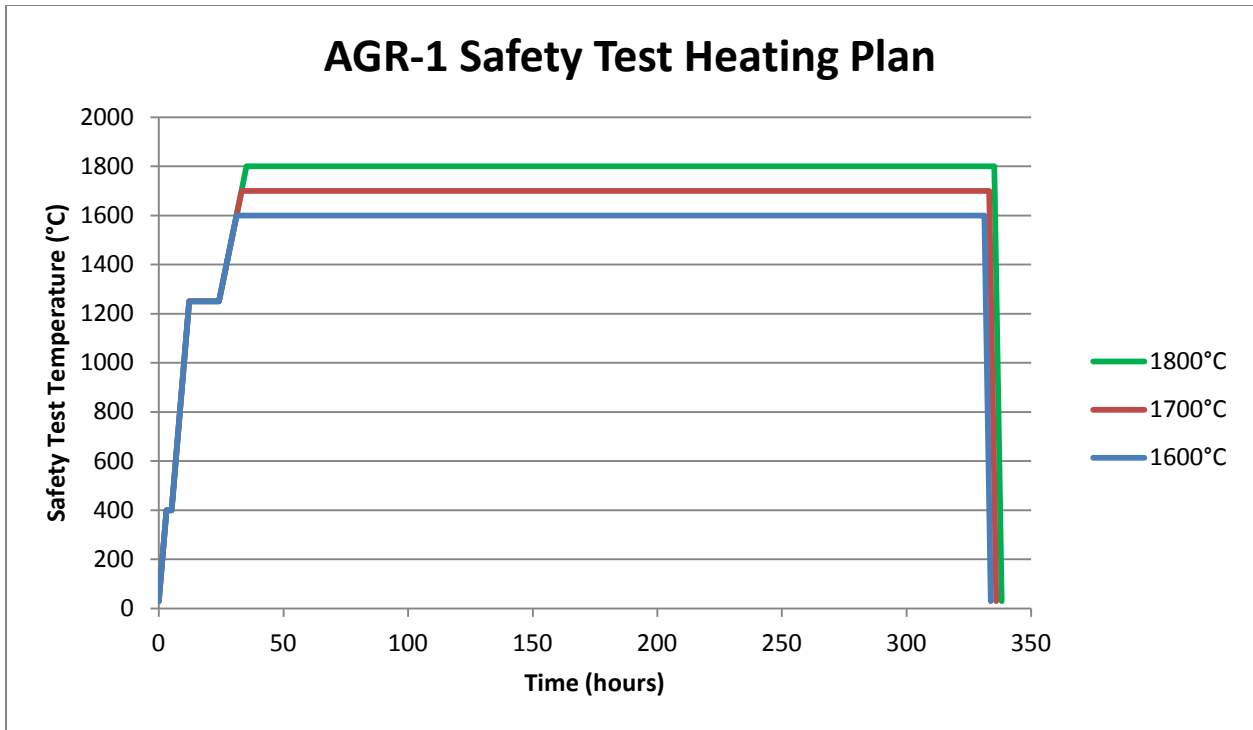
Figure 2. AGR-1 safety test temperature profile.

3. PARFUME MODELING

AGR-1 test train was irradiated in the 38.1 mm (1.5 inch) diameter B-10 position of the ATR at INL. An ATR core cross section indicating this location is displayed in Figure 3. The test train contains six capsules arranged vertically as shown in Figure 4. Each AGR-1 capsule is 152.4 mm (6 inch) long and contains 12 fuel compacts arranged in three vertical stacks with each stack containing four compacts. Figure 5 illustrates a radial view of a capsule.

Figure 3. ATR core cross section displaying the B-10 position.
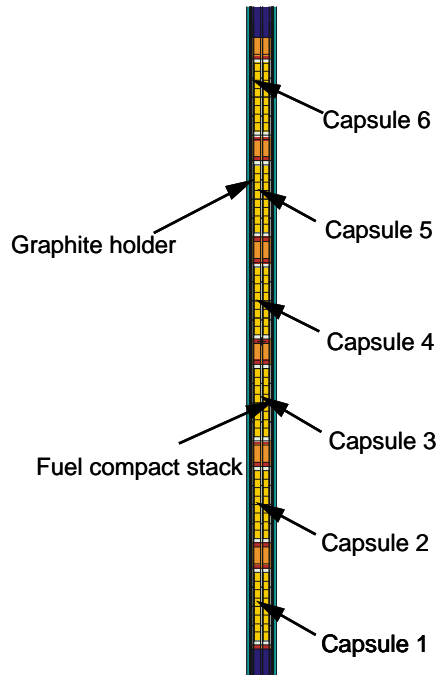
Figure 4. Axial schematic of the AGR-1 capsules.
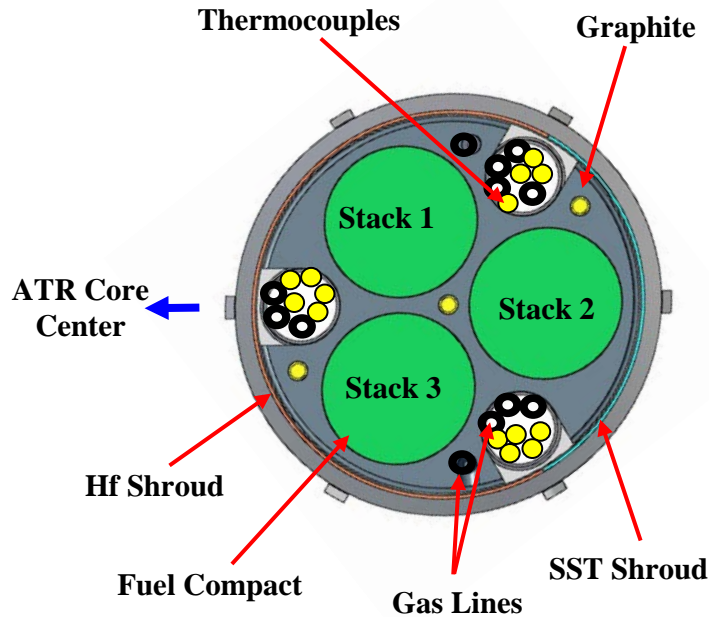
Figure 5. Radial schematic of an AGR-1 capsule.

AGR-1 compacts are right cylinders nominally 25.1 mm in length and 12.4 mm in diameter. Each compact contains ~4,100 fuel par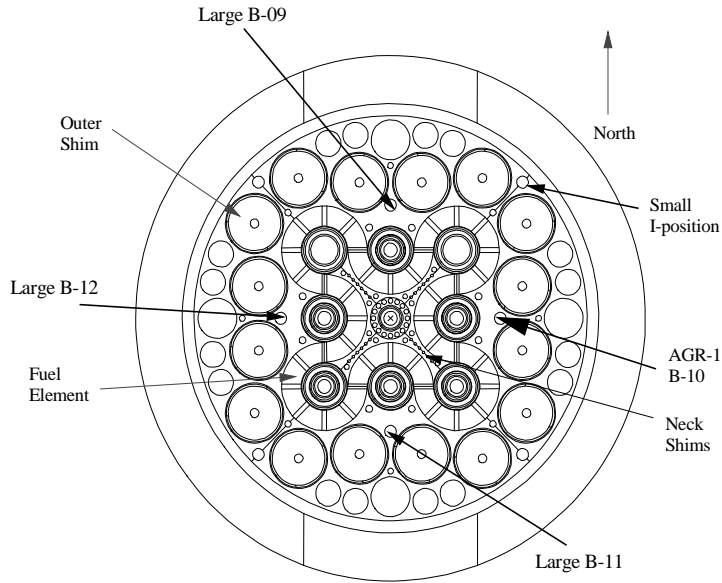ticles uniformly dispersed in a matrix composed of a thermosetting carbonaceous material. Each particle has a nominal diameter of ~800 μm and contains a kernel consisting of uranium oxycarbide (UCO) fuel. The kernel is coated with a porous buffer layer to accommodate fission product accumulation, a SiC layer to retain the fission products, and inner and outer pyrocarbon (IPyC and OPyC) layers to protect the silicon carbide (SiC) as depicted in Figure 6. AGR-1 irradiation in ATR reached 620.2 Effective Full Power Days (EFPD) (Collin 2012). Key aspects of the AGR-1 characteristics needed for PARFUME modeling are described below.

Figure 6. Schematic of a typical TRISO-coated fuel particle.

3.1 Boundary and Initial Conditions

PARFUME is designed to evaluate fuel performance based on user inputs for neutron fluence and burnup with a corresponding set of thermal conditions. Results from neutronics analyses and/or measur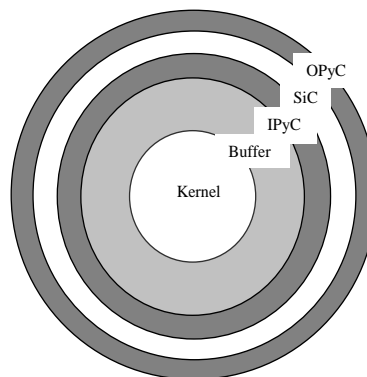ed values are possible sources for fluence and burnup inputs. The neutronics and thermal conditions for the 18 compacts undergoing safety tests are based on results obtained from as-run neutronics calculations and as-run thermal analysis (Sterbentz 2011, Hawkes 2012) a presented in Table 1.

The 620.2 days of irradiation are modeled for each compact with the end-of-irradiation values of burnup and fast neutron fluence displayed in Table 1. Burnup and fast neutron fluence are assumed to follow linear evolutions during irradiation. The assumption is validated by as-run neutronics calculations (Sterbentz 2011) as illustrated by the burnup and fast neutron fluence compact history presented in Appendix A.

The temperature profile of each compact is volume-averaged over the compact. The boundary condition assumes an OPyC temperature constant throughout irradiation and equal to the TAVA temperature of the compact at the end of irradiation (EoI) as calculated by as-run thermal analyses (Hawkes 2012) and displayed in Table 1. From that boundary temperature, PARFUME calculates the temperature profile between the OPyC and the kernel center (40 to 60°C higher than the OPyC temperature at the end of irradiation), taking into account that the temperature profile is affected throughout irradiation by the width of the IPyC-Buffer gap. Appendix A contains plots of the calculated daily temperature of a selected subset of compacts during irradiation (omitted compacts have similar irradiation characteristics as those shown). Each plot shows the compact TAVA temperature chosen for modeling.

Following irradiation the compacts undergo a safety testing phase according to the heating plan displayed in Figure 2 and the maximum safety test temperatures listed in Table 1. The heating plan for all compacts consists of two temperature ramps of 120°C/hr followed by temperature plateaus of 2 hours and 12 hours respectively, and then a temperature ramp of 40°C/hr until the maximum temperature (1600, 1700, or 1800°C) is reached. A 300-hr heating phase follows at maximum temperature and then the compacts are brought back to room temperature (30°C) with a ramp of -600°C/hr (Demkowicz 2011).

3.2   Input Parameters

The PARFUME input parameters needed to model the AGR-1 safety tests for particle failure probability are listed in Table 2. They originate from:

- The AGR-1 Irradiation Experiment Test Plan (Maki 2009) for the fuel characteristics, particle geometry, compact characteristics, and material non-mechanical properties.
- A CEGA Corporation report (CEGA 1993) for the material mechanical properties.
- Neutronics calculations and thermal analysis for the boundary conditions (see Section 3.1).

In addition, diffusion coefficients used for fission product transport are extracted from the International Atomic Energy Agency (IAEA) Technical Document 978 (IAEA 1997) (see Section 3.4).

Table 2. Parameters used in the PARFUME modeling of the AGR-1 safety tests.

Category	Parameter	Fuel type[a] Mean Value ± Standard Deviation		
		Baseline	Variant 1	Variant 3
Fuel characteristics	U235 enrichment (wt%)[b]	19.736		
	Oxygen/uranium (atomic ratio)[b]	1.3613		
	Carbon/uranium (atomic ratio)[b]	0.3253		
	Uranium contamination fraction[b]	3.64e-7	2.75e-7	1.26e-7
Particle geometry	Kernel diameter (μm)	349.7 ± 9.0		
	Buffer thickness (μm)	103.5 ± 8.2	102.5 ± 7.1	104.2 ± 7.8
	IPyC thickness (μm)	39.4 ± 2.3	40.5 ± 2.4	38.8 ± 2.1
	SiC thickness (μm)	35.3 ± 1.3	35.7 ± 1.2	35.9 ± 2.1
	OPyC thickness (μm)	41.0 ± 2.1	41.1 ± 2.4	39.3 ± 2.1
	Particle asphericity @ SiC (aspect ratio)	1.040		
Compact characteristics	Diameter (mm)	12.36	12.36	12.34
	Number of particles per compact	4154	4145	4132
	Compact matrix density (g.cm^{-3})	1.297	1.256	1.344
Material properties	IPyC Weibull modulus[b]	9.5		
	SiC Weibull modulus[b]	6.0		
	OPyC Weibull modulus[b]	9.5		
	IPyC / SiC bond strength (MPa)[c]	100.0		
	PyC Poisson's ratio in creep[b]	0.5		
	PyC creep coefficient amplifier	2.0		
	Kernel density (g.cm^{-3})[b]	10.924		
	Buffer density (g.cm^{-3})[b]	1.10		
	IPyC density (g.cm^{-3})[c]	1.904	1.853	1.904
	OPyC density (g.cm^{-3})[c]	1.907	1.898	1.911
	IPyC (post compact anneal) BAF[c]	1.022	1.014	1.029
	OPyC (post compact anneal) BAF[c]	1.019	1.013	1.021
Boundary conditions	Ambient pressure (MPa)	0.1		

a. Baseline fuel in Capsules 3 and 6, Variant 1 in Capsule 5, and Variant 3 in Capsule 4.
b. Standard deviation not considered in PARFUME.
c. Standard deviation not included in the AGR-1 Safety Test Predictions.

As indicated in Table 2, a baseline fuel type and two fuel variant types are tested. Baseline fuel is used in Capsules 3 and 6, Variant 1 fuel is used in Capsule 5, and Variant 3 fuel is used in Capsule 4. Statistical variations are considered relative to the fuel particle geometry only (kernel diameter, buffer, pyrolitic carbon (PyC), and SiC thicknesses). PARFUME also has the capability to address statistical variations in creep, bond strength, PyC densities, and PyC Bacon anisotropy factors (BAF). With the exception of creep and bond strength, the AGR-1 Irradiation Experiment Test Plan (Maki 2009) provides information regarding these variations. However, results from sensitivity calculations indicated that these variations have little impact on the probability of AGR-1 fuel particle failure (Miller 2007). Because the effects are so small, statistical variations in PyC densities and BAF are not considered in the AGR-1 Safety Test Predictions.

The asphericity mentioned in Table 2 is considered at the SiC layer, as required by PARFUME inputs. Asphericity measurements reported in the AGR-1 Irradiation Experiment Test Plan correspond to asphericity at the OPyC layer. The asphericity of AGR-1 fuel particles at the SiC layer was not measured during the coating process, but post-coating optical inspection showed that asphericity at that layer is limited. Asphericity at the SiC layer was measured at a mean value of 1.037 for AGR-2 UCO fuel (Collin 2011). A value of 1.040 is therefore a conservative upper limit. Furthermore, previous sensitivity studies concluded that variations in asphericity at this level had a negligible impact on the probability of AGR-1 fuel particle failure (Miller 2007).

The material mechanical properties used in PARFUME are obtained from a report compiled by the CEGA Corporation (CEGA 1993). Table 2 displays parameters used in PARFUME user inputs. Material properties directly incorporated into the PARFUME code source are discussed by (Miller 2007 and 2009).

3.3   Failure Mechanisms

The potential failure mechanisms considered in PARFUME currently consist of (Miller 2009):

- Pressure vessel failure
- Cracking of the IPyC layer
- Partial debonding of the IPyC from the SiC
- Pressure vessel failure of an aspherical particle
- Amoeba effect
- Palladium attack of the SiC layer

Pressure vessel failure occurs in a one-dimensional (1-D) spherical particle as pressure from released fission gases builds up and becomes high enough that the tangential stress in the SiC layer reaches the SiC fracture strength for that particle. Carbon monoxide (CO) production theoretically contributes to the pressure build-up but little CO production is expected in UCO fuel[a]. In the case of pressure vessel failure the particle is treated as 1-D because of the symmetry in the tangential and azimuthal directions in the perfectly spherical geometry.

In addition to the 1-D behavior of a symmetrical spherical fuel particle, PARFUME also considers multi-dimensional behavior. This includes cracking of the IPyC layer, partial debonding of the IPyC from the SiC, pressure vessel failure of an aspherical particle, Amoeba effect, and thinning of the SiC layer as follows:

- IPyC cracking occurs when irradiation-induced shrinkage of the IPyC induces a tensile stress that exceeds the tensile strength in that layer. A radial crack then develops in the IPyC layer that creates local tensile stress in the SiC layer, leading to possible particle failure.
- Partial debonding of the IPyC from the SiC occurs when irradiation-induced shrinkage of the IPyC induces a radial tensile stress at the interface between the IPyC and SiC layers that exceeds the bond strength between the two layers.
- Asphericity affects the probability of failure by high internal pressure. PARFUME incorporates the effects of asphericity for particles that have a flat facet but are otherwise spherical. Because of discontinuities in the faceted particle geometry, the faceted portion of that particle typically incurs higher stress than spherical or ellipsoidal portions from pressure of released fission gases. If the pressure builds up high enough, the tensile stress in the faceted portion can exceed the fracture strength of the SiC and lead to particle failure. Effects of ellipsoidal asphericity are small in comparison and therefore not included in the code (Miller 1994).
- Kernel migration, also called Amoeba effect, occurs when the fuel kernel of a particle migrates into the SiC layer under the influence of a temperature gradient. Particle failure is assumed to occur when the kernel comes into contact with the SiC layer. This effect is prominent with UO_2 kernels and very small with UCO kernels.
- Fission product palladium (Pd) can attack and penetrate the SiC layer, causing a thinning of the SiC thickness that can eventually lead to particle failure. Although particle failure is generally assumed when penetration through the thickness of the SiC is complete (Miller 2006), PARFUME does not currently treat Pd attack as a standard failure mechanism but rather just computes Pd penetration as a flag for users.

---

[a] The CO production model in PARFUME was shut off in the calculation of the AGR-1 Safety Test Predictions because of inaccuracies found during the completion of this work.

In all of these thermomechanical calculations, the buffer is assumed to have completely detached from the IPyC layer, hence forming a gap. The buffer densifies with increasing neutron fluence while the kernel swells with increasing burnup: this change in gap is important for calculating kernel temperature and fission product diffusion. However, in the case of failure probability evaluations, the TRISO coating system is mechanically separated from the kernel and buffer.

To model the multi-dimensional behavior associated with IPyC cracking, debonding, and asphericity previous versions of PARFUME used the results of the detailed finite element analysis program Abaqus (Abaqus 2007) for cracked, debonded, and/or aspherical particles in conjunction with results from the PARFUME closed form 1-D solution to make a statistical approximation of the stress levels in any particle (Miller 2002). These combined results determined the multidimensional statistical parameters for IPyC cracking and particle asphericity required as user inputs. This historical approach has been replaced by an automated calculation of multidimensional input parameters (for IPyC cracking and asphericity) directly embedded in the PARFUME source code (Skerjanc 2011). In the case of the AGR-1 Safety Test Predictions, the correlation coefficients for IPyC cracking are obtained through that feature, while the correlation coefficients for asphericity are calculated by Abaqus. The statistical parameters used in the AGR-1 Safety Test Predictions are given in Appendix B.

Because AGR particle fabrication is originally based on German processes, the IPyC-SiC bond strength is set at a value that is considered to be representative for German particles (100 MPa). At this bond strength, IPyC-SiC debonding is not predicted by PARFUME for AGR-type particles. As a consequence, debonding is not included in the calculation of the multidimensional input parameters and it is not considered as a potential failure mechanism in the AGR-1 Safety Test Predictions.

Chemical attack of the SiC by palladium is modeled in PARFUME by calculating the penetration of palladium in the SiC layer. The penetration rate is calculated by an Arrhenius function fitted to in-reactor data (Petti 2004). It is given by:

$$P = 38.232e^{-11342.3/T} \ (\mu m/day)$$

where

T = temperature (K)

3.4   Fission Product Transport

Fission product (FP) transport in PARFUME is based on coding extracted from the Tritium Migration Analysis Program Version 4 (TMAP4) computer code. Originally developed to assist in the evaluation of tritium losses from fusion reactor systems, TMAP4 incorporates a 1-D diffusion capability that determines the thermal response of structures and solves equations for solute atom movement through surfaces and in bulk materials (Longhurst 1992).

The coding extracted from TMAP4 was modified for use within PARFUME to calculate FP transport from the kernel through the successive coating layers of a TRISO-coated fuel particle, from individual TRISO-coated fuel particles to the surrounding matrix, and from the surrounding matrix to the outside of the fuel sphere or compact, which constitutes the release of the fission products.

Fission product transport in PARFUME is a three-step process that includes a fuel element thermal analysis, thermal and FP transport analyses for fuel particles, and a fuel element FP transport analysis ultimately leading to fission product release. Thermal analyses are performed to acknowledge the temperature dependence of diffusion. Diffusion is first calculated for individual fuel particles. Results from each particle then serve as time- and position-dependent FP sources for the subsequent fuel element transport analysis.

The AGR-1 Safety Test Predictions calculate the transport of the four following fission products: silver (Ag), cesium (Cs), krypton (Kr), and strontium (Sr). Diffusion coefficients used in PARFUME for each of these species in the successive coating layers and graphite materials are derived from the IAEA (IAEA 1997) and displayed in Table 3. The corresponding diffusivities can be calculated using these diffusion coefficients in the following Arrhenius-type equation:

$$D = D_{0,1}e^{-\frac{Q_{0,1}}{RT}} + D_{0,2}e^{-\frac{Q_{0,2}}{RT}}$$

where

$D_{0,i}$ =   pre-exponential factor (m^2/s)
$Q_{0,i}$ =   activation energy (kJ/mol)
R =   gas constant (8.3142×10^{-3} kJ/mol/K)
T =   temperature (K)

The diffusion coefficient of Cs in SiC has a fluence-dependent component ($D_{0,1}/Q_{0,1}$). In the frame of the AGR-1 Safety Test Predictions this component was calculated with a value of the fluence equal to zero. This approximation has no impact on the fractional release calculated during the safety testing phase, as the second component ($D_{0,2}/Q_{0,2}$) is largely dominant at these safety test temperatures.

Table 3. Diffusion coefficients used in PARFUME.

Species	$D_{0,i}$ (m²/s) $Q_{0,i}$ (kJ/mol)	Kernel	Buffer	IPyC / OPyC	SiC	Matrix graphite	Structural graphite
Ag	$D_{0,1}$ $Q_{0,1}$	6.7e-9 165	1.0e-8 0	5.3e-9 154	3.6e-9 215	1.6 258	1.6 258
	$D_{0,2}$ $Q_{0,2}$	-	-	-	-	-	-
Cs	$D_{0,1}$ $Q_{0,1}$	5.6e-8 209	1.0e-8 0	6.3e-8 222	5.5e-14*e$^{\Gamma/4.5}$ [b] 125	3.6e-4 189	1.7e-6 149
	$D_{0,2}$ $Q_{0,2}$	5.2e-4 362	-	-	1.6e-2 514	-	-
Kr	$D_{0,1}$ $Q_{0,1}$	1.3e-12 / 8.8e-15 [a] 126 / 54 [a]	1.0e-8 0	2.9e-8 291	3.7e1 / 8.6e-10 [c] 657 / 326 [c]	6.0e-6 0	6.0e-6 0
	$D_{0,2}$ $Q_{0,2}$	0 / 6.0e-1 [a] 0 / 480 [a]	-	2.0e5 923	-	-	-
Sr	$D_{0,1}$ $Q_{0,1}$	2.2e-3 488	1.0e-8 0	2.3e-6 197	1.2e-9 205	1.0e-2 303	1.7e-2 268
	$D_{0,2}$ $Q_{0,2}$	-	-	-	1.8e6 791	-	-

a. First values used in irradiation conditions / Second values used in accidental conditions.

b. Γ: fast neutron fluence (10^{25} n.m^{-2}, E > 0.18 MeV).

c. First values used above 1626 K / Second values used below 1626 K.

4.   RESULTS

PARFUME was run with the Fast Integration scheme to calculate the particle failure probabilities, and with the Monte Carlo scheme to obtain the fractional releases of fission products. An example of a PARFUME input deck is given in Appendix E.

Results on failure probability and palladium penetration are given in Section 4.1, results on fission product release constitute Section 4.2.

4.1   Failure Probability

PARFUME calculates the probability of fuel particle failure due to the following failure mechanisms:

- Pressure vessel failure
- Cracking of the IPyC layer
- Partial debonding of the IPyC from the SiC
- Amoeba effect

Pressure vessel failure can occur in both spherical and aspherical particles. Aspherical particles are more prone to failing under pressure as their faceted portions are more sensitive to pressure. The AGR-1 Safety Test Predictions conservatively assume that all particles in the compacts have an asphericity of 1.040 (see Section 3.2). As explained in Section 3.3, partial debonding of the IPyC from the SiC is not expected to be able to lead to particle failure because of the assumed high IPyC-SiC bond strength. It is therefore not considered a potential failure mechanism in the AGR-1 Safety Test Predictions. In addition to these failure mechanisms, PARFUME also calculates the penetration of palladium in the SiC layer, which allows users to assess potential failures by comparing the penetration depth to the SiC thickness.

Table 4 lists the failure probabilities for all the compacts at the end of irradiation. It shows the SiC failure probability is solely associated with IPyC cracking. Failure probabilities range from 9.60×10^{-8} for Compact 6-2-3 to 1.57×10^{-6} for Compact 3-2-2. Kernel migration (Amoeba effect), historically observed in UO_2 fuel (Petti 2005), is not predicted for UCO at the AGR-1 irradiation temperatures. With maximum pressures limited to less than 10 MPa in the fuel particles, no pressure vessel failure is predicted during irradiation. The number of failed particles predicted by PARFUME during irradiation is also displayed in Table 4. As can be seen, PARFUME does not predict any particle failure during irradiation.

Figure 7 shows the profile of the SiC failure probability throughout irradiation and safety testing for a representative compact (Compact 4-2-2). The failure probability builds up in the first 50 EFPD, as IPyC starts to shrink under irradiation. As the irradiation temperature rises, the stress due to shrinkage in the IPyC layer increases. As an offset to shrinkage, irradiation-induced creep also rises with temperature, eventually overcoming the shrinkage effect and bringing some relief to the IPyC layer. The failure probability subsequently peaks and remains constant throughout the rest of the irradiation. Similar plots for the other compacts are shown in Appendix C.

Figure 8 plots the SiC failure probability at the end of irradiation as a function of the irradiation temperature for the compacts grouped by capsule type. It shows the effect of temperature on IPyC cracking. At higher temperature, creep relieves the tangential stress produced by IPyC shrinkage, leading to a decreased probability of SiC failure with temperature. Figure 9 and Figure 10 show the influence of burnup and fast neutron fluence on the SiC failure probability — no trend can be observed on these plots.

Table 4. Failure probabilities at the end of irradiation.

Compact	Probability of SiC failure				Probability of IPyC Cracking	Probability of IPyC Debonding[a]	Number of Failed Particles
	Amoeba	IPyC Cracking	IPyC Debonding[a]	Pressure			
6-4-1	0	9.07E-07	-	0	4.57E-02	-	0
6-2-1	0	9.85E-08	-	0	1.40E-02	-	0
6-4-3	0	9.05E-07	-	0	4.56E-02	-	0
6-2-3	0	9.60E-08	-	0	1.38E-02	-	0
5-1-1	0	1.26E-06	-	0	6.24E-02	-	0
5-3-3	0	1.23E-06	-	0	6.15E-02	-	0
5-1-3	0	1.23E-06	-	0	6.14E-02	-	0
4-4-1	0	5.89E-07	-	0	3.58E-02	-	0
4-3-1	0	2.57E-07	-	0	2.30E-02	-	0
4-3-2	0	5.91E-07	-	0	3.59E-02	-	0
4-2-2	0	4.89E-07	-	0	3.24E-02	-	0
4-1-2	0	8.35E-07	-	0	4.31E-02	-	0
4-4-3	0	5.61E-07	-	0	3.48E-02	-	0
4-3-3	0	2.45E-07	-	0	2.25E-02	-	0
3-3-1	0	7.15E-07	-	0	4.01E-02	-	0
3-3-2	0	1.53E-06	-	0	6.12E-02	-	0
3-2-2	0	1.57E-06	-	0	6.21E-02	-	0
3-2-3	0	6.83E-07	-	0	3.92E-02	-	0

a. Because of the strong IPyC-SiC bond anticipated in AGR-1 fuel, partial debonding is not considered in the AGR-1 Safety Test Predictions (see Section 3.3).
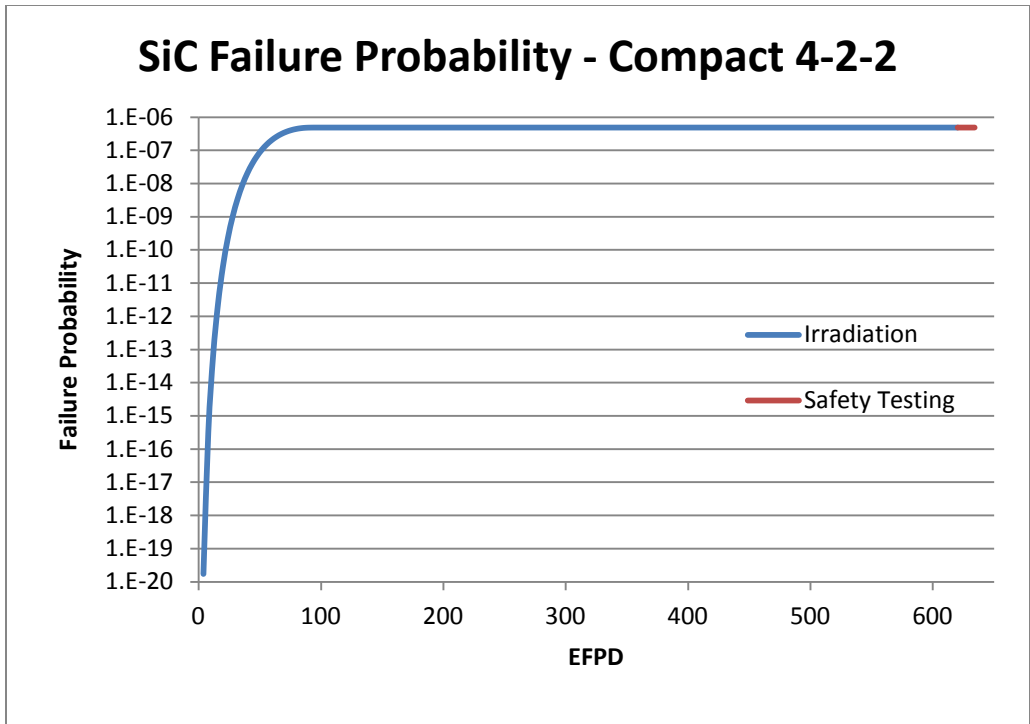
Figure 7. SiC failure probability for Compact 4-2-2.
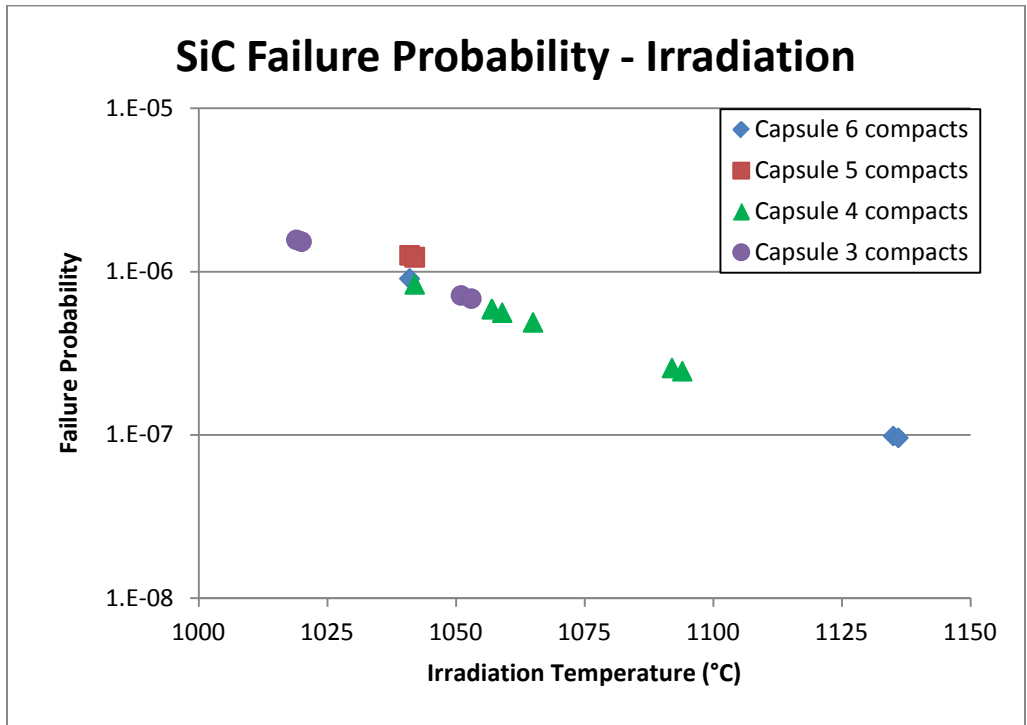
Figure 8. SiC failure probability at the end of irradiation as a function of irradiation temperature.
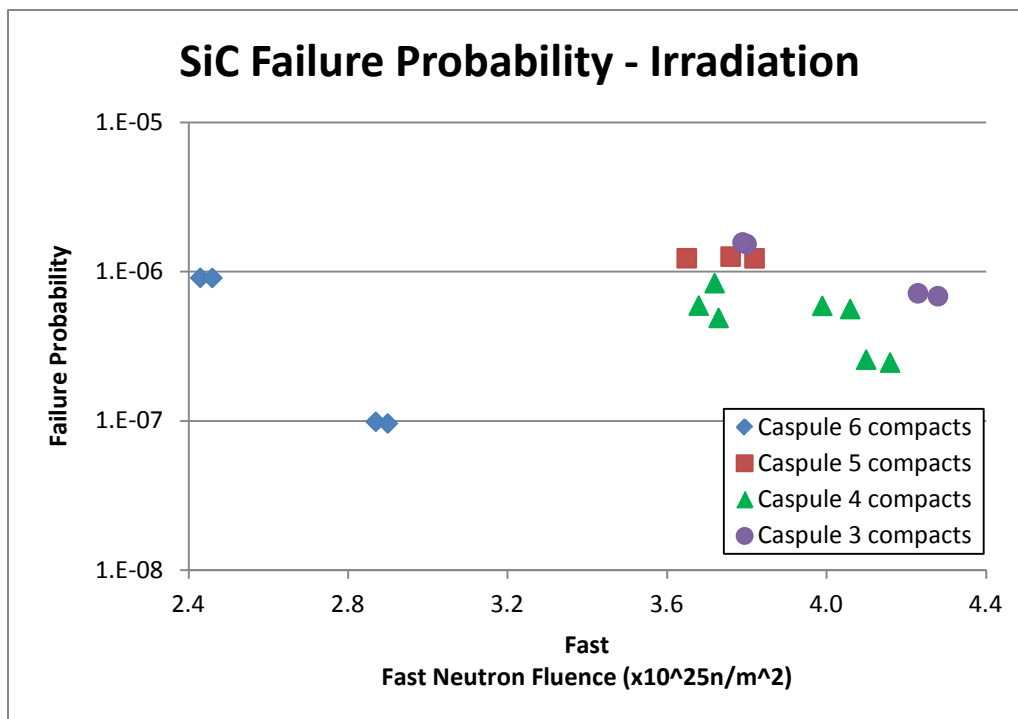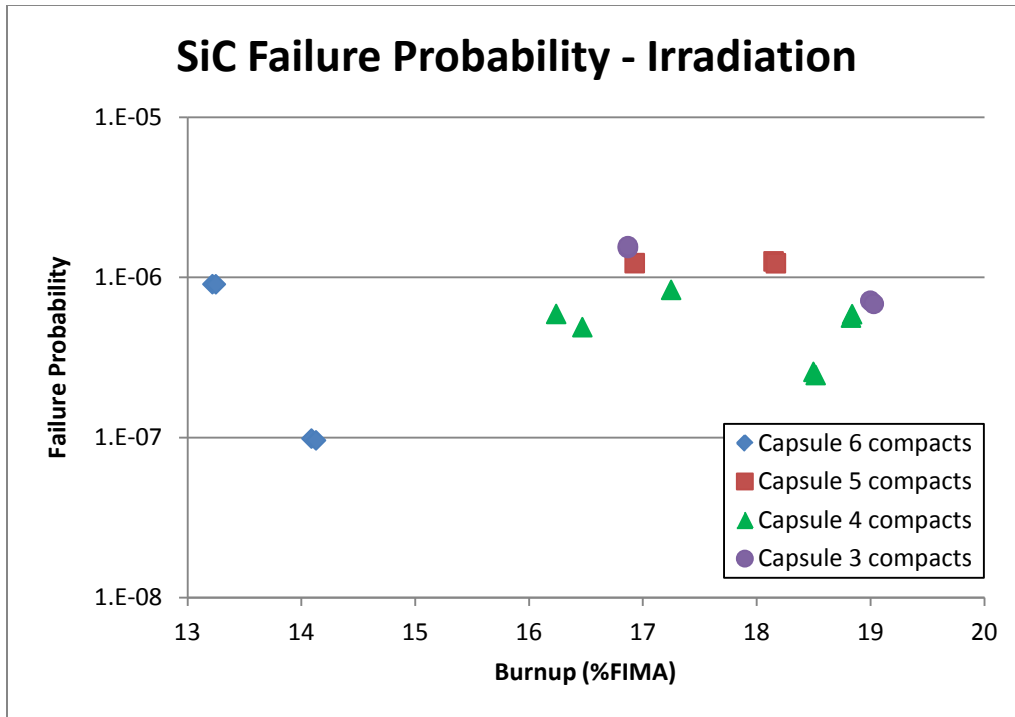
Figure 9. SiC failure probability at the end of irradiation as a function of burnup and fast fluence.

Table 5 displays the SiC failure probabilities for all the compacts at the end of safety testing. Kernel migration is not observed because the kernel is not subjected to any temperature gradient during safety testing. Irradiation-induced IPyC cracking is not further affected by heat-up as the compacts are no longer exposed to neutron flux. The contribution of IPyC cracking to SiC failure probability thus remains at the level reached during irradiation. The high test temperature (1800°C) creates extra pressure in the particles (up to 30 MPa) that can contribute to their failure. In the case of Compact 5-1-3, the contribution of pressure amounts to about 1% of the total SiC failure probability. Overall, PARFUME does not predict any particle failure during the heating phase.

Table 5. Failure probabilities at the end of irradiation plus safety testing.

Compact	Probability of SiC failure				Probability of IPyC Cracking	Probability of IPyC Debonding[a]	Number of Failed Particles
	Amoeba	IPyC Cracking	IPyC Debonding[a]	Pressure			
6-4-1	0	9.07e-07	-	0	4.57e-02	-	0
6-2-1	0	9.85e-08	-	0	1.40e-02	-	0
6-4-3	0	9.05e-07	-	0	4.56e-02	-	0
6-2-3	0	9.60e-08	-	0	1.38e-02	-	0
5-1-1	0	1.26e-06	-	0	6.24e-02	-	0
5-3-3	0	1.23e-06	-	0	6.15e-02	-	0
5-1-3	0	1.23e-06	-	1.44e-08	6.14e-02	-	0
4-4-1	0	5.89e-07	-	0	3.58e-02	-	0
4-3-1	0	2.57e-07	-	0	2.30e-02	-	0
4-3-2	0	5.91e-07	-	0	3.59e-02	-	0
4-2-2	0	4.89e-07	-	0	3.24e-02	-	0
4-1-2	0	8.35e-07	-	0	4.31e-02	-	0
4-4-3	0	5.61e-07	-	0	3.48e-02	-	0
4-3-3	0	2.45e-07	-	0	2.25e-02	-	0
3-3-1	0	7.15e-07	-	0	4.01e-02	-	0
3-3-2	0	1.53e-06	-	0	6.12e-02	-	0
3-2-2	0	1.57e-06	-	0	6.21e-02	-	0
3-2-3	0	6.83e-07	-	0	3.92e-02	-	0

b. Because of the strong IPyC-SiC bond anticipated in AGR-1 fuel, partial debonding is not considered in the AGR-1 Safety Test Predictions (see Section 3.3).

In addition to the failure probabilities listed in Table 4 and Table 5, PARFUME also calculates the penetration of palladium in the SiC layer. The calculation is performed using a temperature-dependent Arrhenius law (see Section 3.3) so the total penetration depth only depends on time at the irradiation and safety test temperatures.

Results are displayed in Table 6 and plotted in Figure 10 for both irradiation and safety testing phases. They show that Pd penetration is limited to less than 10 μm during irradiation and that the high safety test temperatures do not add any significant contribution to the overall penetration. Compared to the SiC thickness of about 35 μm (see Table 2) palladium penetration is not expected to lead to SiC failure.

The results on Pd penetration only apply to the 18 compacts of the AGR-1 Safety Testing. Other compacts may experience higher penetration depths but, based on these results and on the irradiation characteristics of all 72 compacts, Pd penetration is not expected to fail any AGR-1 particle.

Table 6. Palladium penetration at the end of irradiation and at the end of safety testing.

Compact	Pd Penetration (μm)		
	Irradiation	Safety Testing	Total
6-4-1	5.22	1.15	6.37
6-2-1	9.23	1.14	10.37
6-4-3	5.23	1.14	6.37
6-2-3	9.29	1.14	10.43
5-1-1	5.86	1.56	7.42
5-3-3	5.77	1.15	6.92
5-1-3	5.91	2.06	7.97
4-4-1	6.49	2.07	8.56
4-3-1	7.92	1.14	9.06
4-3-2	6.21	2.06	8.27
4-2-2	6.54	1.14	7.68
4-1-2	5.76	1.15	6.91
4-4-3	6.58	1.56	8.14
4-3-3	8.02	1.14	9.16
3-3-1	6.32	1.56	7.88
3-3-2	5.01	1.15	6.16
3-2-2	4.98	1.15	6.13
3-2-3	6.40	2.07	8.47
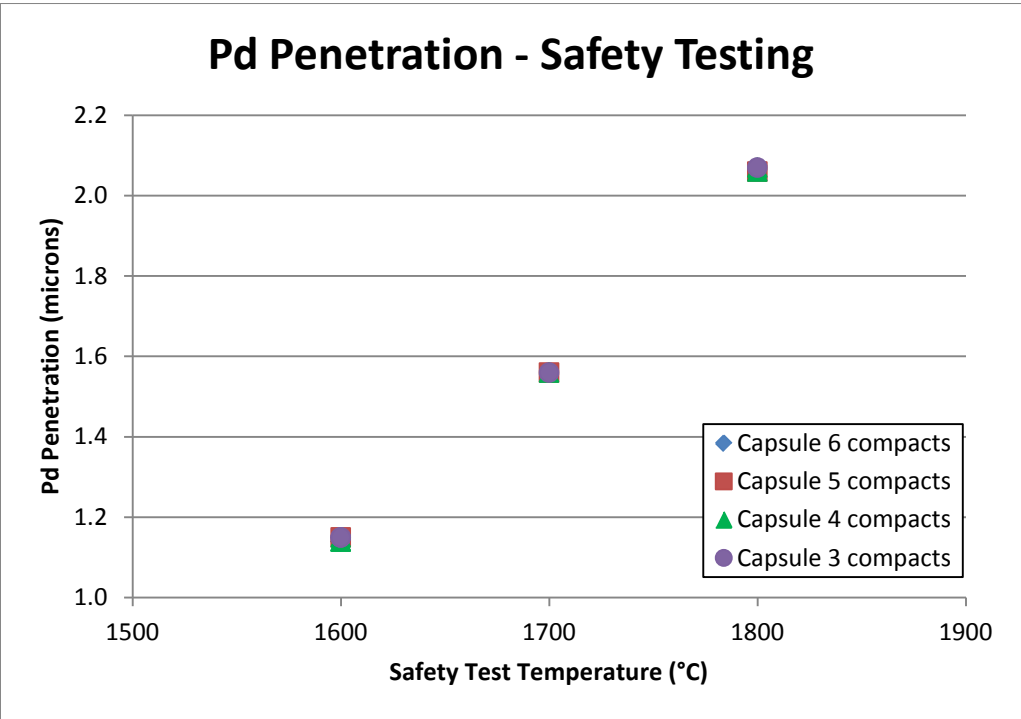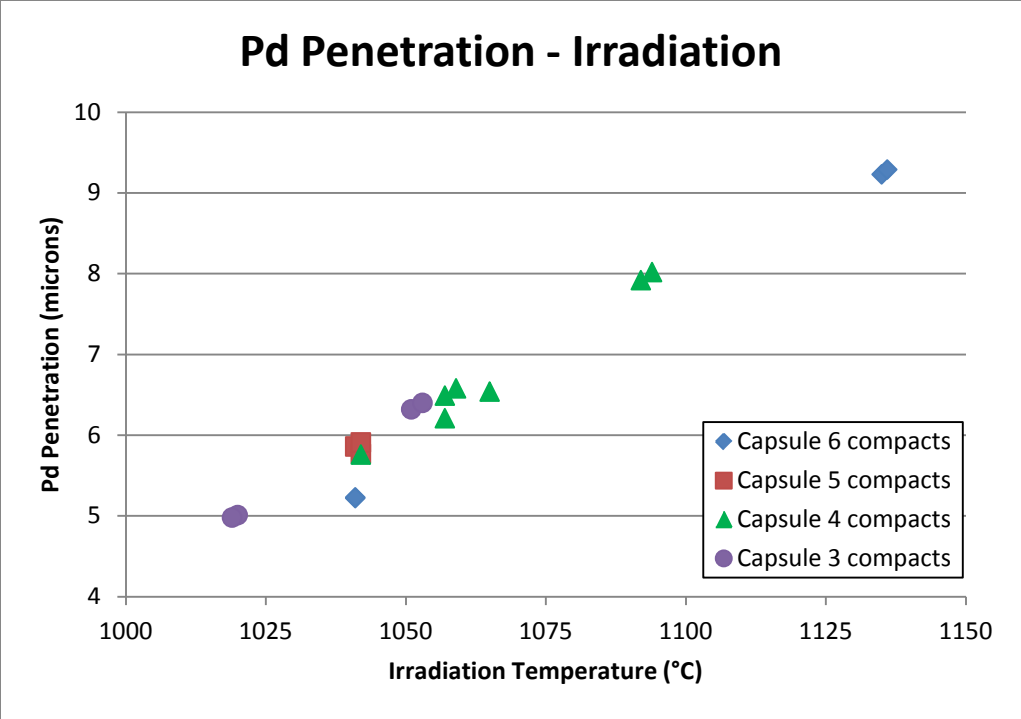
Figure 10. Palladium penetration at the end of irradiation and at the end of safety testing.

4.2   Fractional Release of the Fission Products

PARFUME calculates fission product transport through particles and compacts and it determines the release of four FP species (Ag, Cs, Kr, and Sr) during irradiation and safety testing phases. Using the diffusivities introduced in Section 3.4 and the irradiation and safety test temperatures of the 18 compacts of the AGR-1 Safety Test Predictions, PARFUME calculates the fractional releases as the ratio of the number of atoms released from the compact to the quantity produced in the compact fuel kernels and through uranium contamination in its matrix material.

Results of these fractional releases at the end of irradiation and safety testing are shown in Table 7 for the four fission product species. The fractional releases during safety testing are calculated based on a zero-release at the end of irradiation, i.e. they do not incorporate any release during the irradiation. Figure 11 and Figure 12 display these values as a function of irradiation and safety rest temperatures for the 18 compacts grouped by capsule type. Finally, Figure 13 shows the fractional release of silver for a representative compact (Compact 4-2-2) as a function of time. The top figure shows the release during both irradiation (620 EFPD) and safety testing (300 hours), while the bottom figure shows a close-up of the safety testing phase with the fractional release calculated from zero release at the beginning of the safety test ("Safety Testing"), or from the fractional release at the end of irradiation ("Irradiation + Safety Testing"). The top figure shows the increasing release of silver during irradiation followed by a jump in fractional release as the compact is heated up at 1600°C. Because of the low fractional release at the end of irradiation (4%) the fractional releases at the end of the safety test are similar in both the "Safety Testing" and "Irradiation + Safety Testing" cases (~60%). Similar figures for the other compacts of the AGR-1 Safety Testing are displayed in Appendix D.

From the table and figures below, the following remarks can be made:

- During irradiation:
    - o Silver is released from the compacts with a fractional release ranging from 1% to 16% (Compact 6-2-3).
    - o Cesium and strontium are mostly retained by the particles with fractional releases limited to less than 3×10^{-5}.
    - o Krypton is almost entirely retained in the particles with a fractional release lower than 2×10^{-7}.
- During safety testing:
    - o Ag fractional release exceeds 50% for all compacts and it reaches 92% at 1800°C (Compact 5-1-3) although it is limited to around 60% for compacts heated up at 1600°C.
    - o Cs fractional release reaches 38% at 1800°C but remains below 0.5% for compacts heated up at 1600°C.
    - o Kr fractional release reaches 3% at 1800°C but Kr remains mainly retained by the particles at 1600°C.
    - o Sr fractional release reaches up to 52% at 1800°C but only 5% at 1600°C.
- The fractional releases during irradiation and safety testing are mainly impacted by the irradiation and safety test temperatures respectively.

Table 7. Fractional release at the end of irradiation and at the end of safety testing.

Compact	Ag		Cs		Kr		Sr	
	Irradiation	Safety Testing[a]	Irradiation	Safety Testing[a]	Irradiation	Safety Testing[a]	Irradiation	Safety Testing[a]
6-4-1	2.23e-02	6.02e-01	4.19e-07	1.89e-03	6.69e-08	2.67e-07	1.10e-07	4.73e-02
6-2-1	1.55e-01	5.27e-01	2.64e-05	3.21e-03	1.98e-07	1.38e-07	2.61e-05	4.79e-02
6-4-3	2.23e-02	6.02e-01	4.19e-07	1.89e-03	6.70e-08	2.66e-07	1.10e-07	4.74e-02
6-2-3	1.57e-01	5.25e-01	2.77e-05	3.24e-03	1.99e-07	1.37e-07	2.77e-05	4.80e-02
5-1-1	2.20e-02	8.11e-01	3.28e-07	6.78e-02	5.16e-08	3.72e-04	1.33e-07	2.03e-01
5-3-3	2.26e-02	6.06e-01	3.32e-07	1.83e-03	5.24e-08	2.02e-07	1.31e-07	4.77e-02
5-1-3	2.27e-02	9.22e-01	3.33e-07	3.71e-01	5.25e-08	3.28e-02	1.42e-07	5.21e-01
4-4-1	3.39e-02	9.11e-01	3.71e-07	3.70e-01	2.71e-08	3.38e-02	3.39e-07	5.21e-01
4-3-1	7.43e-02	5.77e-01	2.78e-06	2.38e-03	4.35e-08	7.59e-08	3.35e-06	4.78e-02
4-3-2	3.38e-02	9.10e-01	3.64e-07	3.69e-01	2.70e-08	3.36e-02	2.75e-07	5.19e-01
4-2-2	4.13e-02	5.94e-01	5.61e-07	2.05e-03	3.05e-08	8.89e-08	4.83e-07	4.75e-02
4-1-2	2.25e-02	6.04e-01	1.98e-07	1.84e-03	2.13e-08	9.85e-08	1.07e-07	4.74e-02
4-4-3	3.57e-02	8.00e-01	4.12e-07	6.80e-02	2.80e-08	3.84e-04	3.92e-07	2.03e-01
4-3-3	7.73e-02	5.75e-01	3.12e-06	2.41e-03	4.45e-08	7.49e-08	3.83e-06	4.78e-02
3-3-1	3.01e-02	8.08e-01	5.10e-07	6.98e-02	8.03e-08	3.67e-04	2.86e-07	2.04e-01
3-3-2	1.16e-02	6.14e-01	3.68e-07	1.79e-03	4.76e-08	2.89e-07	5.96e-08	4.80e-02
3-2-2	1.12e-02	6.15e-01	3.67e-07	1.78e-03	4.68e-08	2.90e-07	5.78e-08	4.80e-02
3-2-3	3.18e-02	9.15e-01	5.38e-07	3.76e-01	8.28e-08	3.26e-02	3.26e-07	5.22e-01

a. The values at the end of safety testing assume no release at the beginning of safety testing and do not use values at the end of irradiation as start-up values.
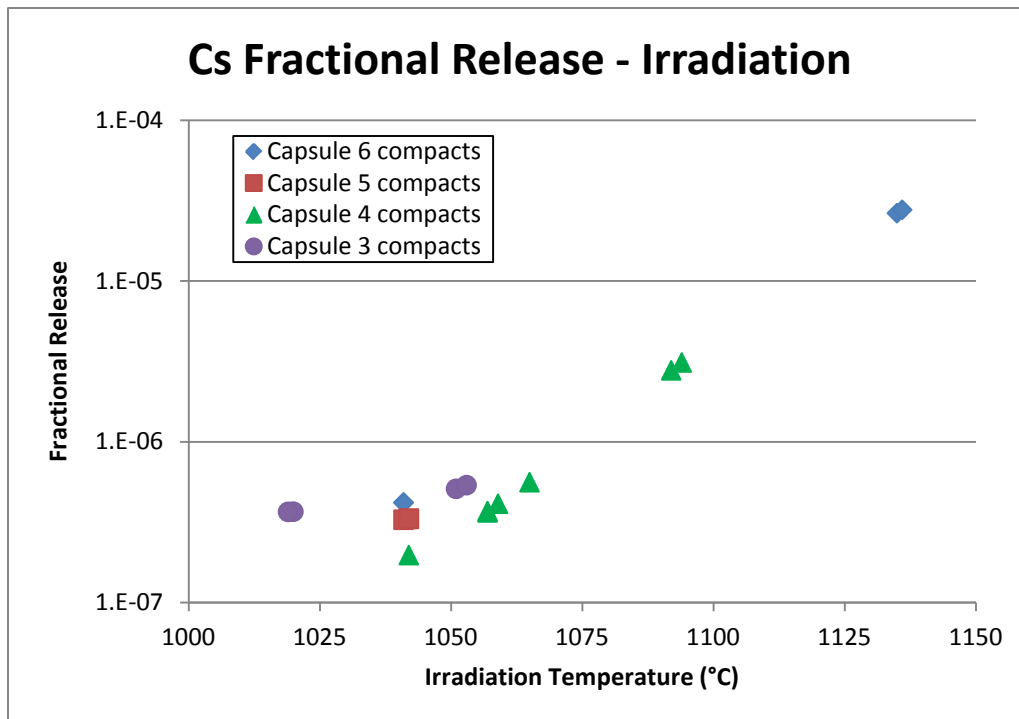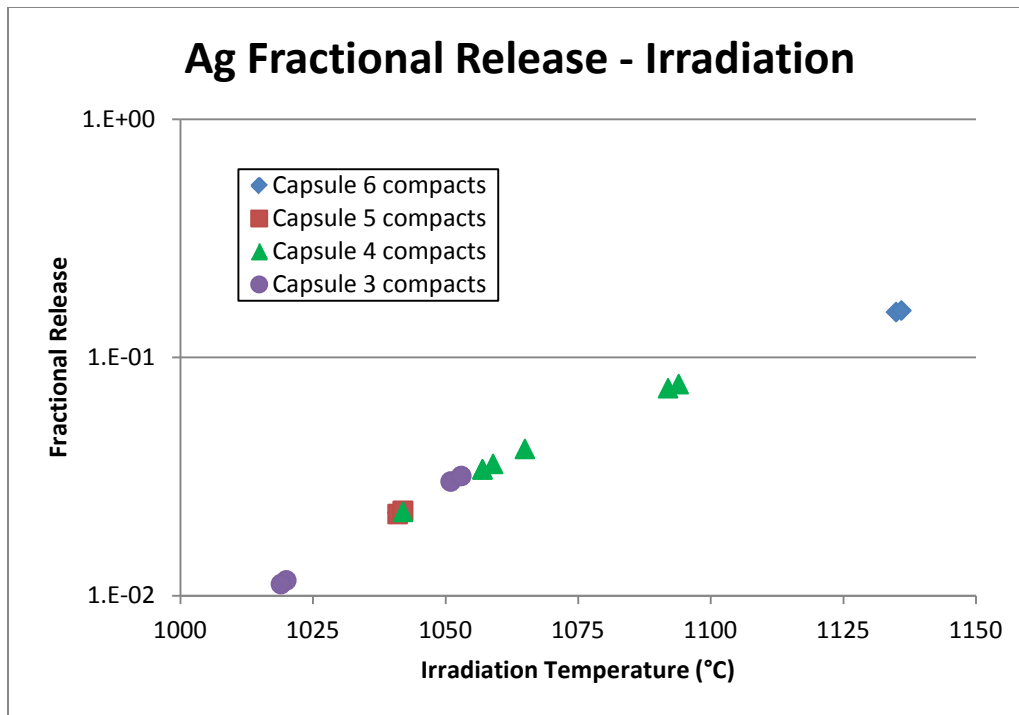
Figure 11a. Silver and cesium fractional releases at the end of irradiation.
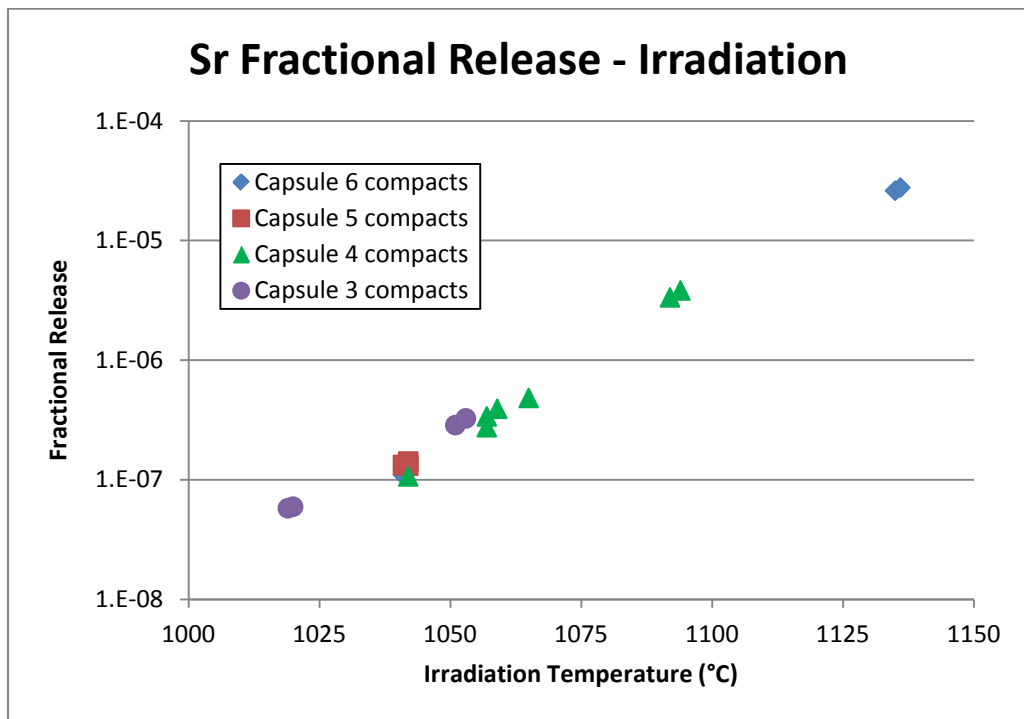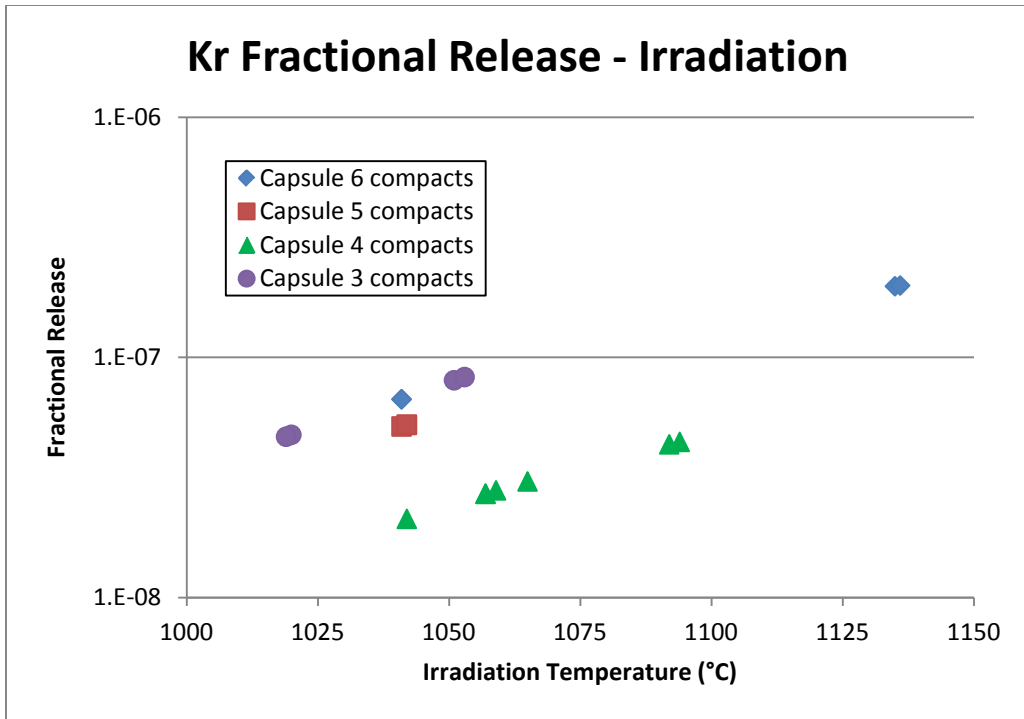
Figure 11b. Krypton and strontium fractional releases at the end of irradiation.
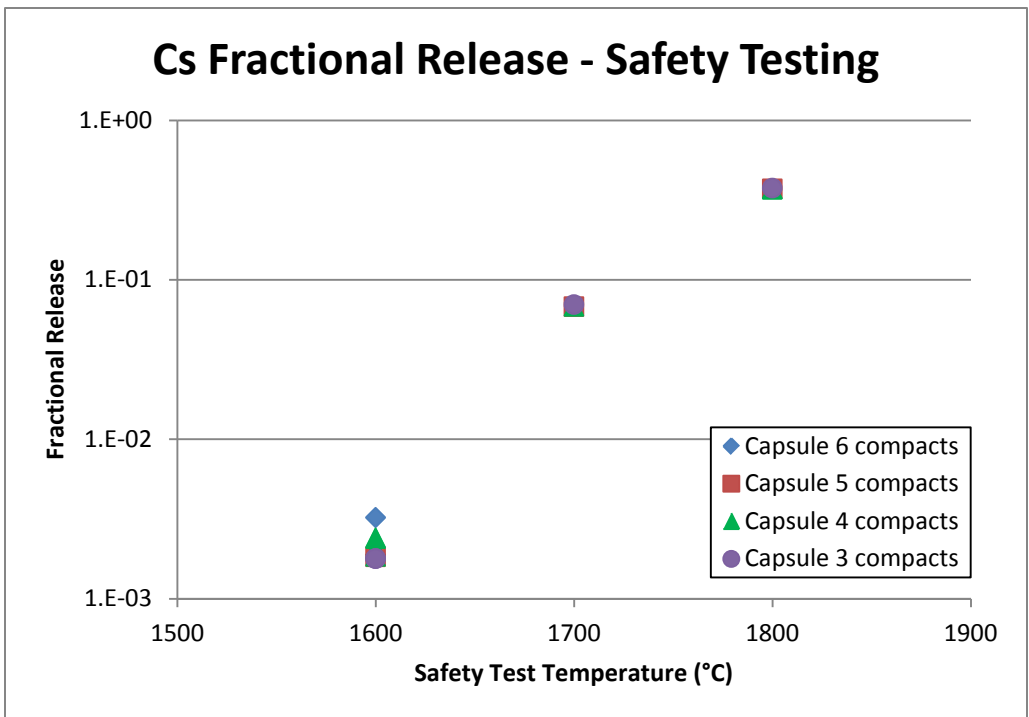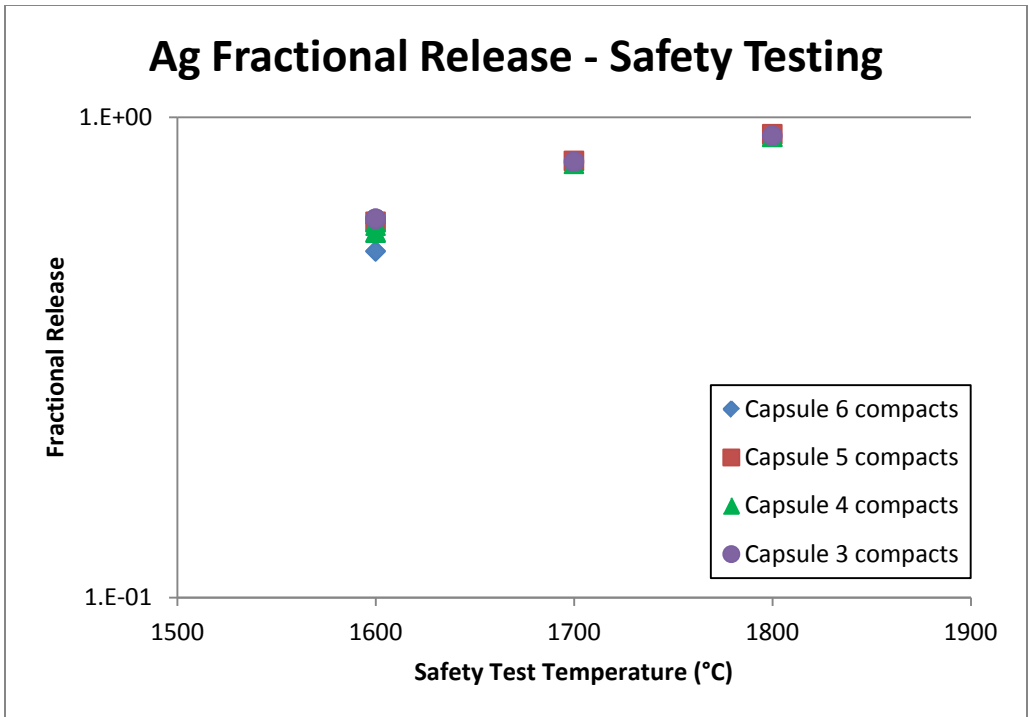
Figure 12a. Silver and cesium fractional releases at the end of safety testing.
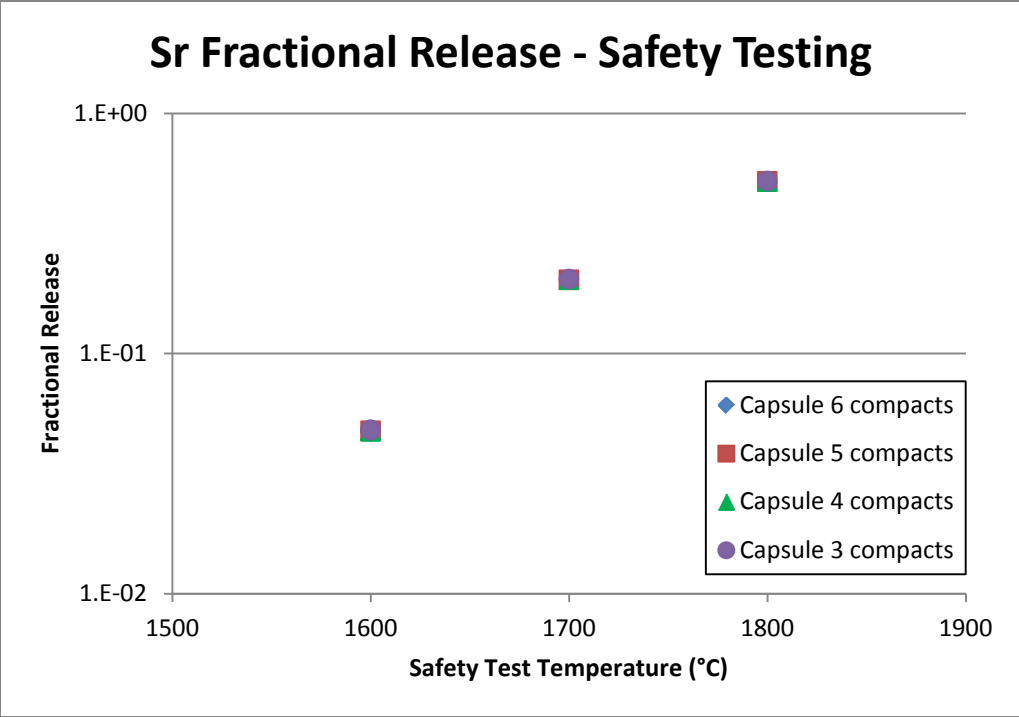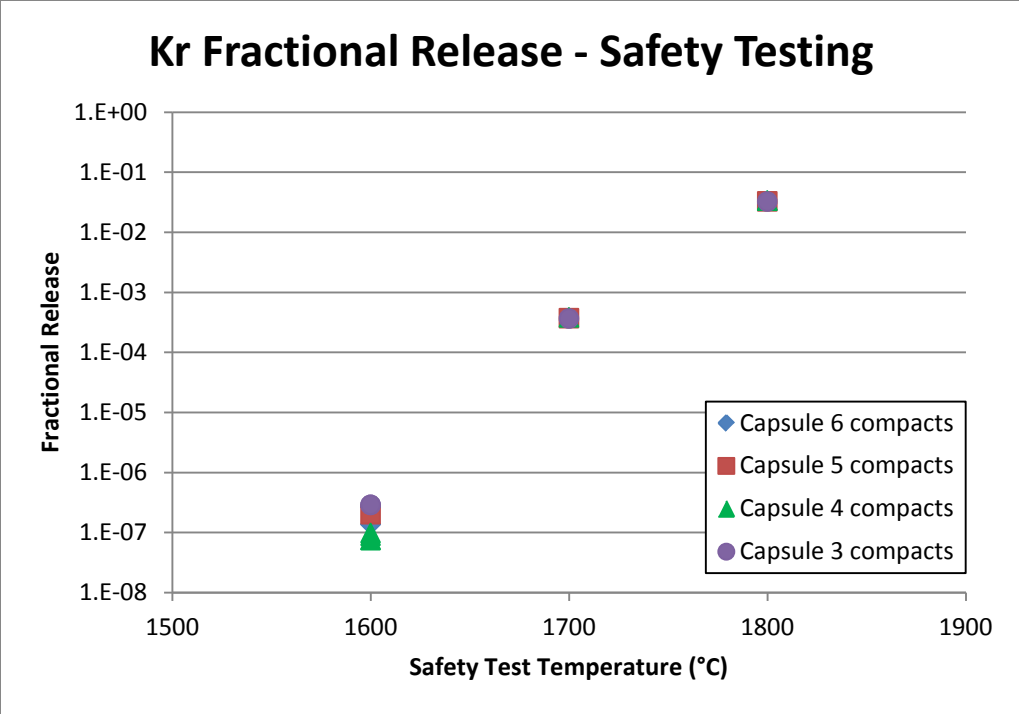
Figure 12b. Krypton and strontium fractional releases at the end of safety testing.
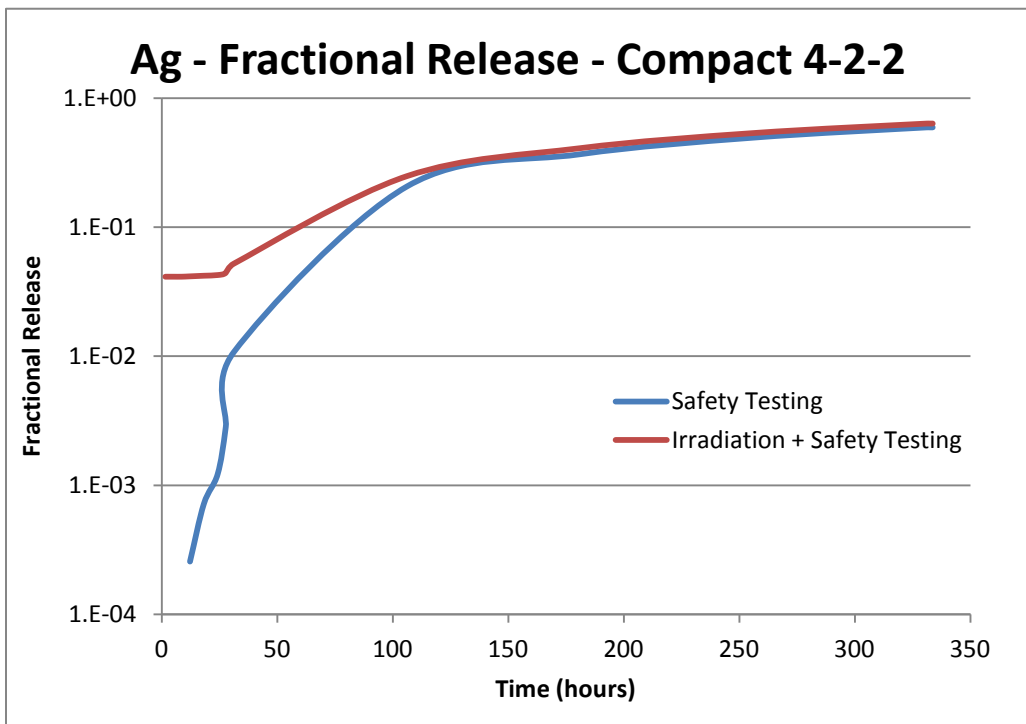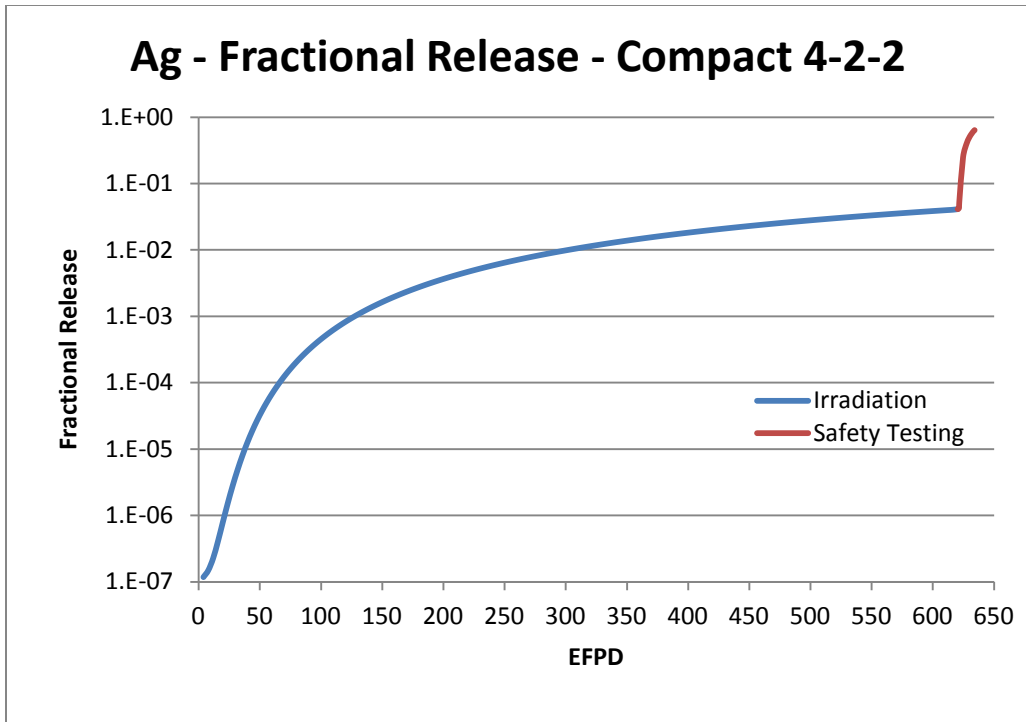
Figure 13. Silver fractional release for Compact 4-2-2.

5. CONCLUSION

PARFUME was used to predict the failure probabilities and fission product fractional releases of the 18 compacts selected for the AGR-1 Safety Testing.

The modeling of the AGR-1 Safety Test Predictions includes the modeling of the AGR-1 irradiation in ATR (620.2 EFPD) and the modeling of post-irradiation heating phase (~30 hours to ramp up + 300 days of heating at target temperature).

From the calculations run, the following conclusions can be drawn:

- PARFUME predicts zero particle failure during irradiation or safety testing: the highest SiC failure probability is 1.6×10^{-6}.
- Kernel migration and pressure have no contribution to the SiC failure probability.
- The failure probability mostly depends on the irradiation temperature and it is not impacted by end-of-irradiation burnup or fast neutron fluence.
- Palladium penetration is limited to around 10 microns, well below the SiC thickness of about 35 microns (but particles from non-selected compacts might have deeper penetrations).
- Fission product release during irradiation is only a concern for silver with a fractional release approaching 16%.
- Fission product release during safety testing reaches 92% for Ag, 38% for Cs, 3% for Kr, and 52% for Sr at 1800°C but it is limited at 1600°C to 61% for Ag, 0.3% for Cs, 5% for Sr, while Kr is mostly retained.

6. REFERENCES

Abaqus/Standard, "Abaqus User's Manual", Version 6.7, 2007.

CEGA Corporation, "NP-MHTGR Material Models of Pyrocarbon and Pyrolytic Silicon Carbide", CEGA-002820, Rev. 1, July 1993.

B. P. Collin, "AGR-2 Irradiation Experiment Test Plan", PLN-3798, Rev. 1, October 2011.

B. P. Collin, "AGR-1 Irradiation Test Final As-Run Report", INL/EXT-10-18097, Rev. 1, May 2012.

P. A. Demkowicz, "Irradiated AGR-1 Compact 6-2-1 Examination Plan", PLN-4064, December 2011.

P. A. Demkowicz, "Inter-office Memorandum: AGR-1 Safety Test Plan", CCN-227349, May 2012.

G. L. Hawkes, "AGR-1 Daily As-run Thermal Analyses", ECAR-968, Rev. 2, January 2012.

HSC Chemistry User's Guide, Version 5.0, Outotec Research Oy, Finland, 2002.

L. C. Hull, "Very High Temperature Reactor Program Data Management and Analysis Plan", PLN-2709, Rev. 3, July 2011.

IAEA, "Fuel performance and fission product behaviour in gas cooled reactors", TECDOC-978, November 1997.

G. R. Longhurst, D. F. Holland, J. L. Jones, B. J. Merrill, "TMAP4 User's Manual", EGG-FSP-10315, June 1992.

J. T. Maki, "AGR-1 Irradiation Experiment Test Plan", INL/EXT-05-00593, Rev. 3, October 2009.

G. K. Miller, D. C. Wadsworth, "Treating asphericity in fuel particle pressure vessel modeling", Journal of Nuclear Materials 211 (1994) 57-69, March 1994.

G. K. Miller, D. A. Petti, D. J. Varacalle, J. T. Maki, "Statistical approach and benchmarking for modeling of multi-dimensional behavior in TRISO-coated fuel particles", Journal of Nuclear Materials 317 (2003) 69-82, December 2002.

G. K. Miller, D. A. Petti, J. T. Maki, D. L. Knudson, "An evaluation of the effects of SiC layer thinning on failure of TRISO-coated fuel particles", Journal of Nuclear Materials 355 (2006) 150-162, May 2006.

G. K. Miller, D. L. Knudson, "AGR-1 Pre-Test Prediction Analysis using the PARFUME Code", EDF-5741, Rev. 1, April 2007.

G. K. Miller, D. A. Petti, J. T. Maki, D. L. Knudson, "PARFUME Theory and Model Basis Report", INL/EXT-08-14497, September 2009.

D. A. Petti, P. Martin, M. Phelip, R. Balinger, "Development of Improved Models and Designs for Coated-Particle Gas Reactor Fuels", INEEL/EXT-05-02615, December 2004.

D.A. Petti, J. T. Maki, "The Challenges Associated with High Burnup and High Temperature for UO_2 TRISO-Coated Particle Fuel", MIT NGNP Symposium, INL/CON-05-00038, February 2005.

W. F. Skerjanc, "Embedding Multi-dimensional Input Parameters for IPyC Cracking and Particle Asphericity in PARFUME", ECAR-1678, September 2011.

J. W. Sterbentz, "JMOCUP As-Run Daily Depletion Calculation for the AGR-1 Experiment in ATR B-10 position", ECAR-958, Rev. 1, August 2011.

APPENDIX A – Compact History

Compact history is given for the 18 compacts of the AGR-1 Safety Testing for

- Burnup
- Fast neutron fluence
- Temperature (subset of compacts – compacts with similar irradiation characteristics are not shown)

All data is available on NGNP Data Management and Analysis System (Hull 2011).

Compact Burnup - Capsule 6

Compact Burnup - Capsule 5

Compact Burnup - Capsule 4

Compact Burnup - Capsule 3
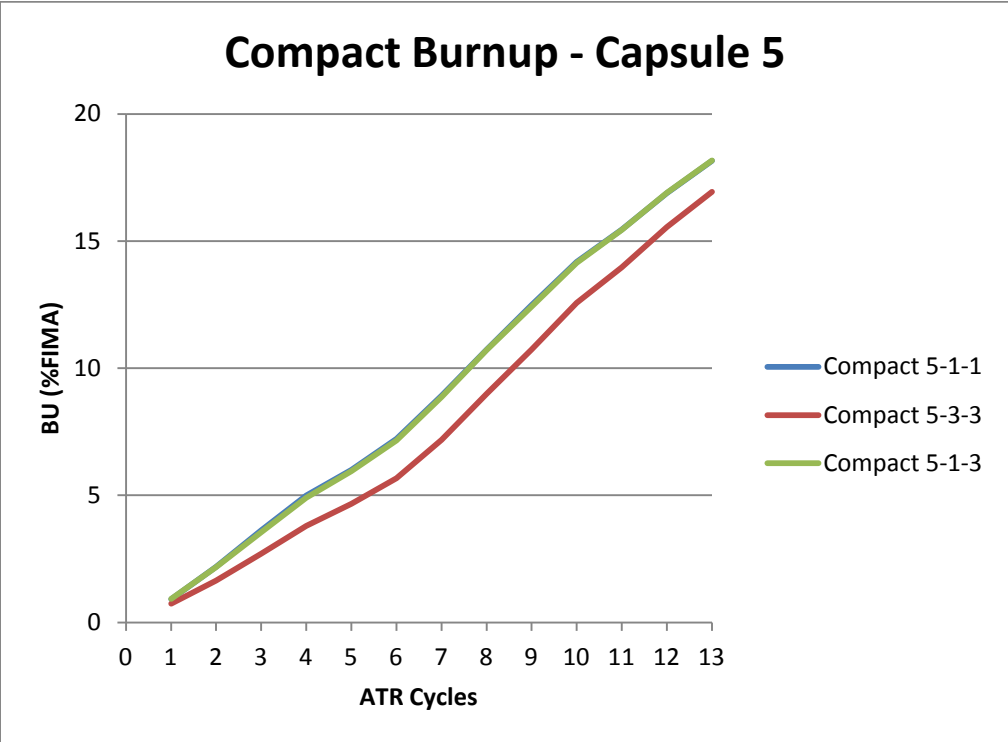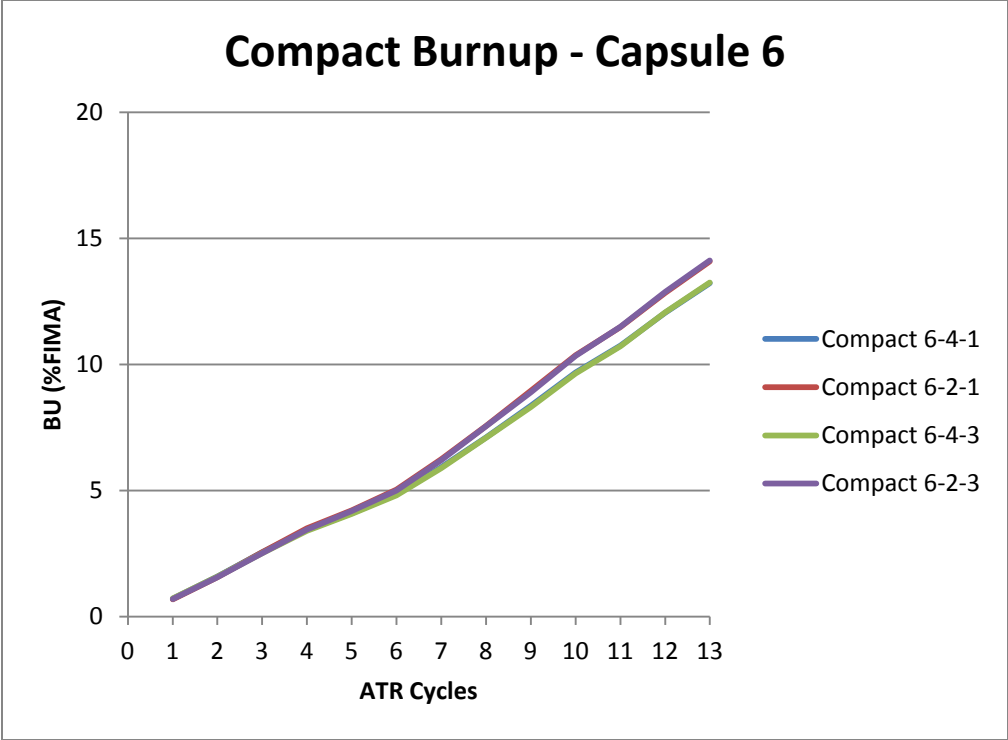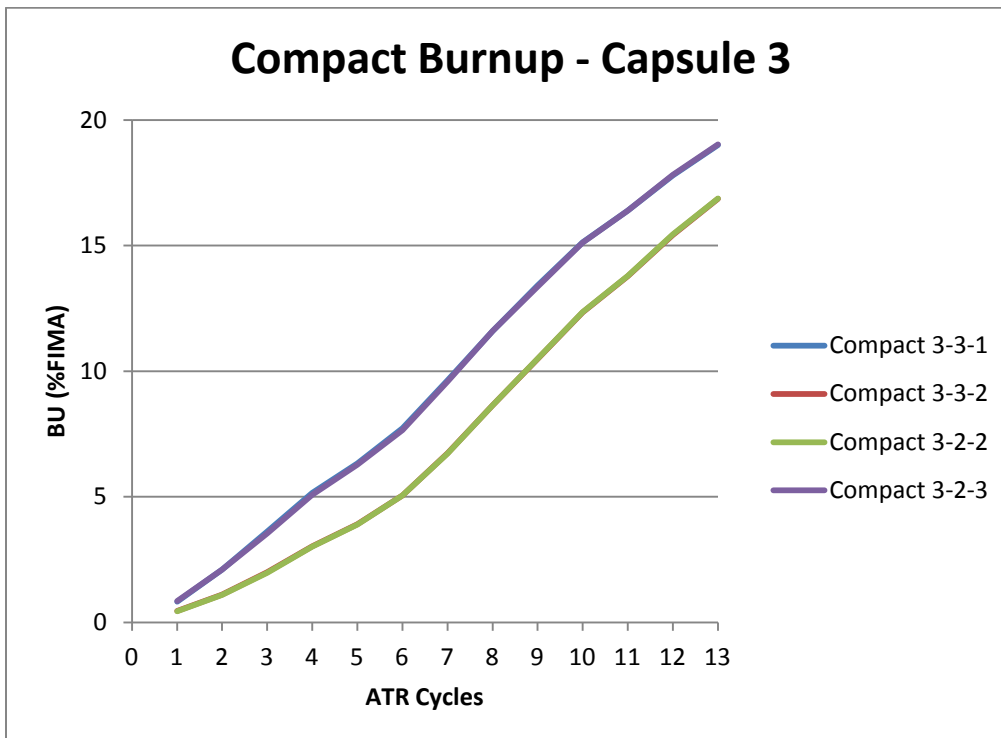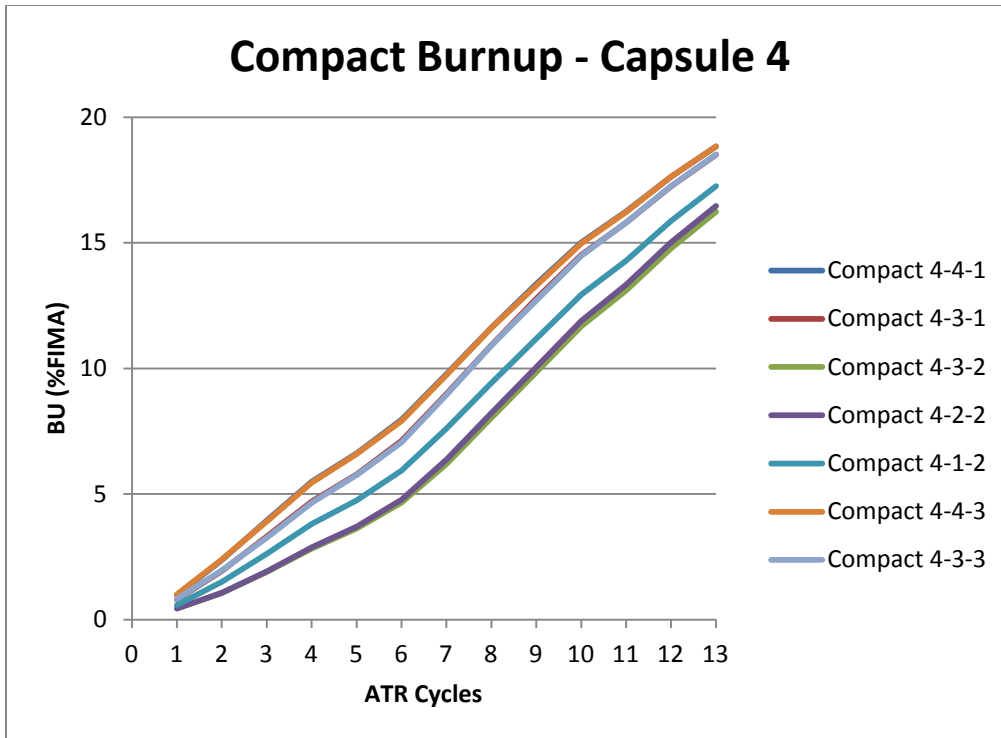
Compact Fast Fluence - Capsule 6
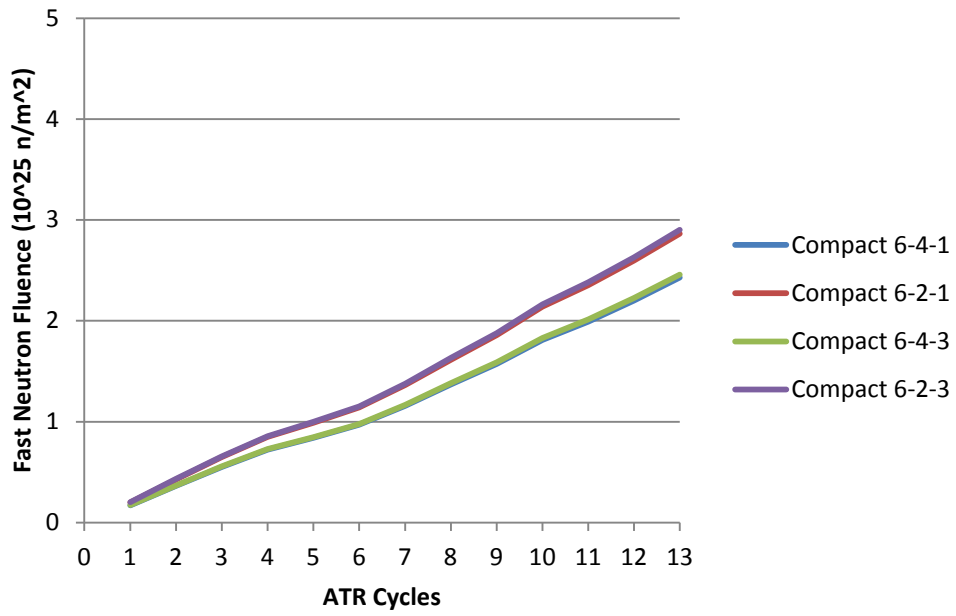
Compact Fast Fluence - Capsule 5
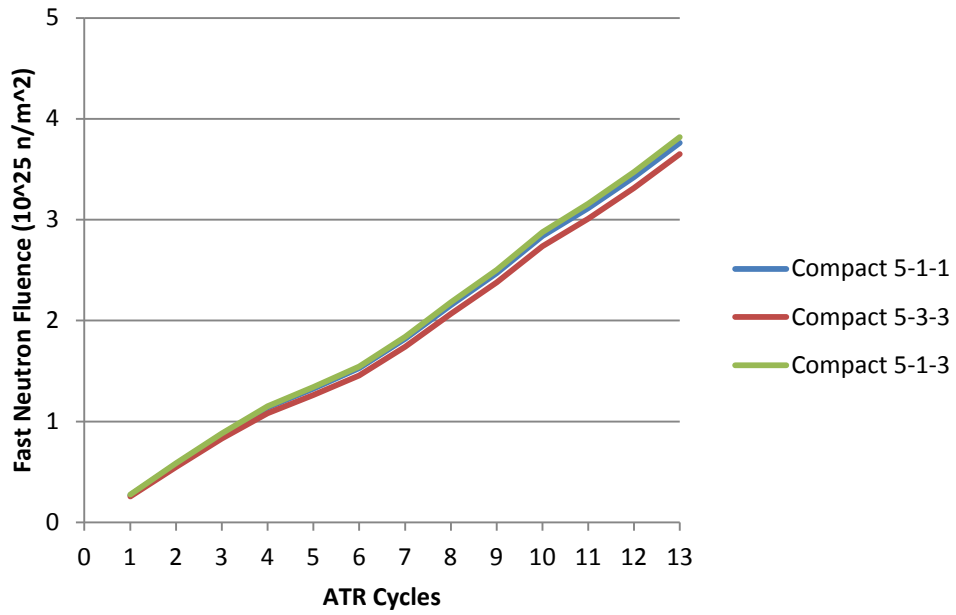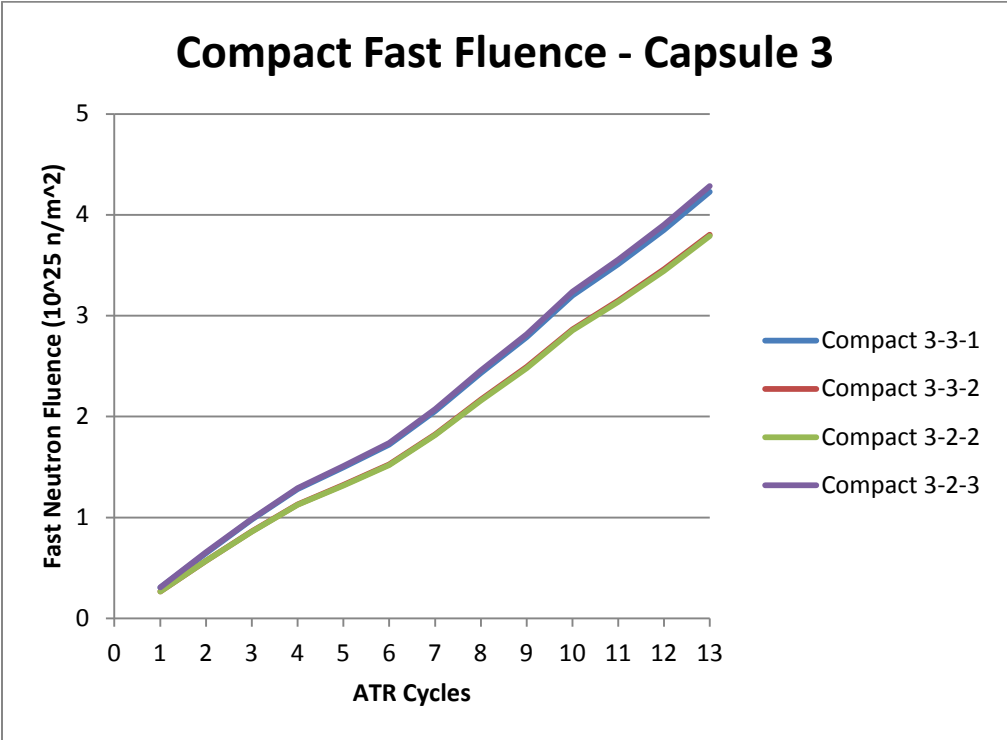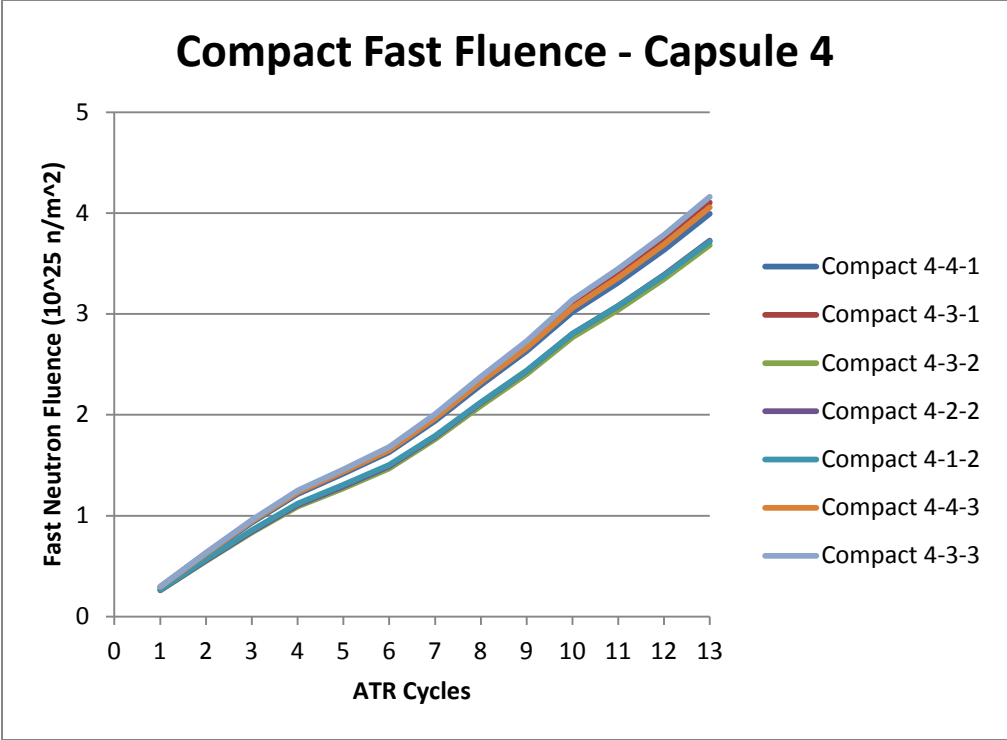
Compact Fast Fluence - Capsule 4
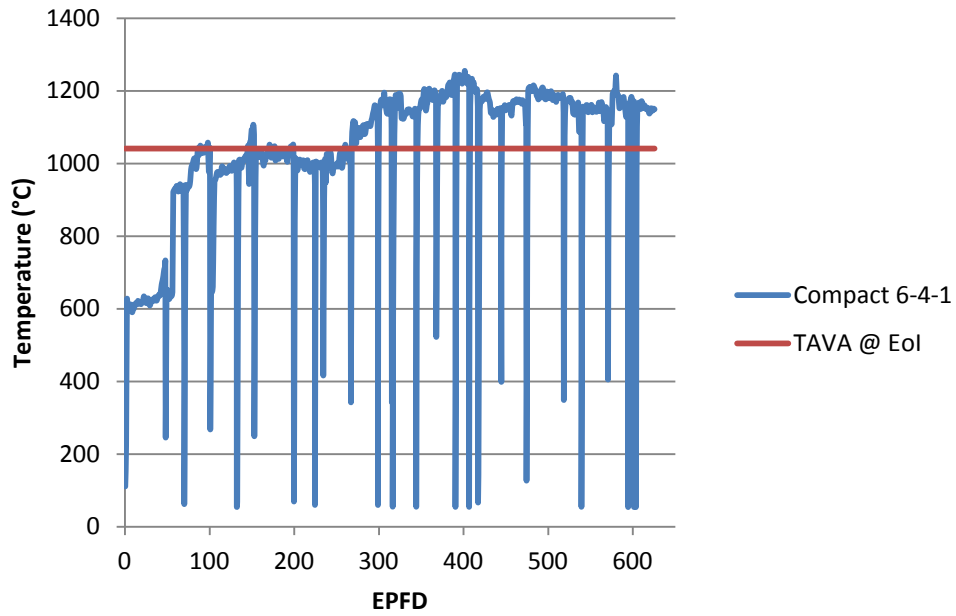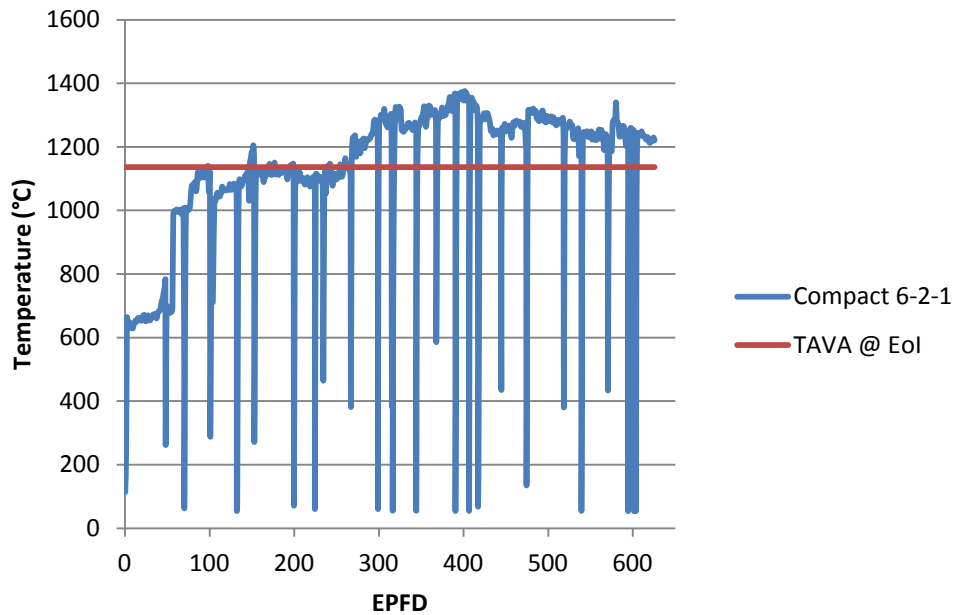
Compact Fast Fluence - Capsule 3

Compact Average Daily Temperature
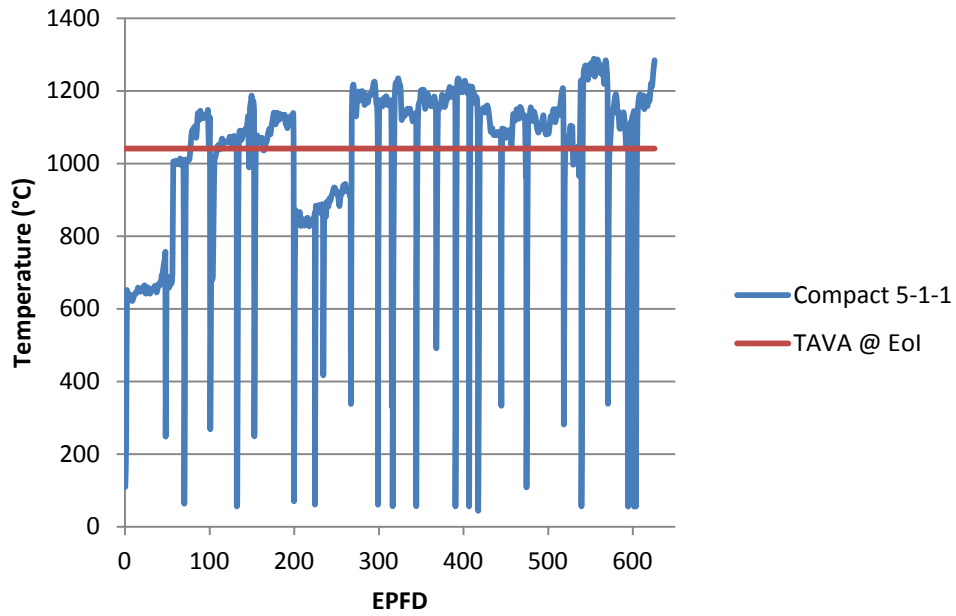
Compact Average Daily Temperature
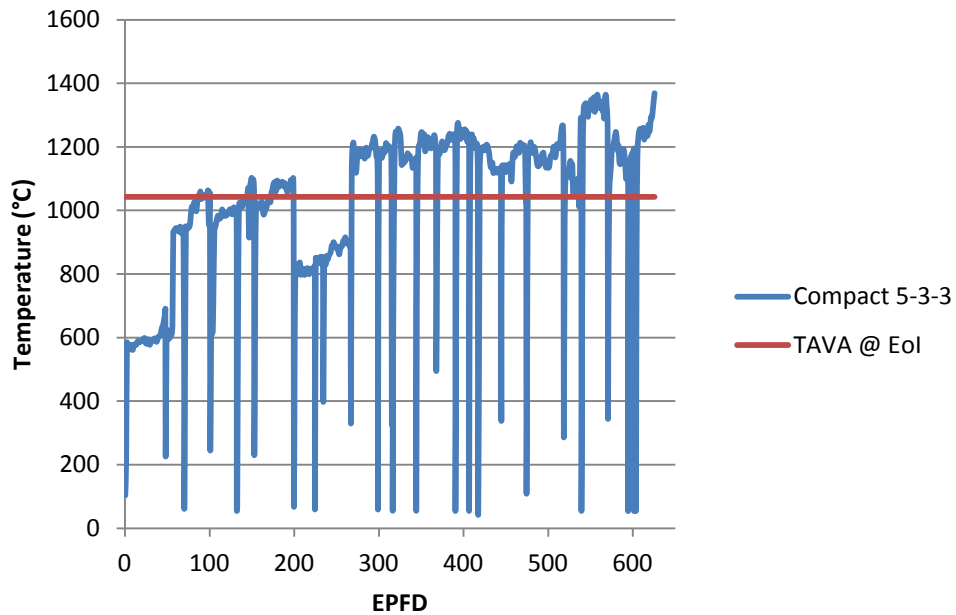
Compact Average Daily Temperature
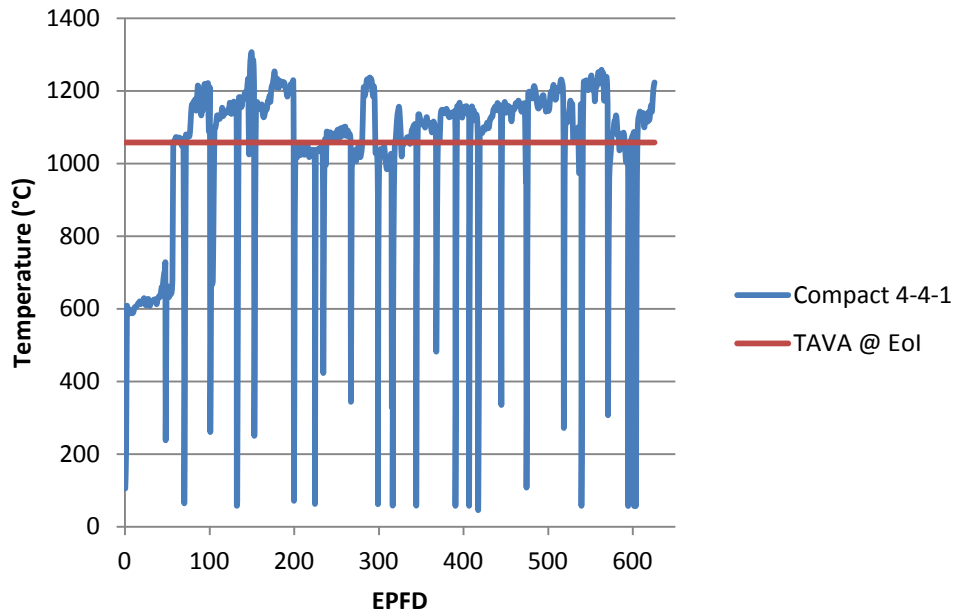
Compact Average Daily Temperature
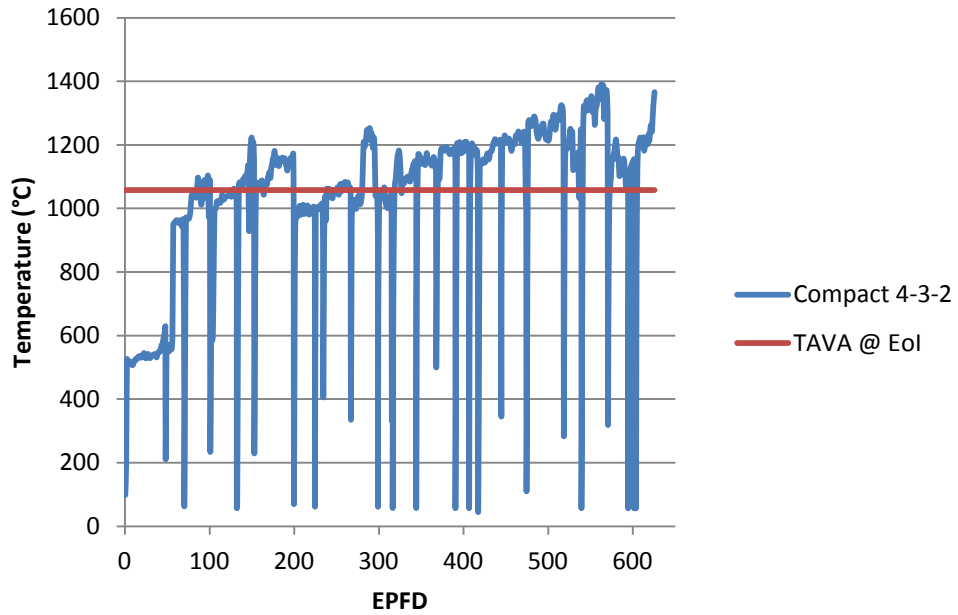
Compact Average Daily Temperature
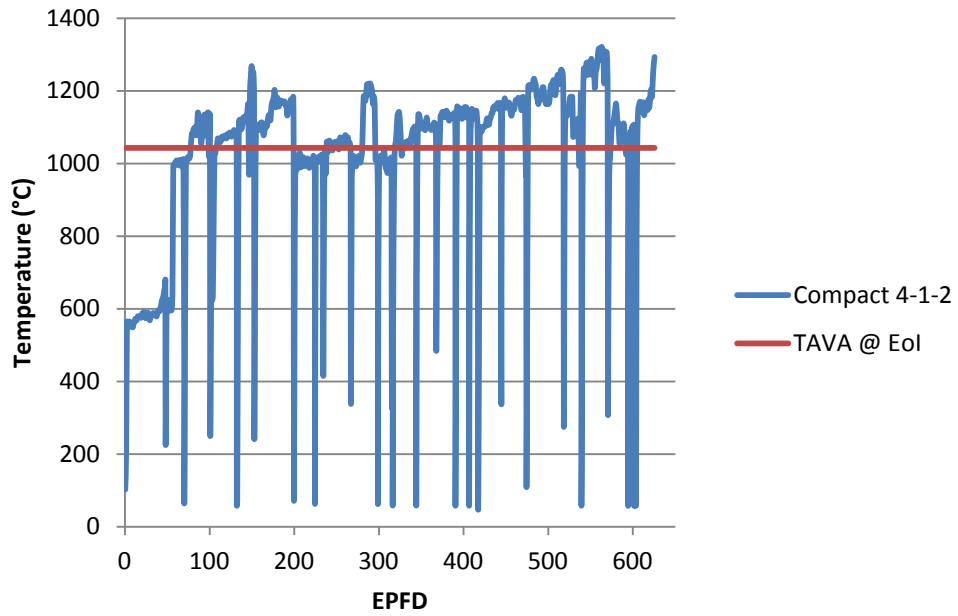
Compact Average Daily Temperature
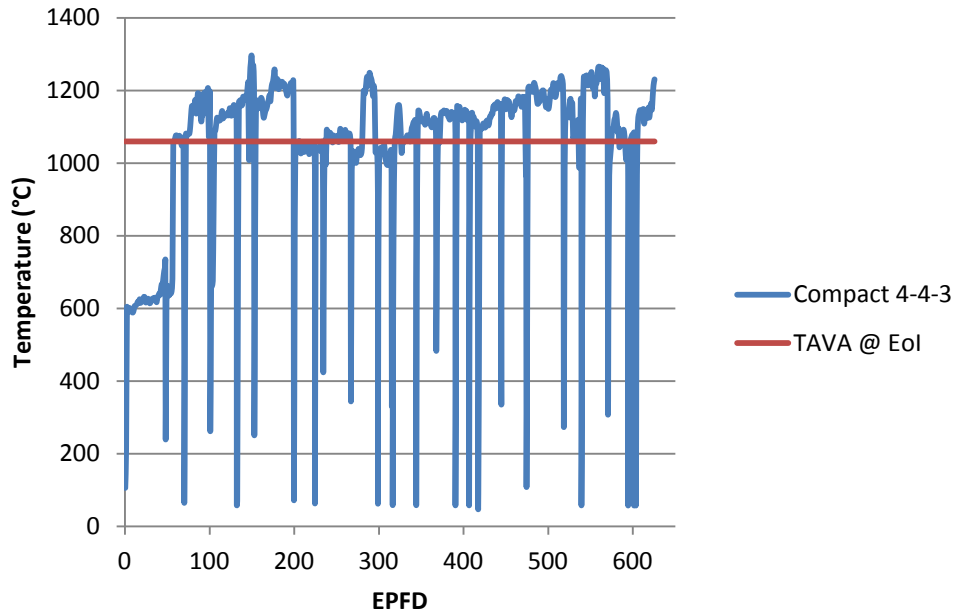
Compact Average Daily Temperature
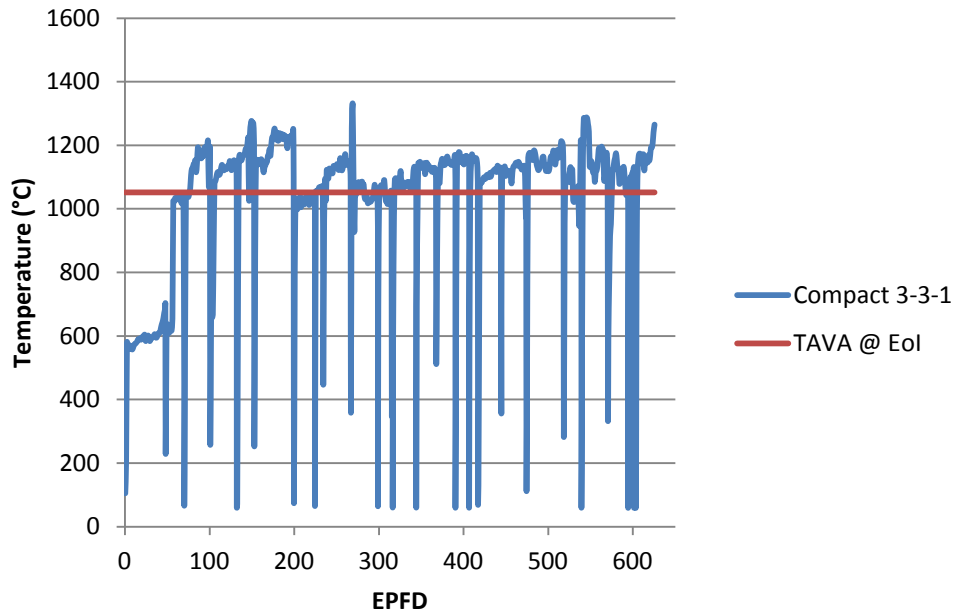
Compact Average Daily Temperature
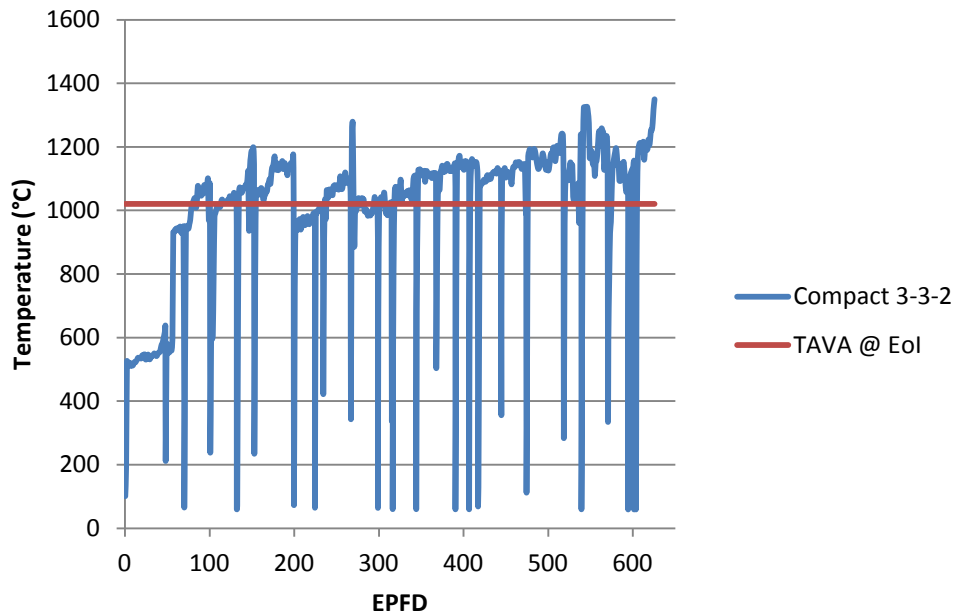
APPENDIX B – Multidimensional Correlation Coefficients

The multidimensional correlation coefficients for IPyC cracking and particle asphericity used in the AGR-1 Safety Test Predictions calculations are given below. The coefficients for IPyC cracking were obtained by the automated calculation embedded in PARFUME, while the coefficients for asphericity were calculated by Abaqus.

Correlation Coefficients for IPyC Cracking			
Compact	Coefficient	C1	C2
6-4-1	IPyC thickness	1.3431e-02	2.9295e-05
	SiC thickness	1.4536e-02	1.5050e-04
	OPyC thickness	-1.2527e-02	2.5890e-04
6-2-1	IPyC thickness	1.3269e-02	2.4470e-05
	SiC thickness	1.5025e-02	1.2797e-04
	OPyC thickness	-1.2008e-02	2.4195e-04
6-4-3	IPyC thickness	1.3431e-02	2.9295e-05
	SiC thickness	1.4536e-02	1.5050e-04
	OPyC thickness	-1.2527e-02	2.5890e-04
6-2-3	IPyC thickness	1.3267e-02	2.4393e-05
	SiC thickness	1.5030e-02	1.2769e-04
	OPyC thickness	-1.2002e-02	2.4177e-04
5-1-1	IPyC thickness	1.3431e-02	2.9295e-05
	SiC thickness	1.4536e-02	1.5050e-04
	OPyC thickness	-1.2527e-02	2.5890e-04
5-3-3	IPyC thickness	1.3430e-02	2.9265e-05
	SiC thickness	1.4541e-02	1.5029e-04
	OPyC thickness	-1.2522e-02	2.5872e-04
5-1-3	IPyC thickness	1.3430e-02	2.9265e-05
	SiC thickness	1.4541e-02	1.5029e-04
	OPyC thickness	-1.2522e-02	2.5872e-04
4-4-1	IPyC thickness	1.3408e-02	2.8761e-05
	SiC thickness	1.4613e-02	1.4712e-04
	OPyC thickness	-1.2438e-02	2.5608e-04
4-3-1	IPyC thickness	1.3352e-02	2.7216e-05
	SiC thickness	1.4789e-02	1.3912e-04
	OPyC thickness	-1.2243e-02	2.4981e-04

Correlation Coefficients for IPyC Cracking			
Compact	Coefficient	C1	C2
4-3-2	IPyC thickness	1.3408e-02	2.8761e-05
	SiC thickness	1.4613e-02	1.4712e-04
	OPyC thickness	-1.2438e-02	2.5608e-04
4-2-2	IPyC thickness	1.3397e-02	2.8456e-05
	SiC thickness	1.4652e-02	1.4536e-04
	OPyC thickness	-1.2393e-02	2.5466e-04
4-1-2	IPyC thickness	1.3430e-02	2.9265e-05
	SiC thickness	1.4541e-02	1.5029e-04
	OPyC thickness	-1.2522e-02	2.5872e-04
4-4-3	IPyC thickness	1.3406e-02	2.8687e-05
	SiC thickness	1.4622e-02	1.4668e-04
	OPyC thickness	-1.2426e-02	2.5572e-04
4-3-3	IPyC thickness	1.3349e-02	2.7110e-05
	SiC thickness	1.4800e-02	1.3863e-04
	OPyC thickness	-1.2232e-02	2.4944e-04
3-3-1	IPyC thickness	1.3417e-02	2.8973e-05
	SiC thickness	1.4583e-02	1.4840e-04
	OPyC thickness	-1.2471e-02	2.5714e-04
3-3-2	IPyC thickness	1.3458e-02	2.9857e-05
	SiC thickness	1.4439e-02	1.5470e-04
	OPyC thickness	-1.2645e-02	2.6254e-04
3-2-2	IPyC thickness	1.3459e-02	2.9880e-05
	SiC thickness	1.4435e-02	1.5489e-04
	OPyC thickness	-1.2651e-02	2.6272e-04
3-2-3	IPyC thickness	1.3414e-02	2.8904e-05
	SiC thickness	1.4593e-02	1.4798e-04
	OPyC thickness	-1.2460e-02	2.5679e-04

SiC Strength and Stress for IPyC Cracking		
Compact	Strength (sigcr0)	Stress (umc)
6-4-1	1138.737	182.148
6-2-1	1140.357	153.437
6-4-3	1138.737	182.148
6-2-3	1140.375	153.158
5-1-1	1138.737	182.147
5-3-3	1138.754	181.819
5-1-3	1138.754	181.819
4-4-1	1139.007	176.947
4-3-1	1139.607	165.998
4-3-2	1139.007	176.947
4-2-2	1139.143	174.392
4-1-2	1138.754	181.819
4-4-3	1139.041	176.306
4-3-3	1139.642	165.391
3-3-1	1138.905	178.884
3-3-2	1138.39	189.138
3-2-2	1138.374	189.475
3-2-3	1138.939	178.236

SiC Strength and Stress for IPyC Asphericity			
Compact	Strength (siga0)	Stress (min) (um)	Stress (max) (delum)
6-4-1	1951.665	456.3	321.8
6-2-1	1662.061	399.1	328.12
6-4-3	1915.635	456.4	326
6-2-3	1643.188	398.6	329.74
5-1-1	754.35	463.1	456.605
5-3-3	1063.094	462.6	441.68
5-1-3	641.775	462.5	489.06
4-4-1	991.269	426.7	408.7
4-3-1	1480.137	406	332.92
4-3-2	831.096	427.1	420.114
4-2-2	1389.312	422.2	368.26
4-1-2	1351.156	436.1	387.48
4-4-3	1300.952	425.6	374.87
4-3-3	1492.375	405	329.73
3-3-1	1349.18	451.6	388.19
3-3-2	1405.964	474.3	410.84
3-2-2	1402.806	475.2	412.57
3-2-3	1167.471	450.4	412.43

APPENDIX C – Failure Probability

SiC failure probability - Compact 6-4-1

SiC failure probability - Compact 6-2-1
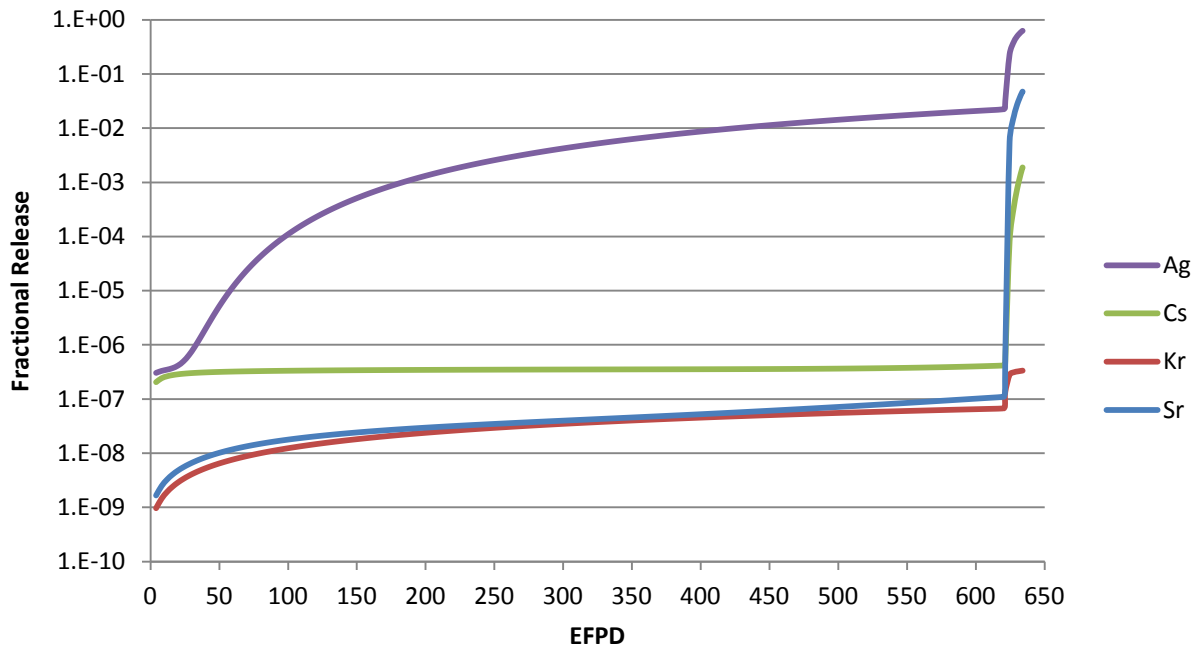
SiC failure probability - Compact 6-4-3

SiC failure probability - Compact 6-2-3
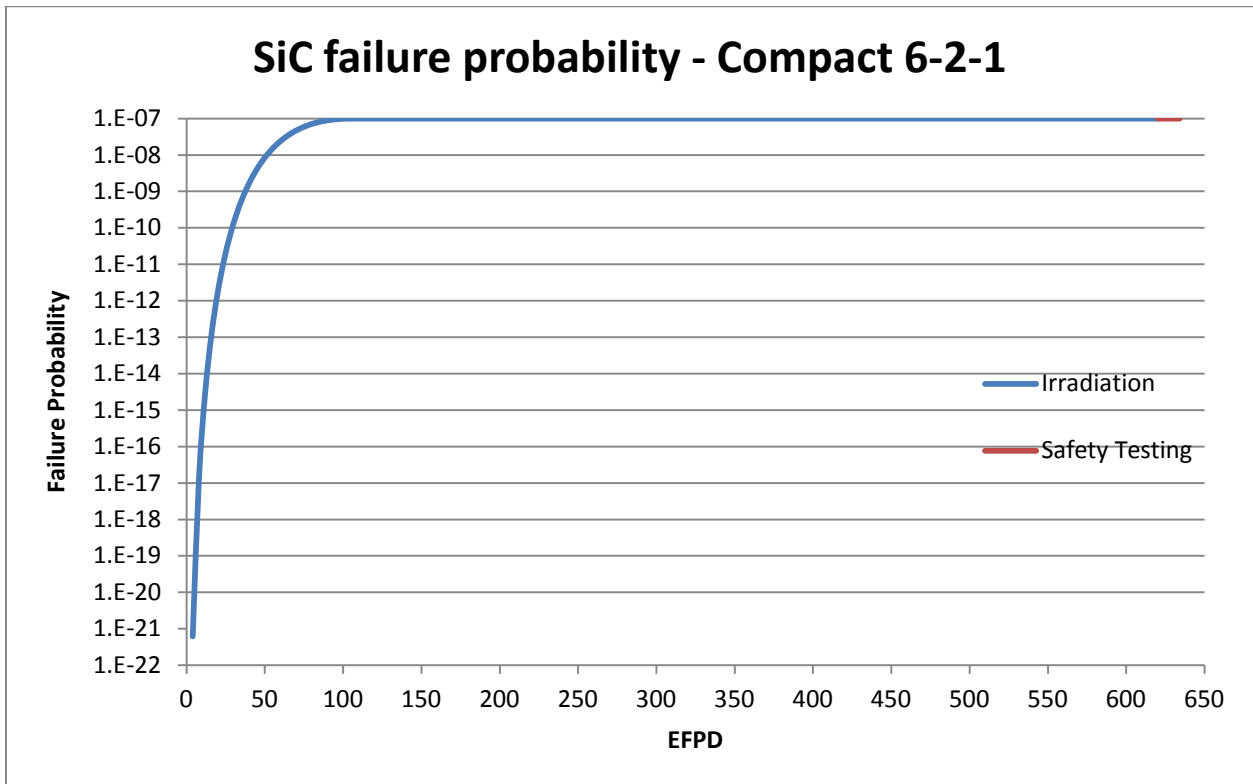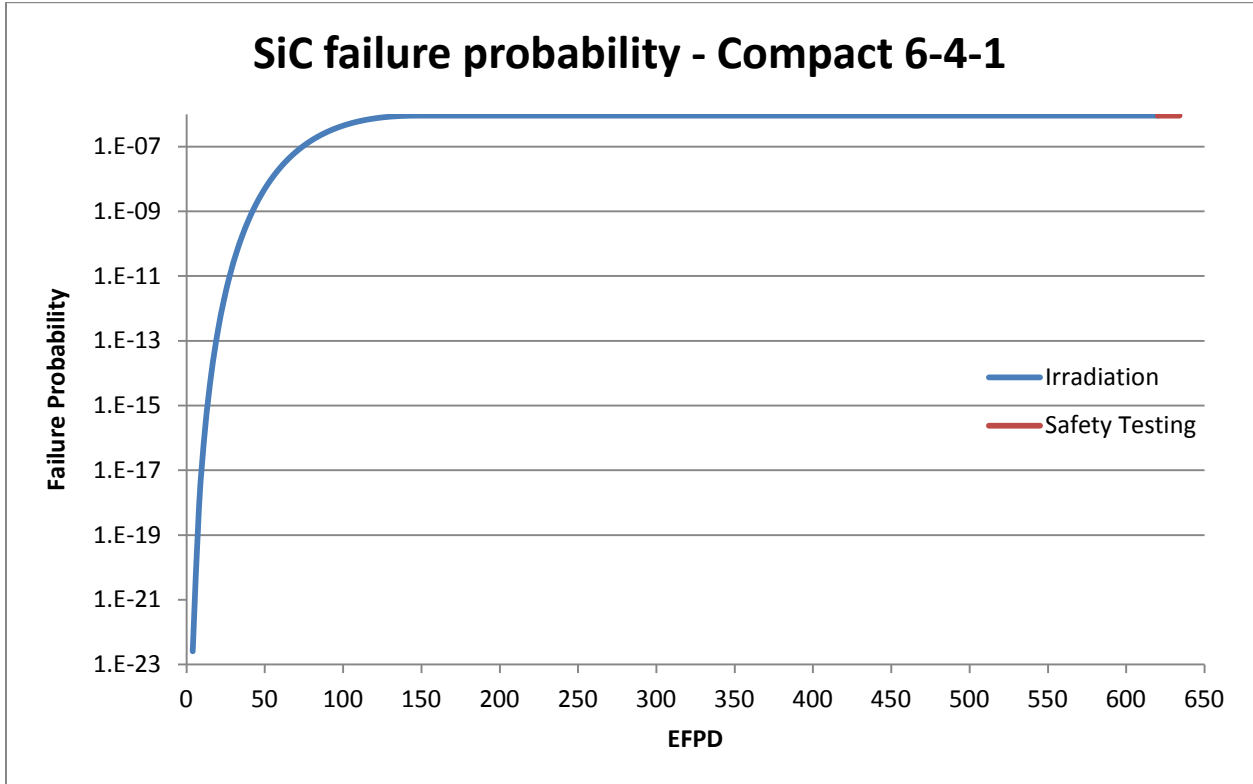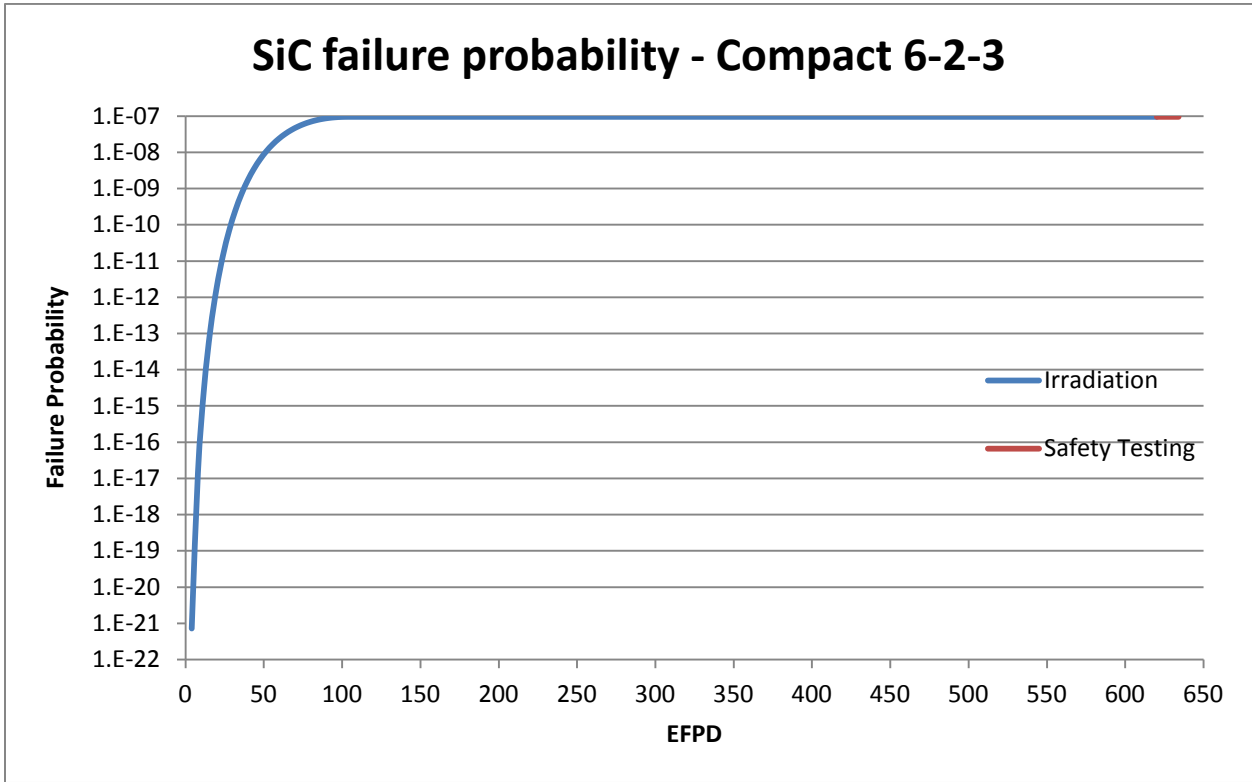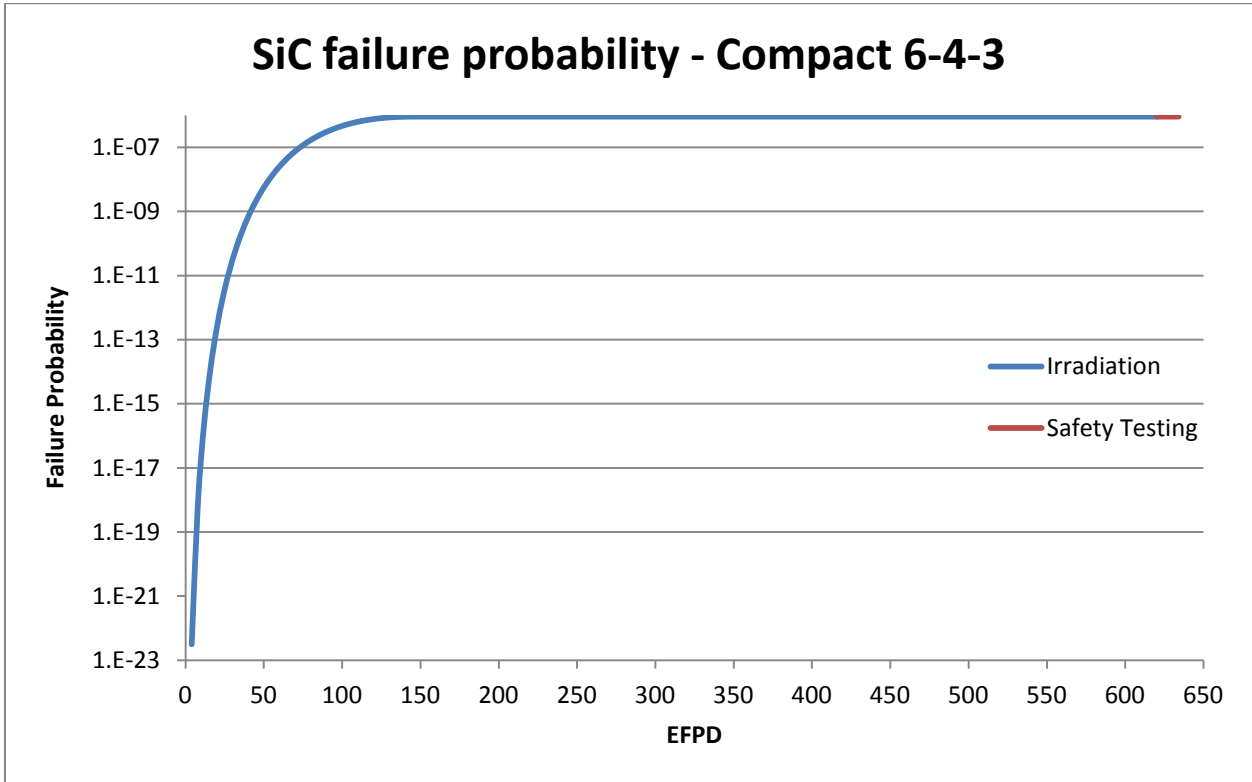
SiC failure probability - Compact 5-1-1
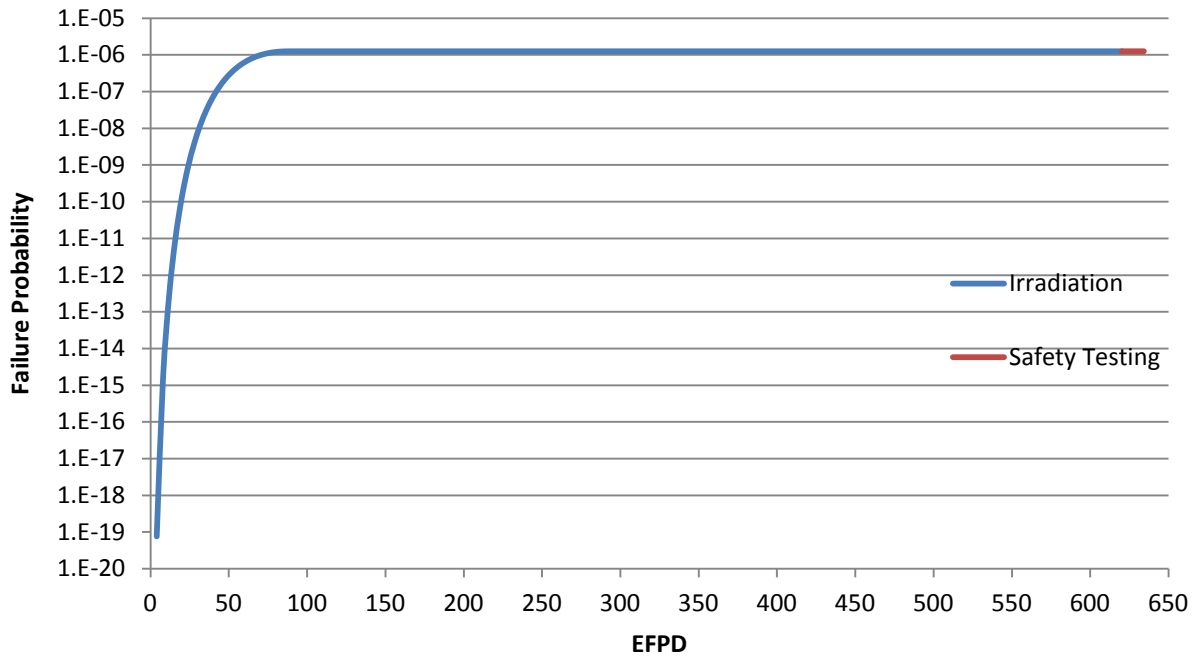
SiC failure probability - Compact 5-3-3
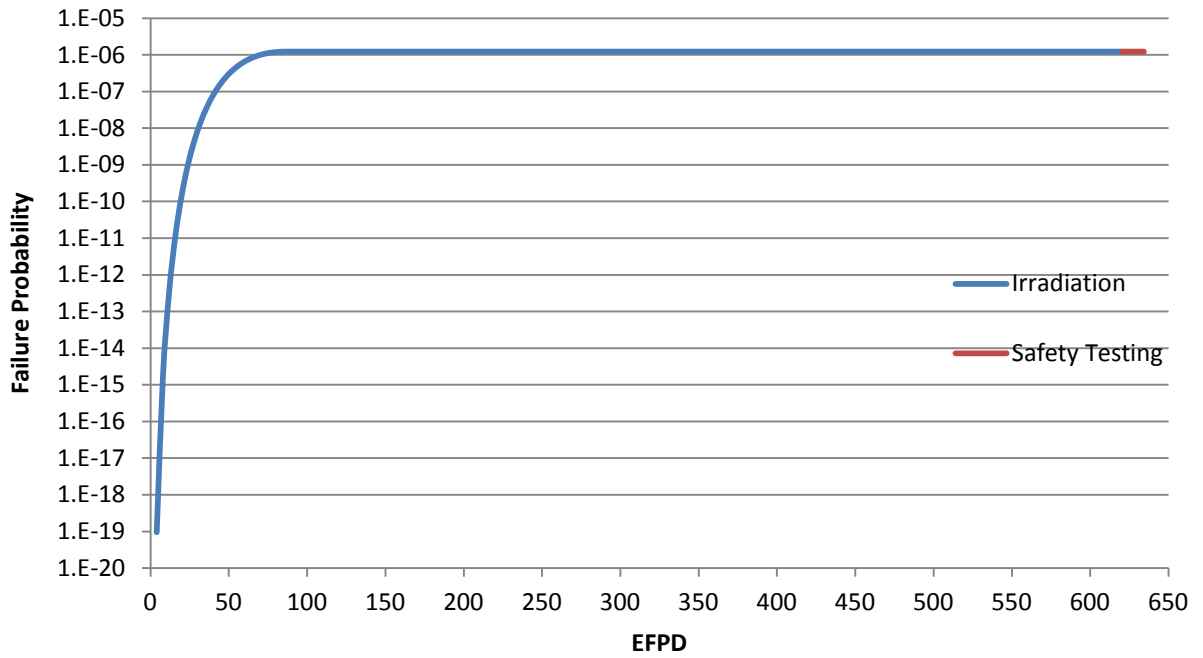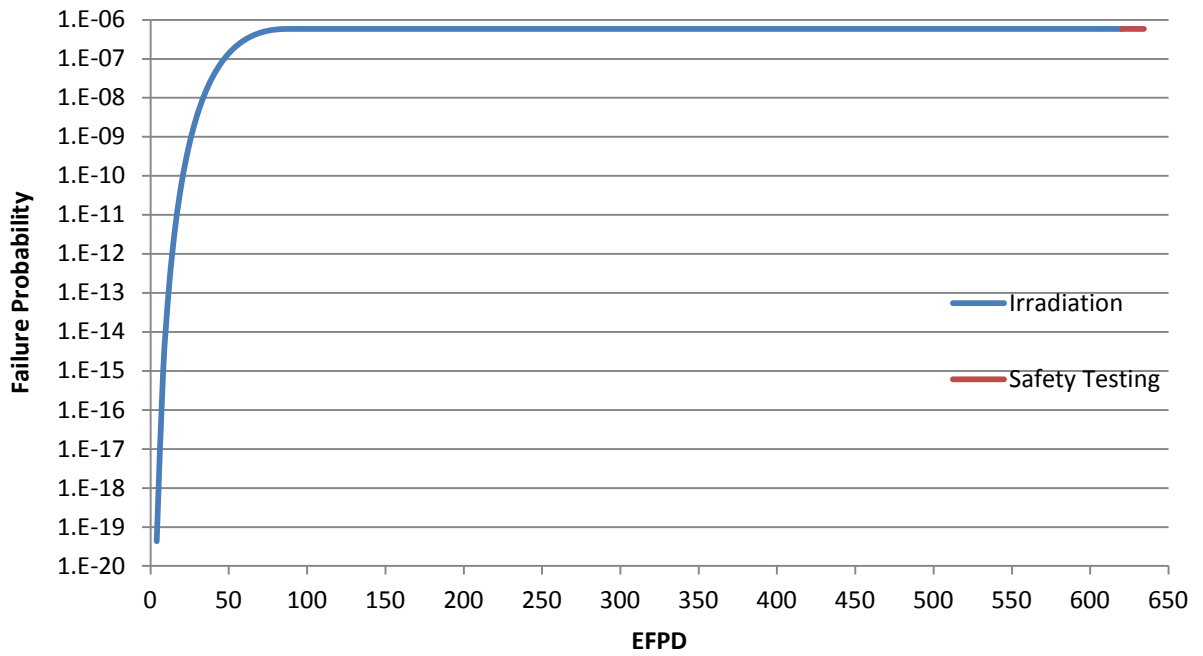
SiC failure probability - Compact 4-3-1
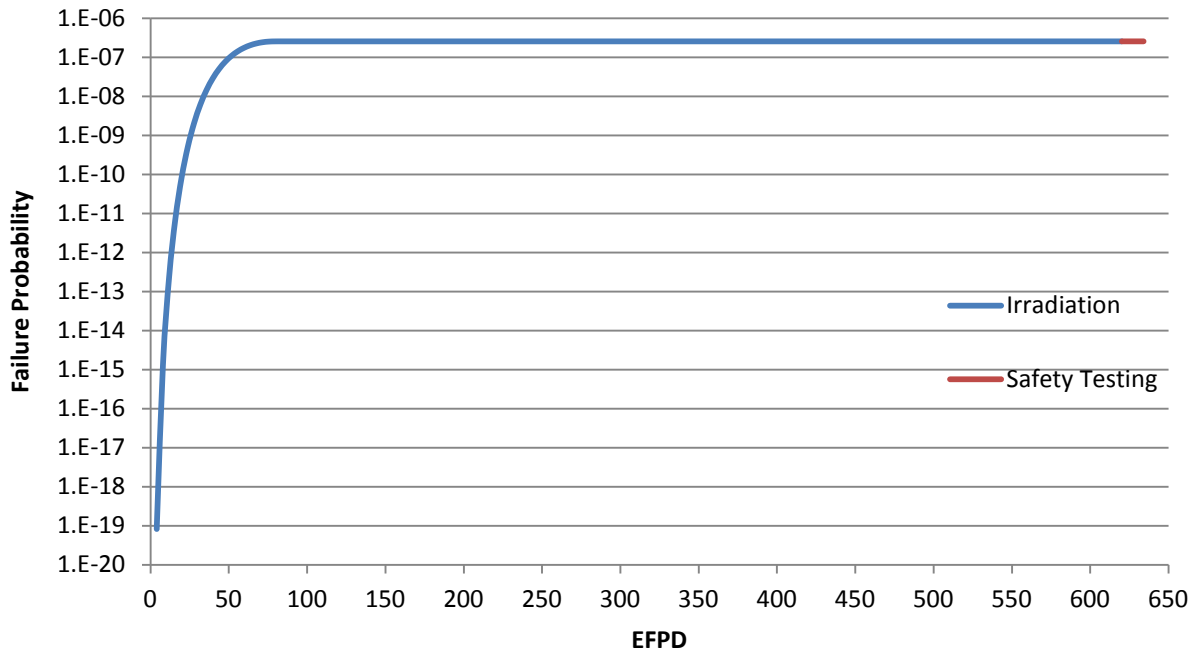
SiC failure probability - Compact 4-3-2

48
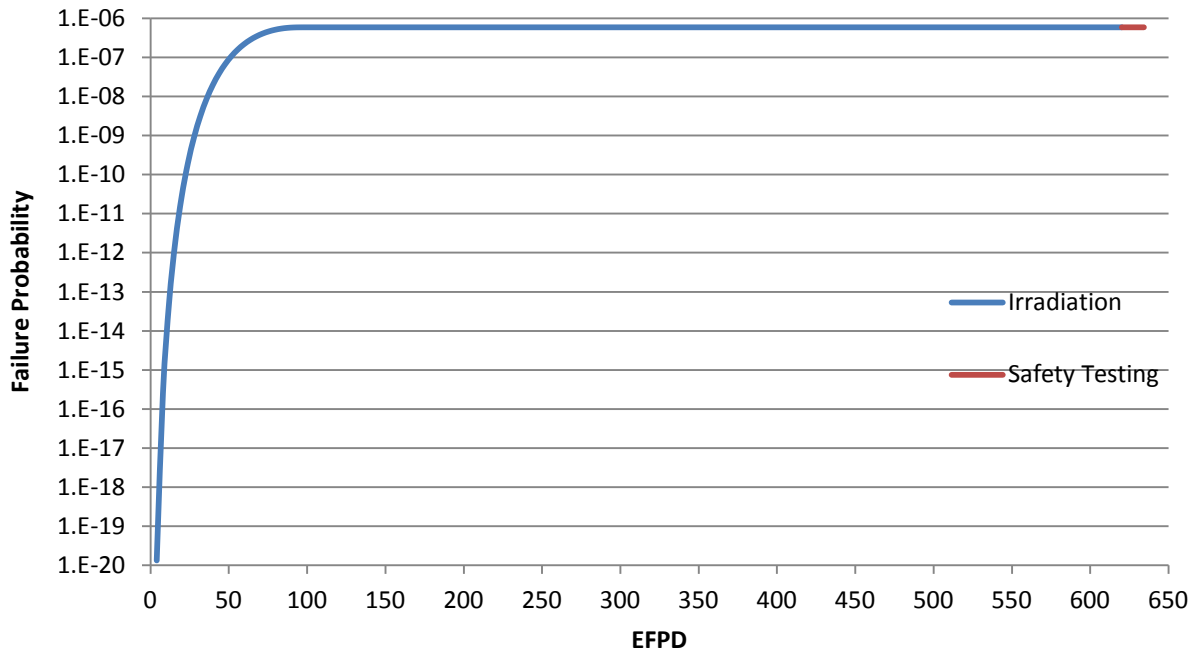
SiC failure probability - Compact 4-2-2
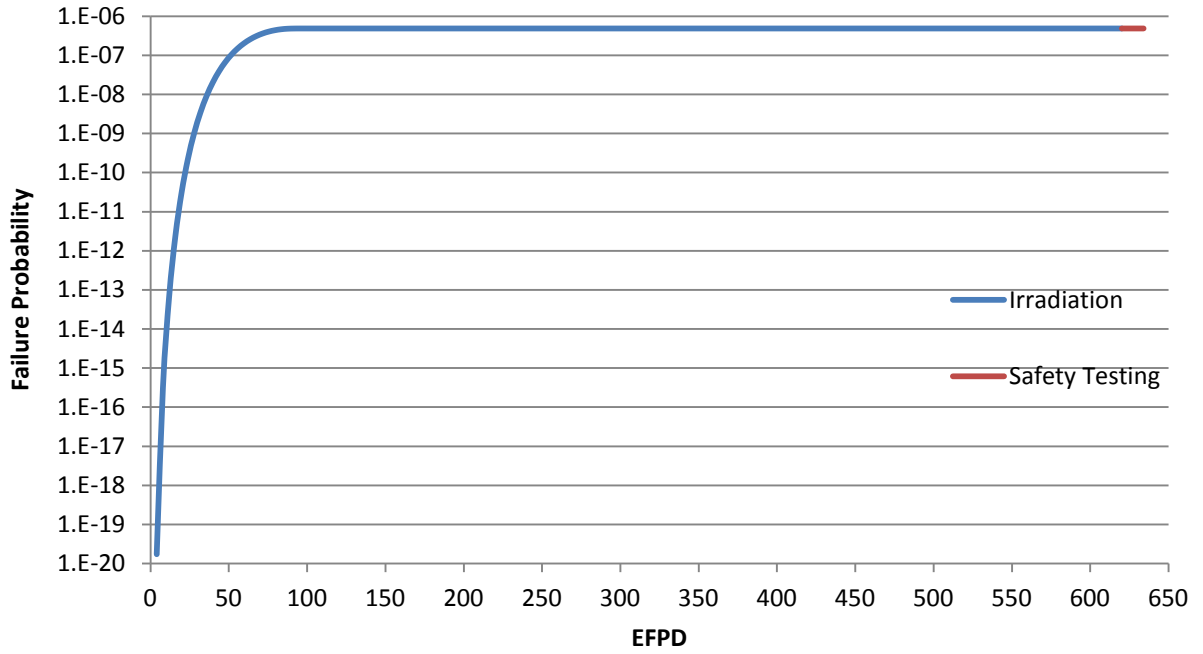
SiC failure probability - Compact 4-1-2
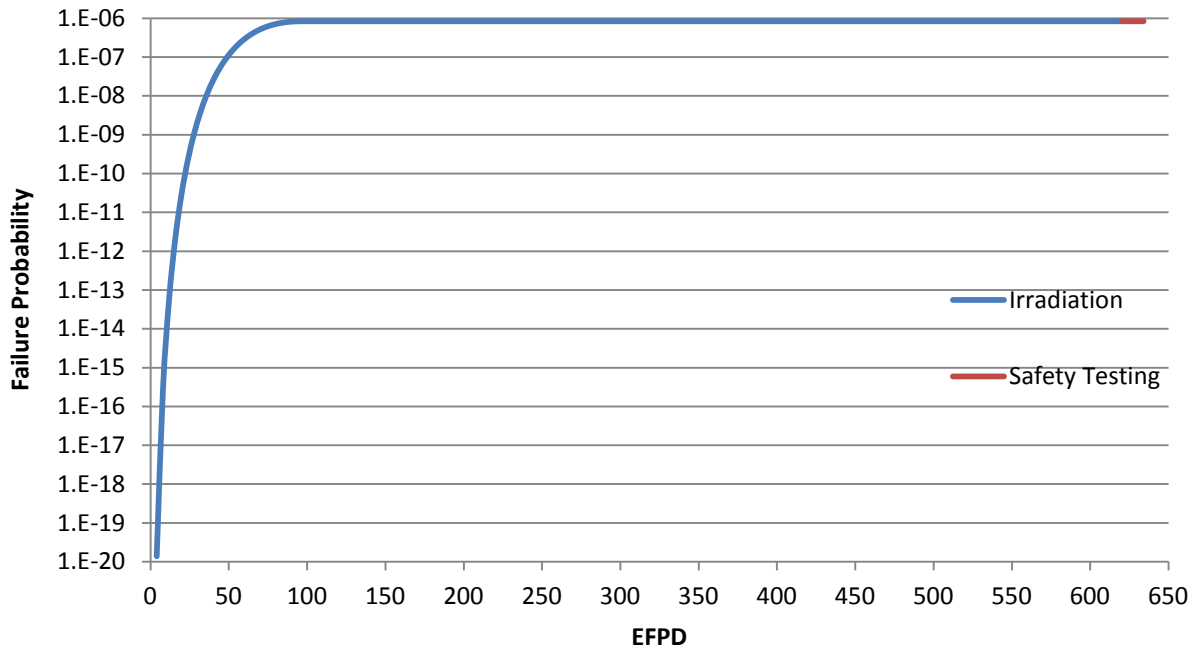
SiC failure probability - Compact 4-4-3
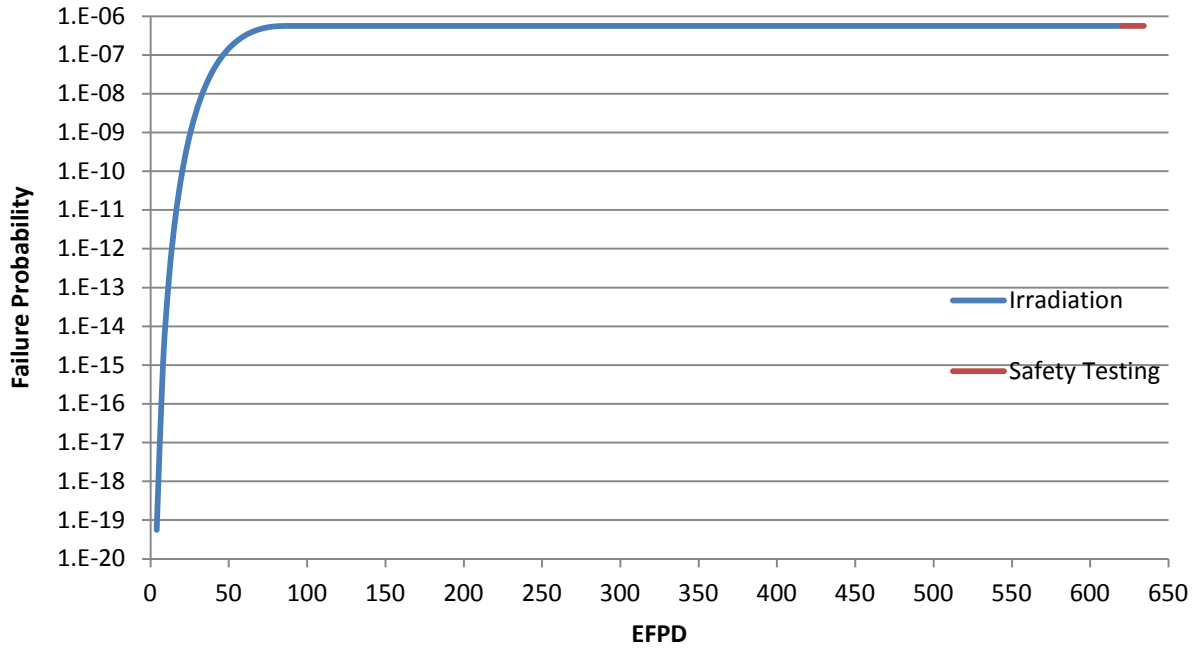
SiC failure probability - Compact 4-3-3

SiC failure probability - Compact 3-3-1

SiC failure probability - Compact 3-3-2
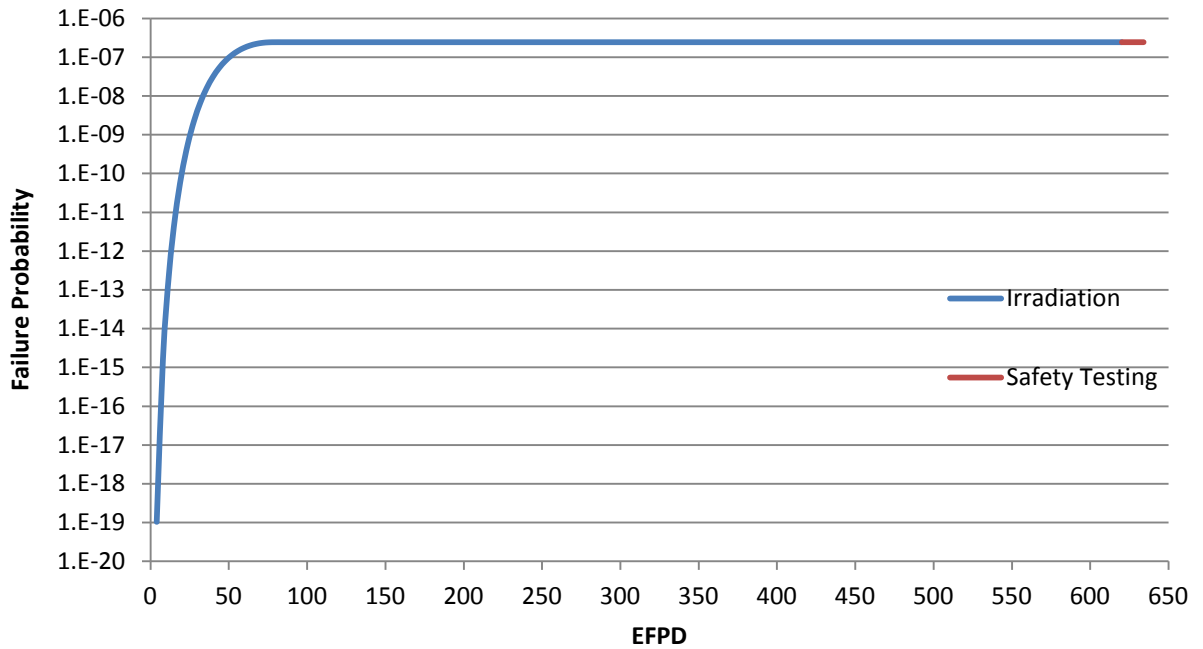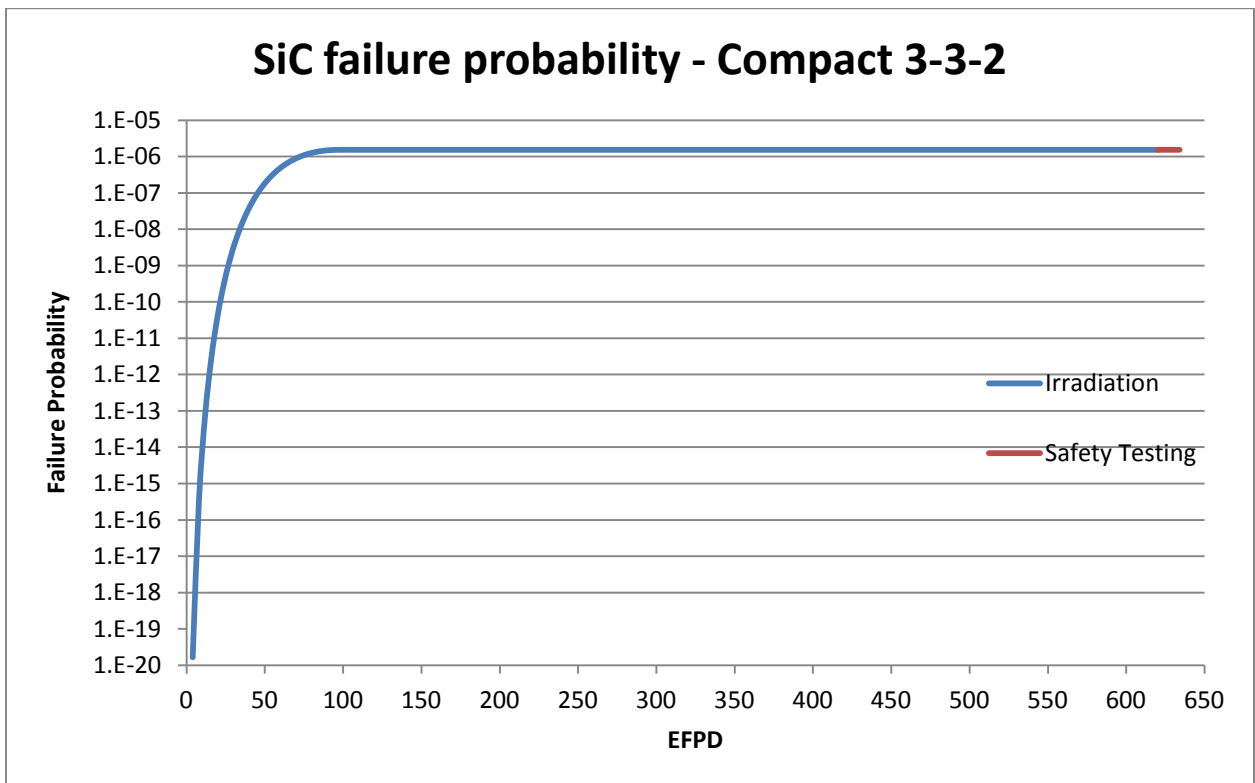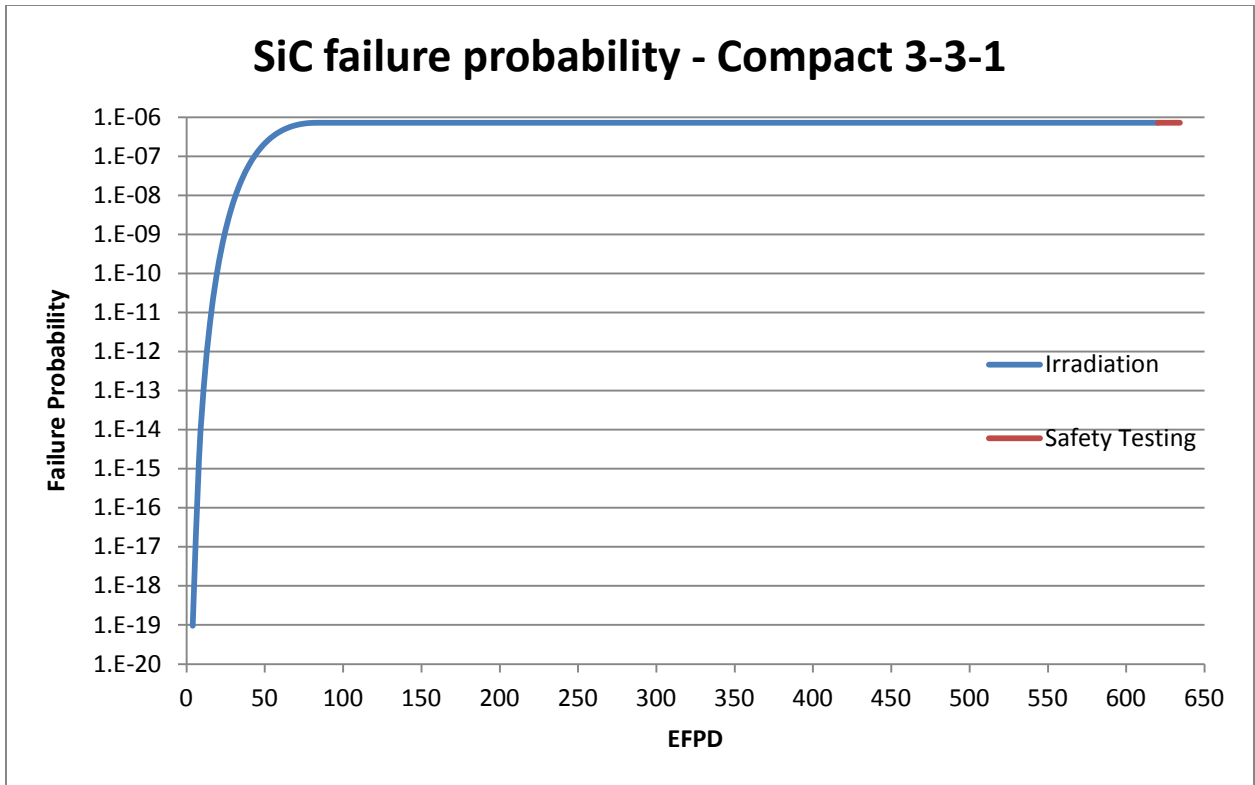
SiC failure probability - Compact 3-2-2
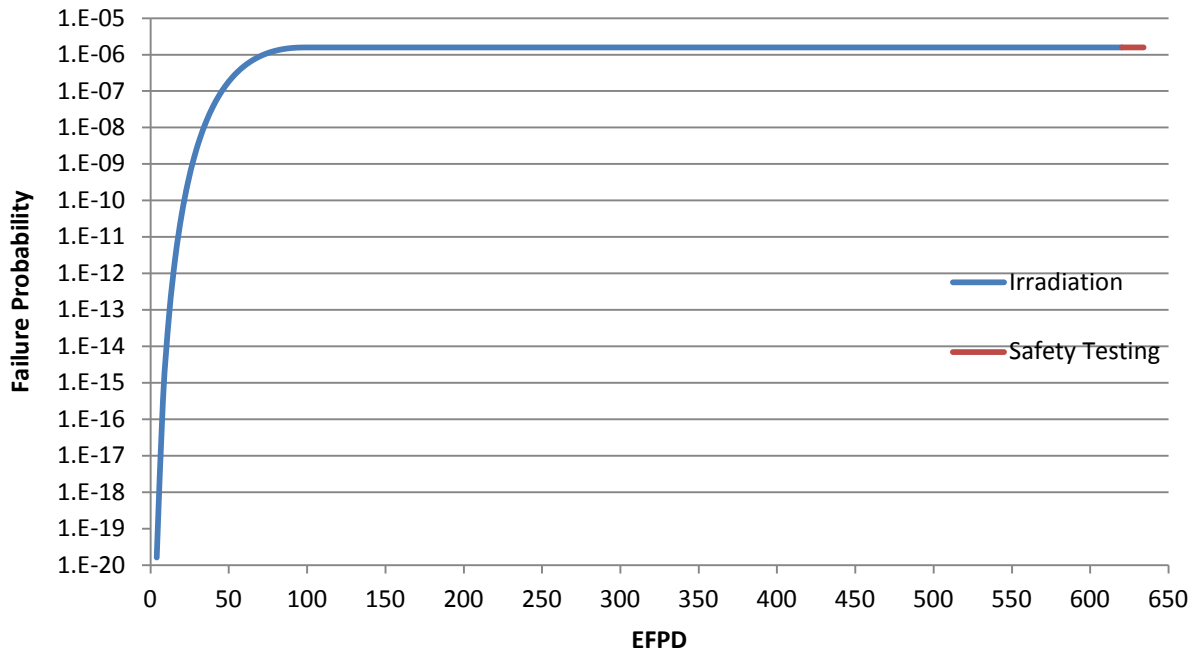
SiC failure probability - Compact 3-2-3
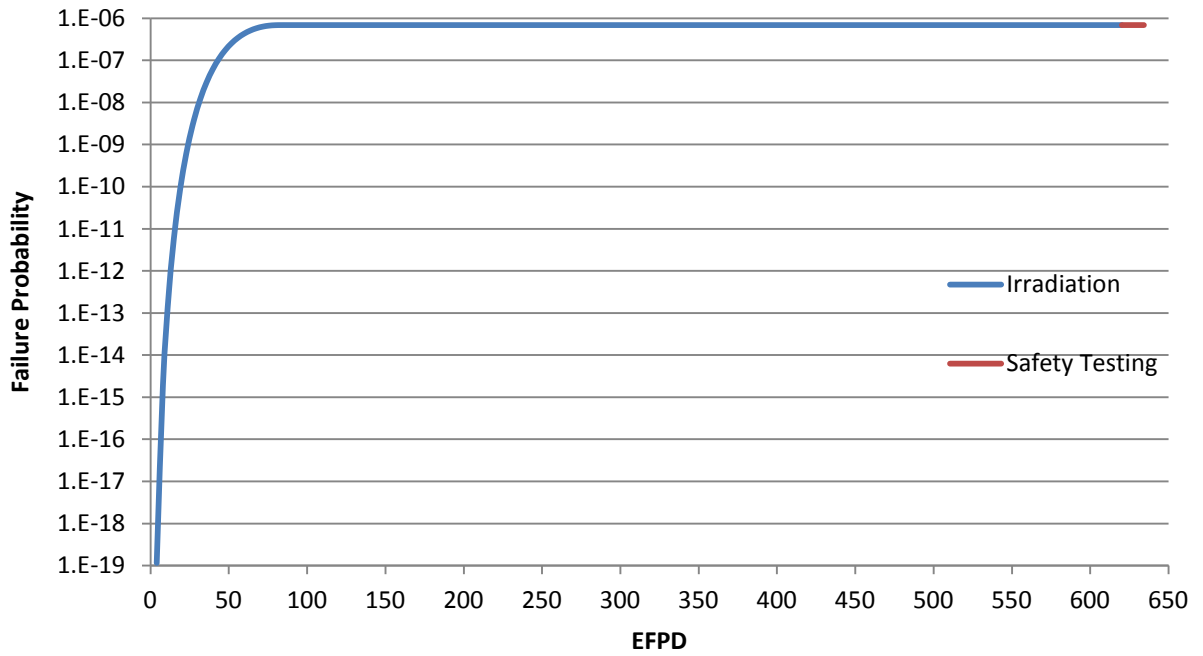
APPENDIX D – Fractional Release of the Fission Products

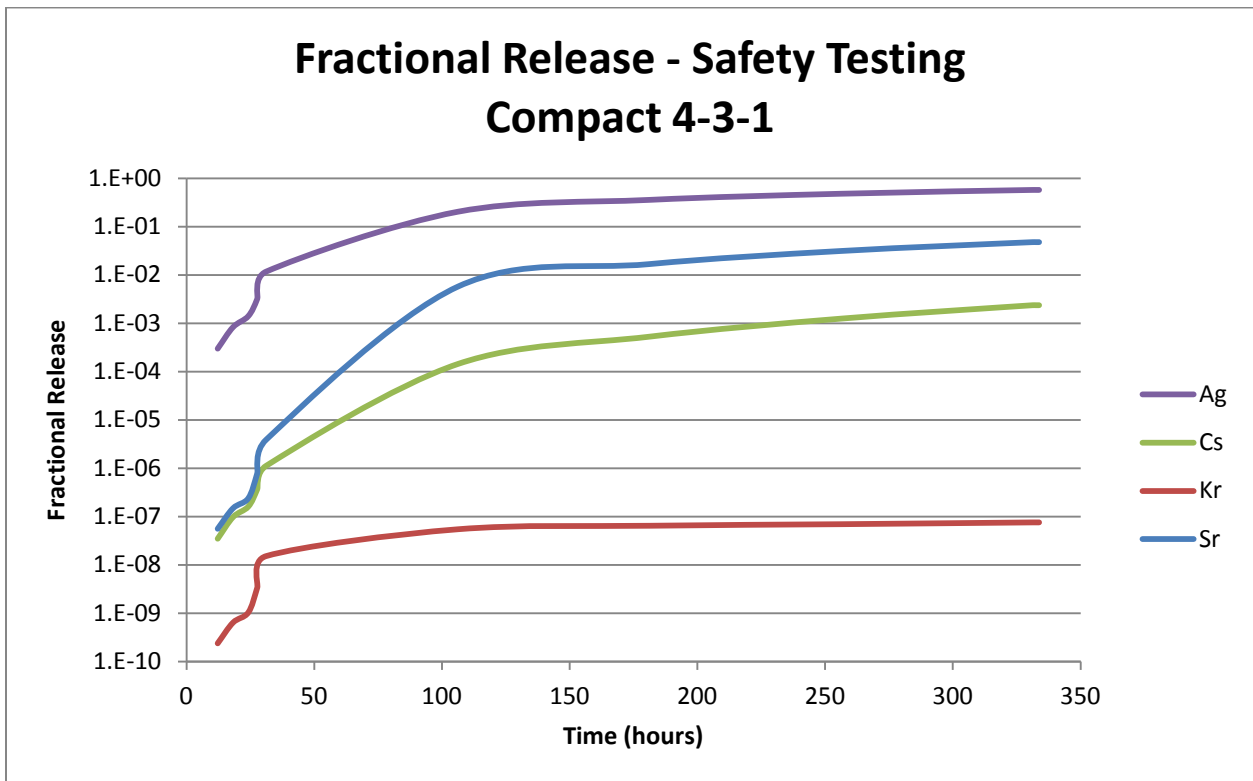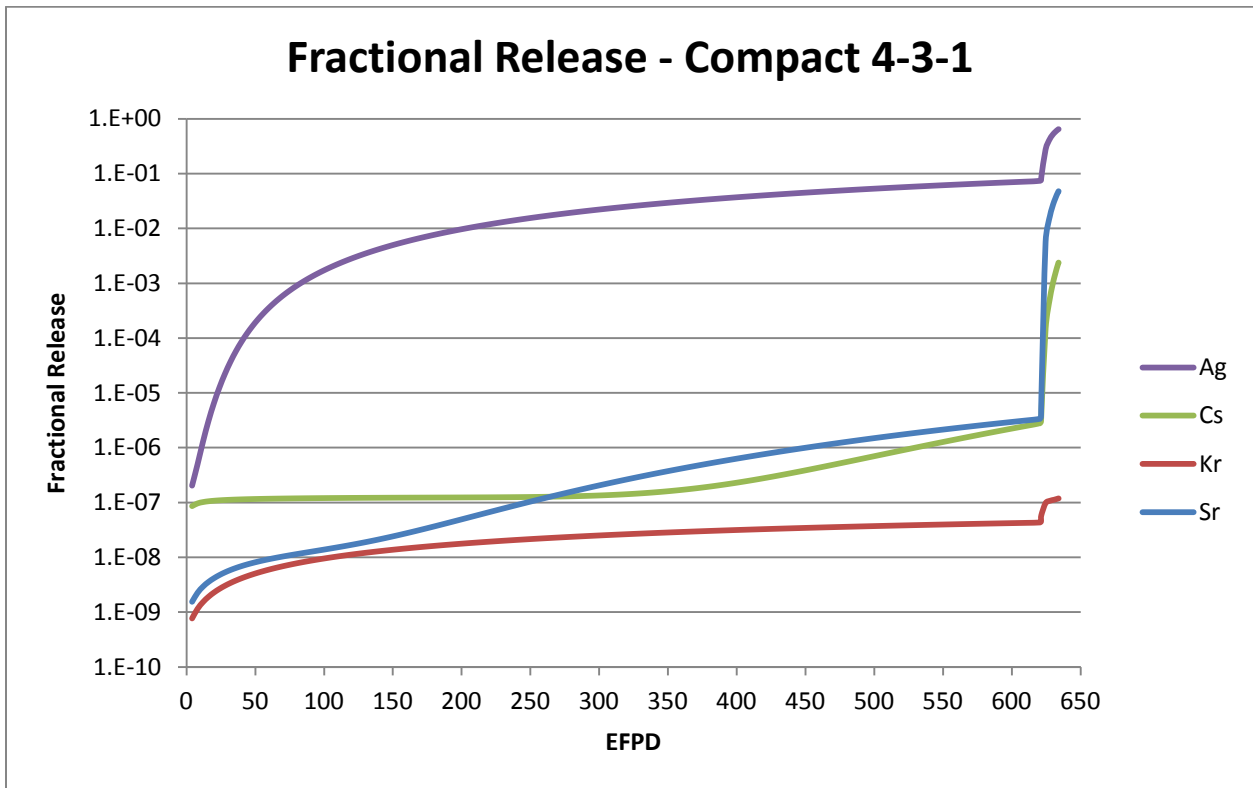Fractional Release - Compact 6-4-1

Fractional Release - Safety Testing Compact 6-4-1

Fractional Release - Compact 6-2-1

Fractional Release - Safety Testing
Compact 6-2-1
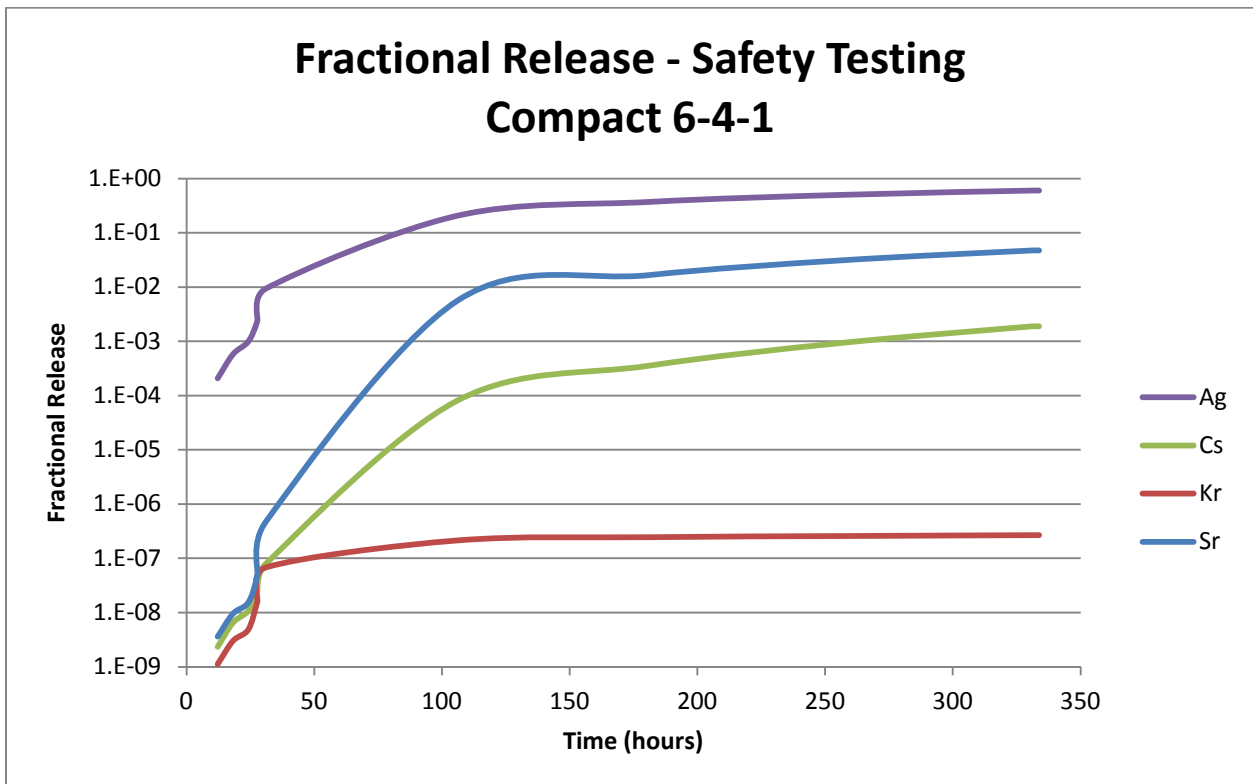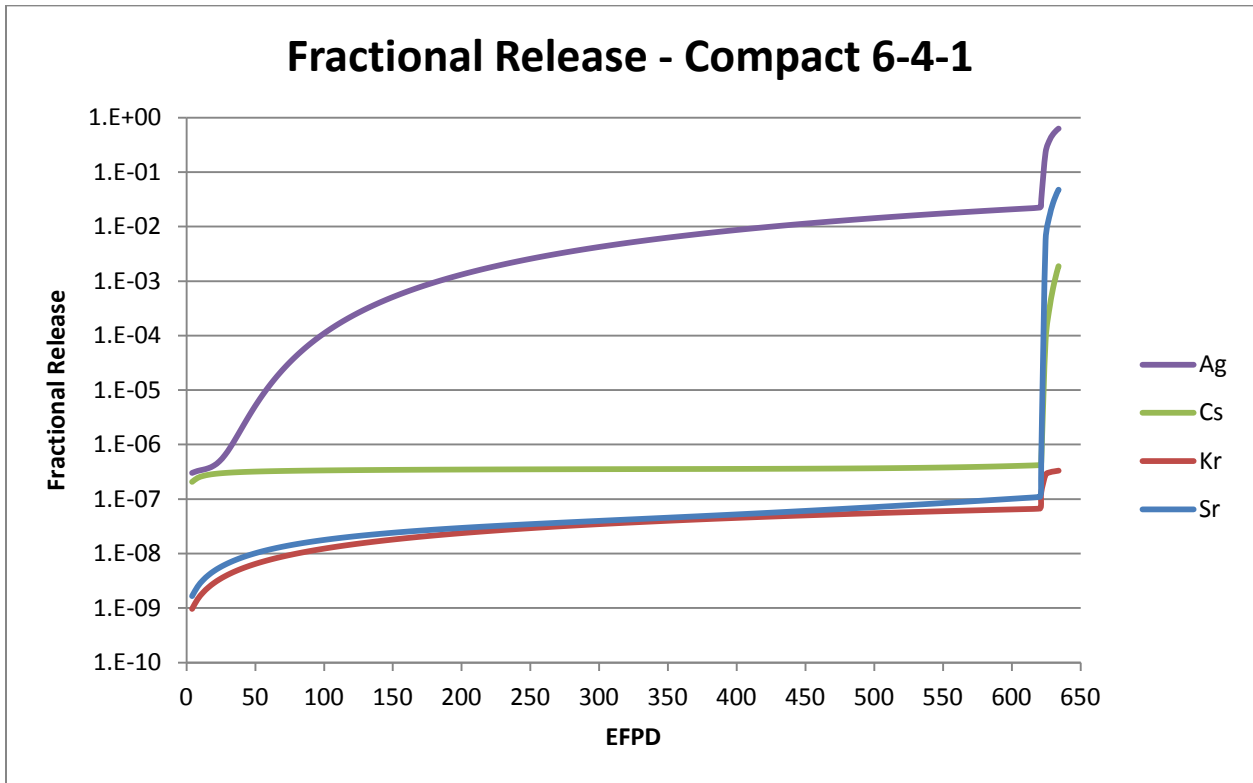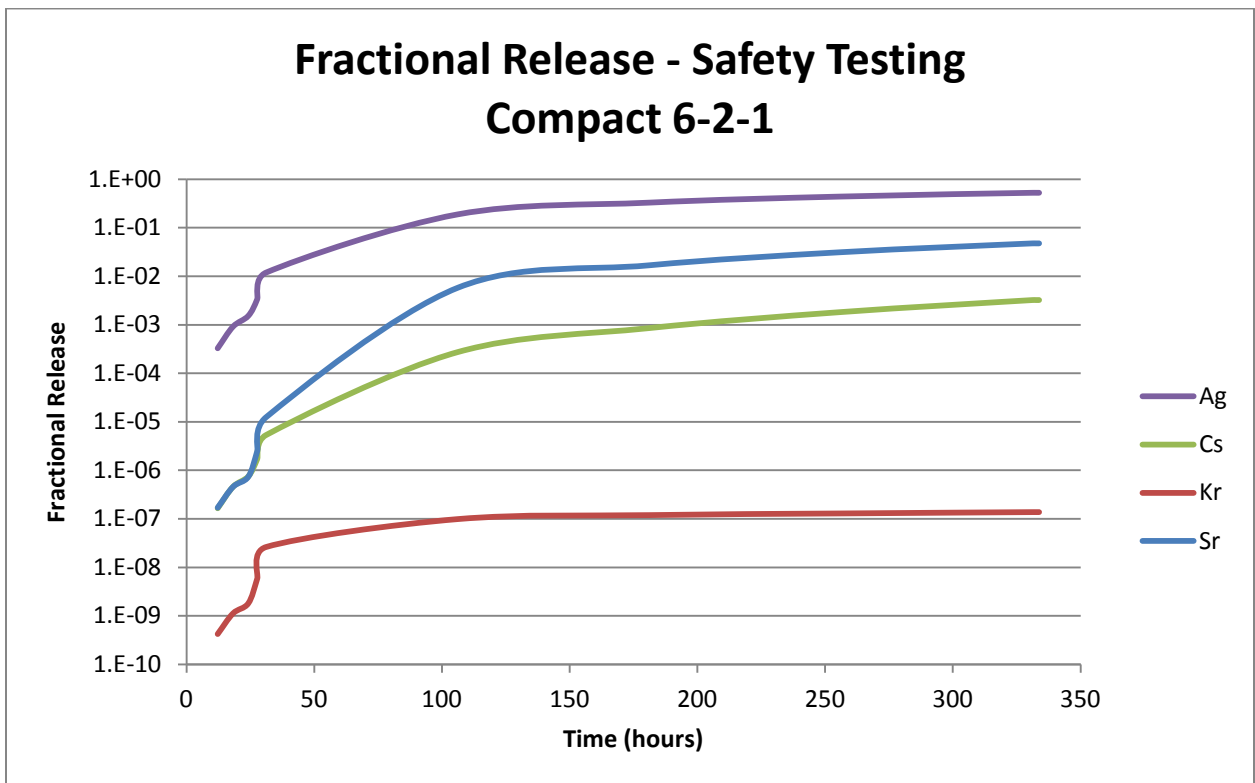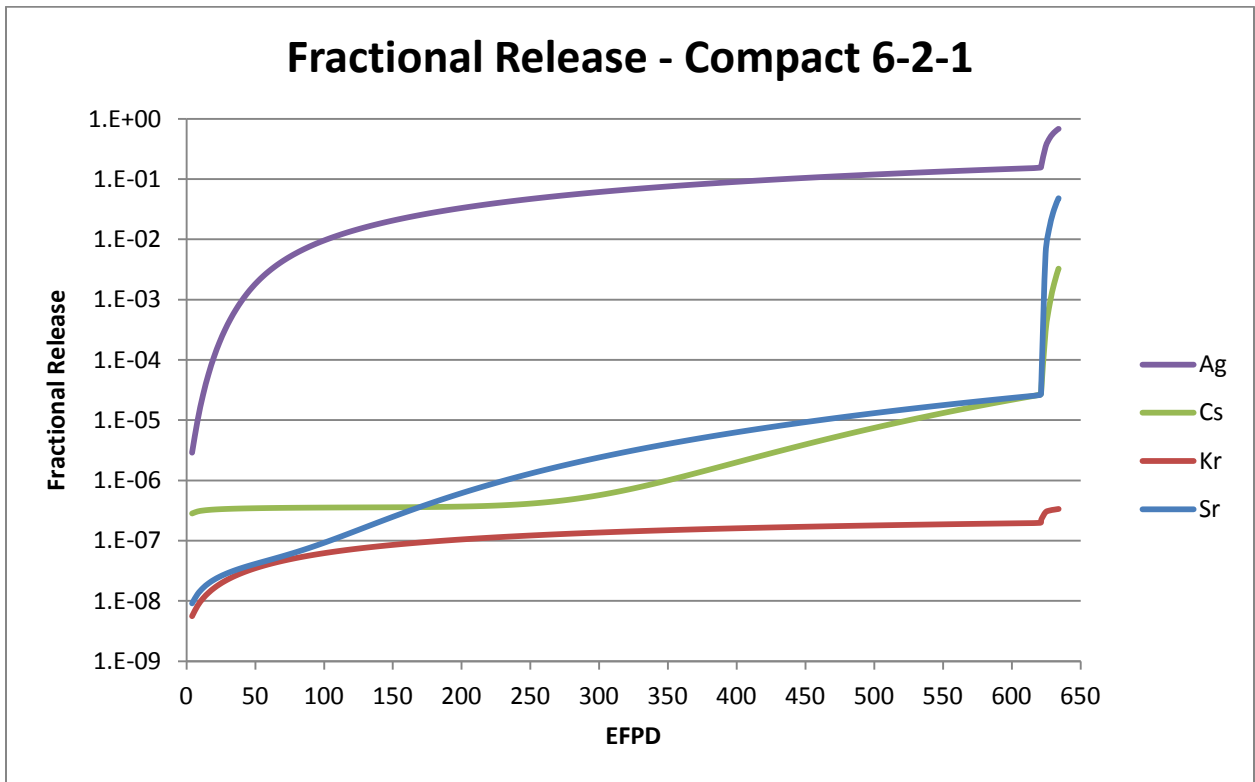
Fractional Release - Compact 6-4-3

Fractional Release - Safety Testing Compact 6-4-3

Fractional Release - Compact 6-2-3

Fractional Release - Safety Testing Compact 6-2-3

Fractional Release - Compact 5-1-1

Fractional Release - Safety Testing Compact 5-1-1

Fractional Release - Compact 5-3-3
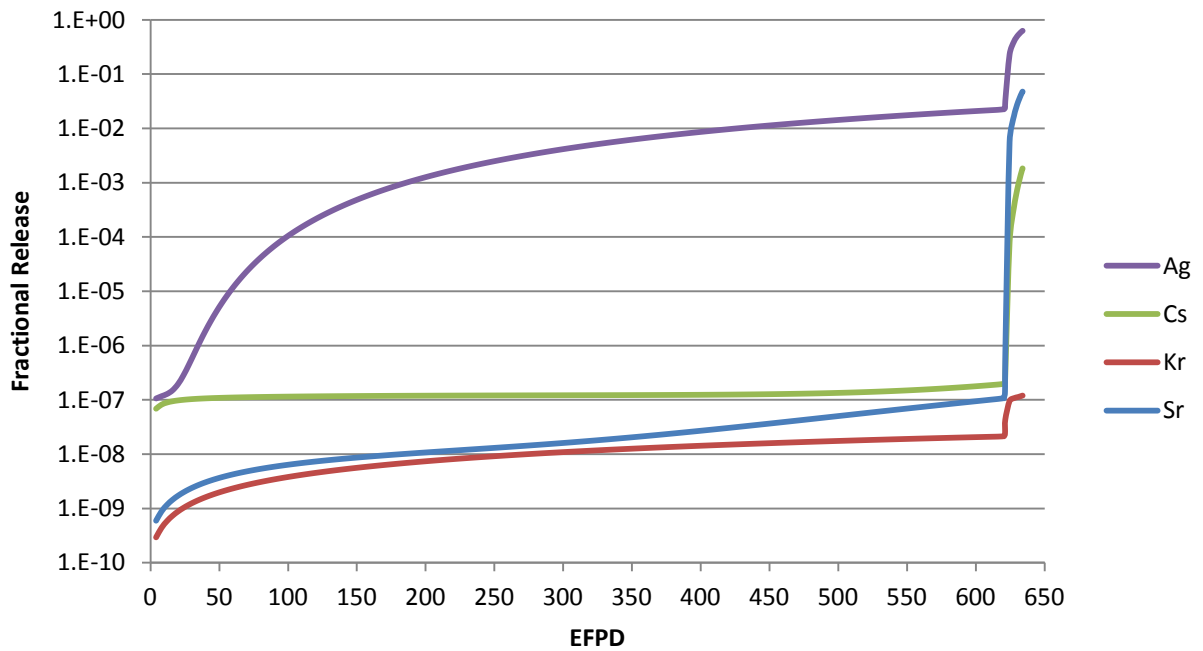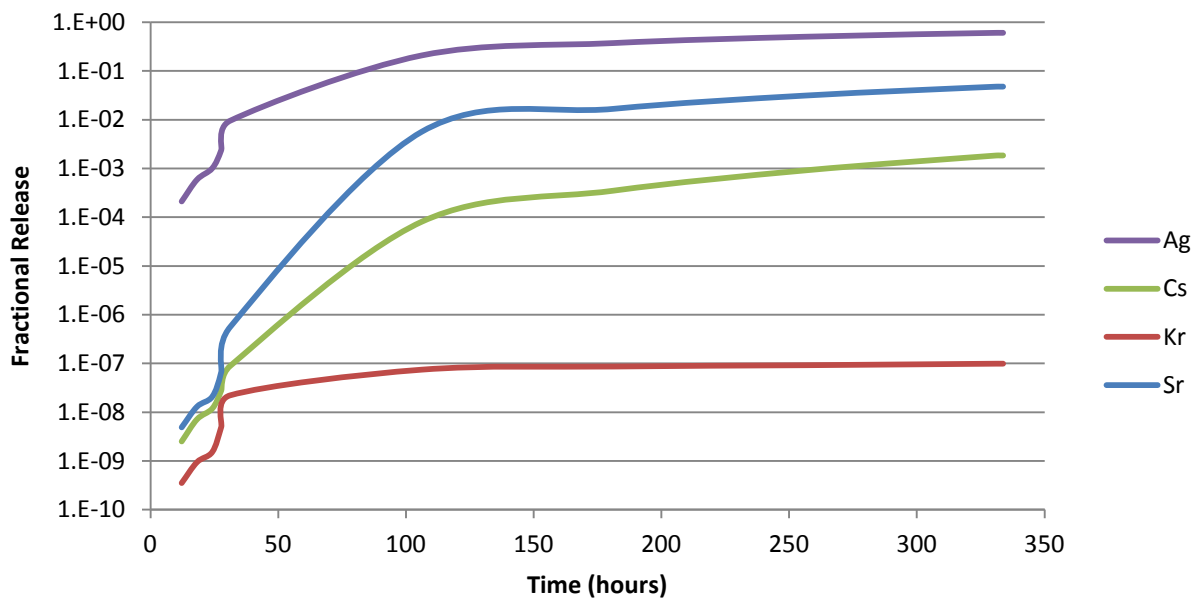

Fractional Release - Safety Testing Compact 5-3-3

Fractional Release - Compact 5-1-3

Fractional Release - Safety Testing Compact 5-1-3

Fractional Release - Compact 4-4-1

Fractional Release - Safety Testing Compact 4-4-1

Fractional Release - Compact 4-3-1

Fractional Release - Safety Testing Compact 4-3-1

Fractional Release - Compact 4-3-2

Fractional Release - Safety Testing Compact 4-3-2

Fractional Release - Compact 4-2-2

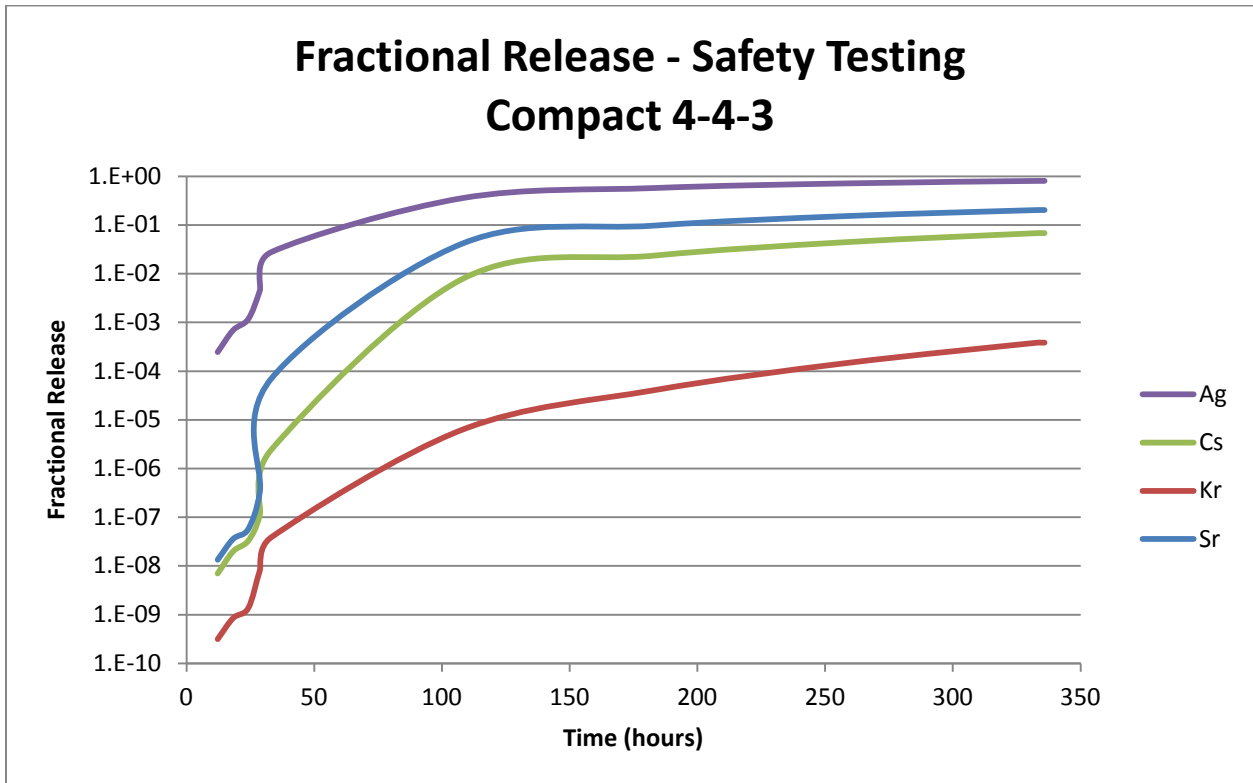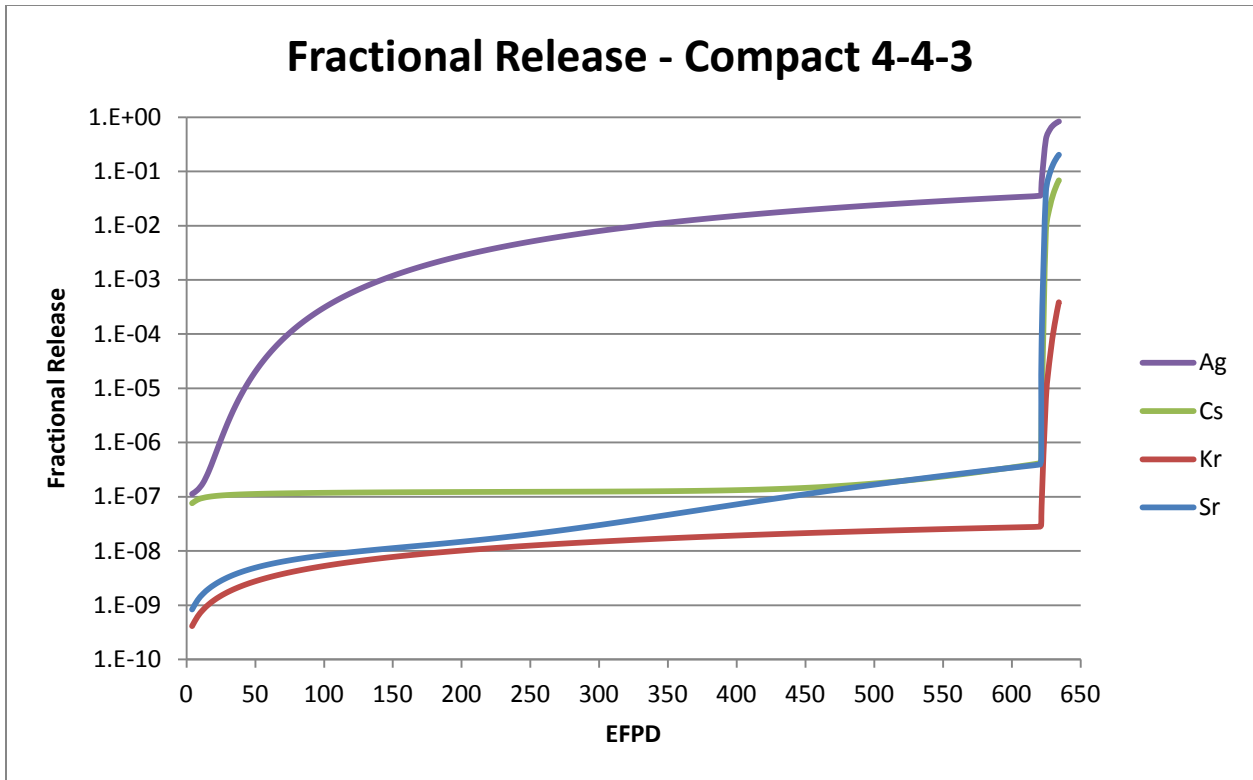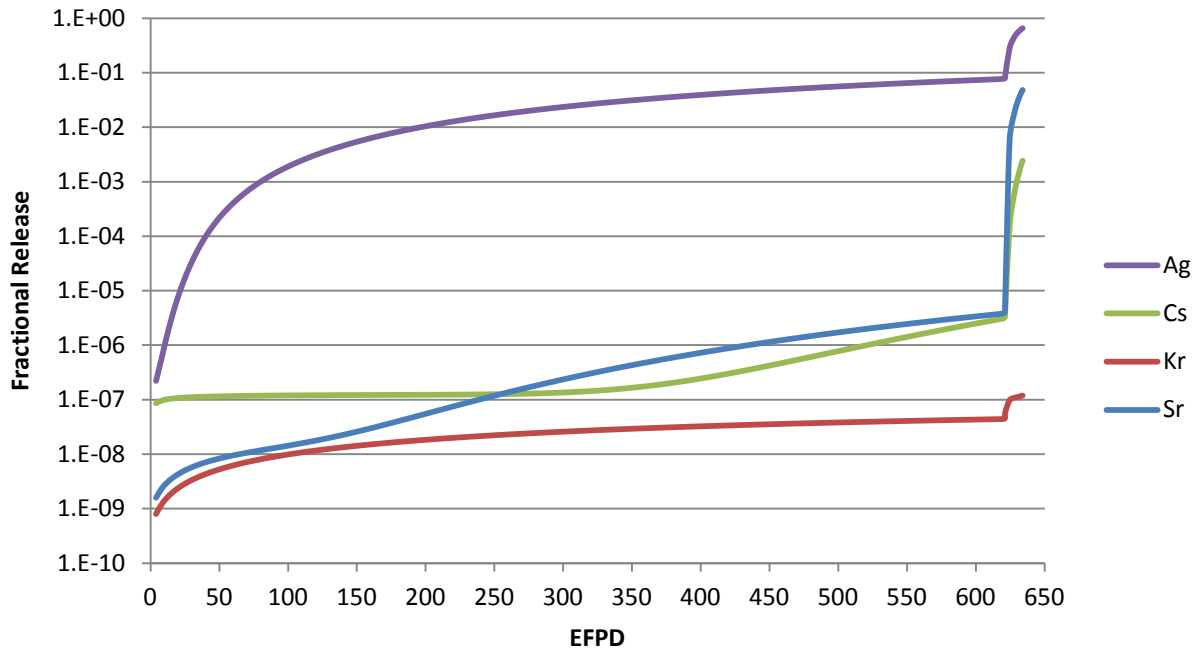**Fractional Release - Safety Testing Compact 4-2-2**

Fractional Release - Compact 4-1-2

Fractional Release - Safety Testing Compact 4-1-2

Fractional Release - Compact 4-4-3

Fractional Release - Safety Testing Compact 4-4-3

Fractional Release - Compact 4-3-3

Fractional Release - Safety Testing Compact 4-3-3

Fractional Release - Compact 3-3-1

Fractional Release - Safety Testing
Compact 3-3-1

Fractional Release - Compact 3-3-2

Fractional Release - Safety Testing
Compact 3-3-2
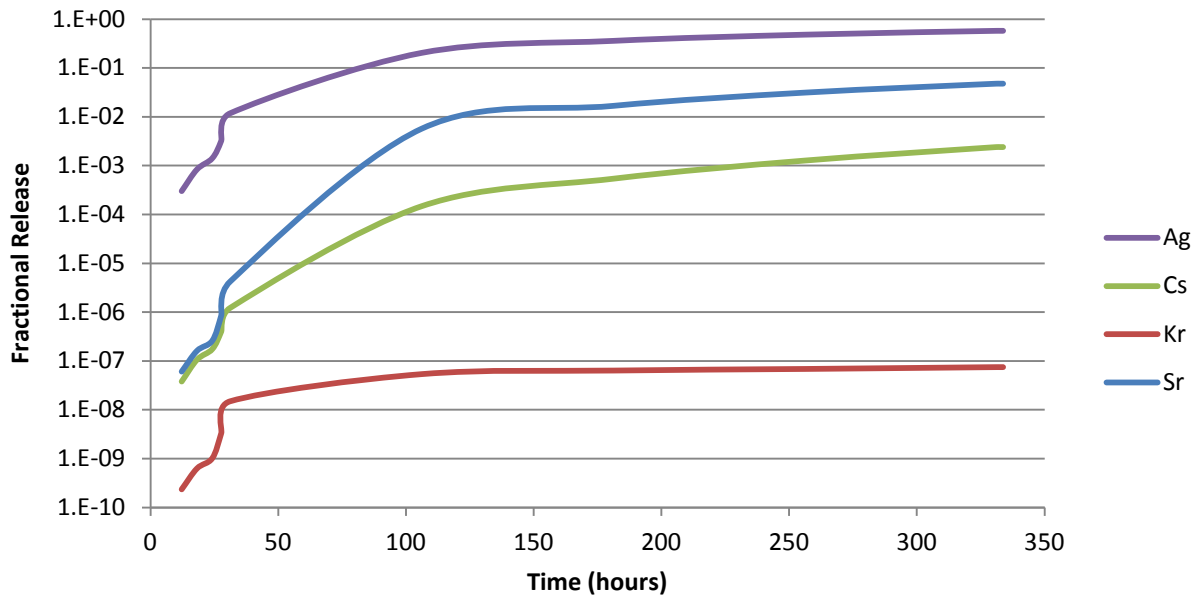
Fractional Release - Compact 3-2-2
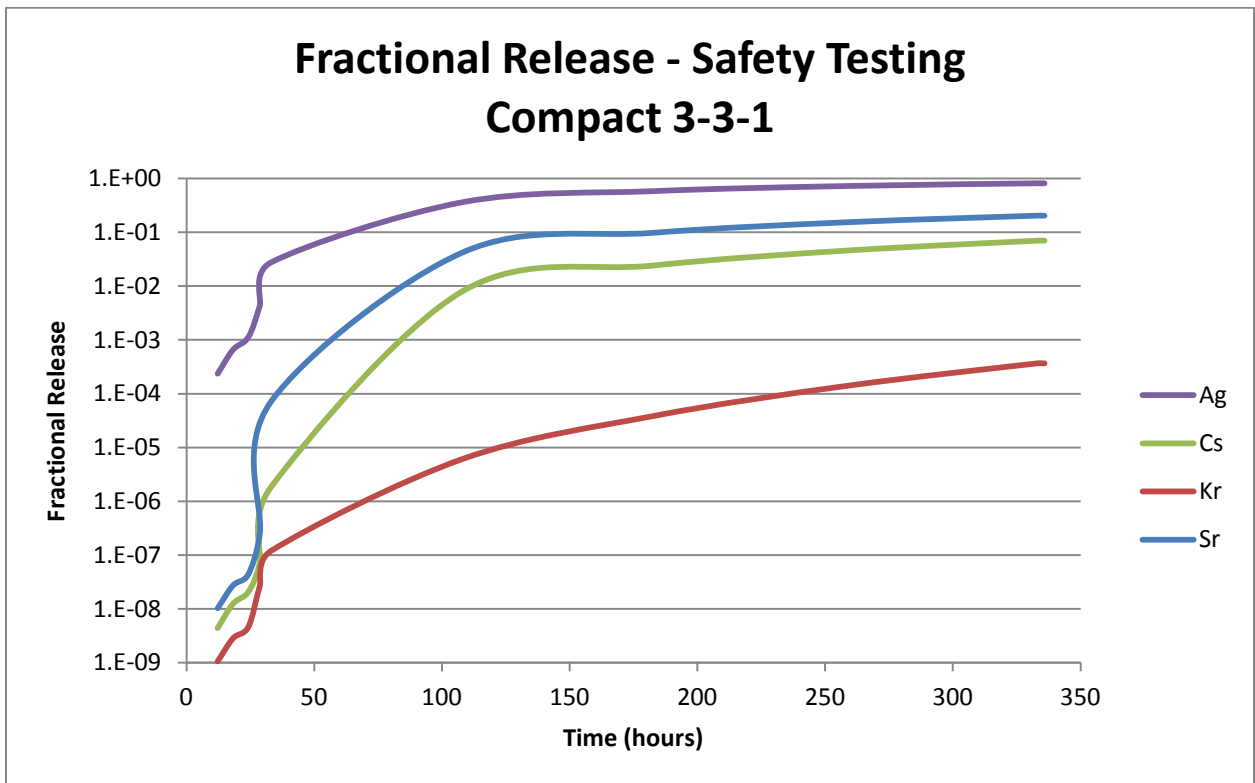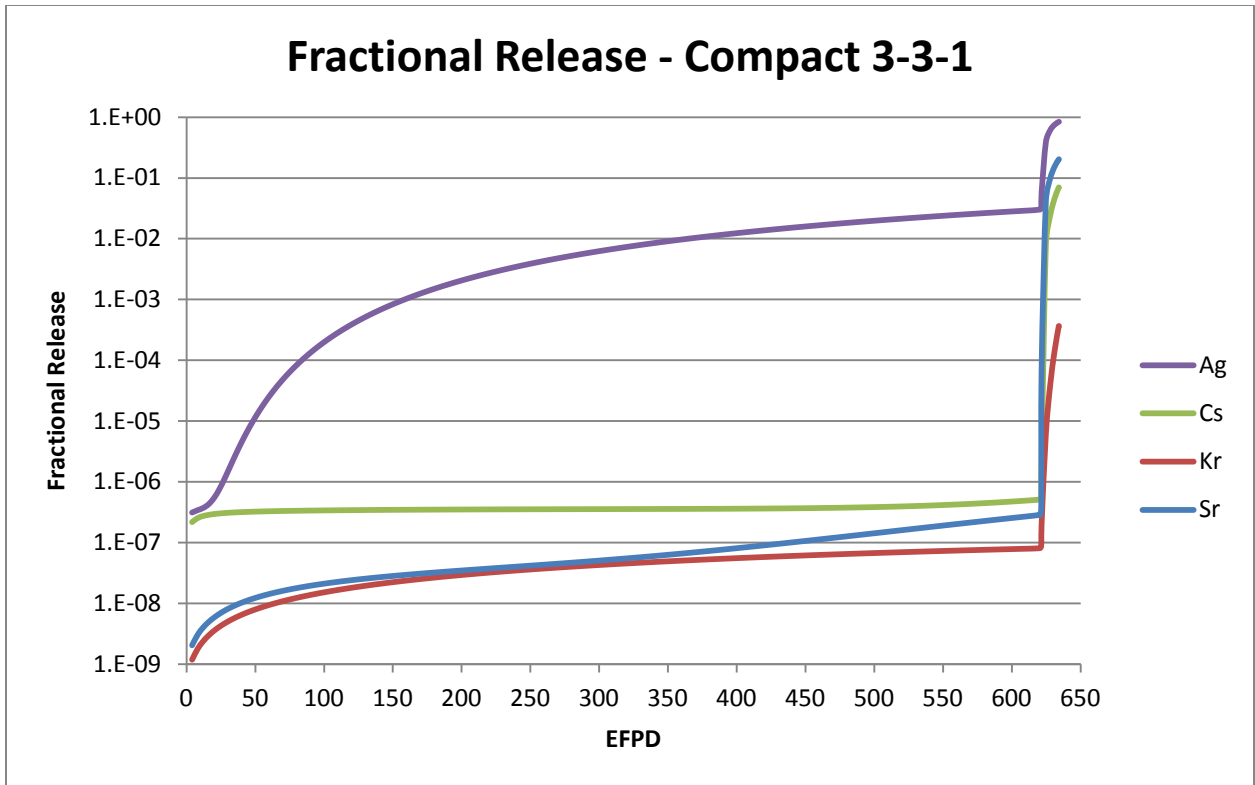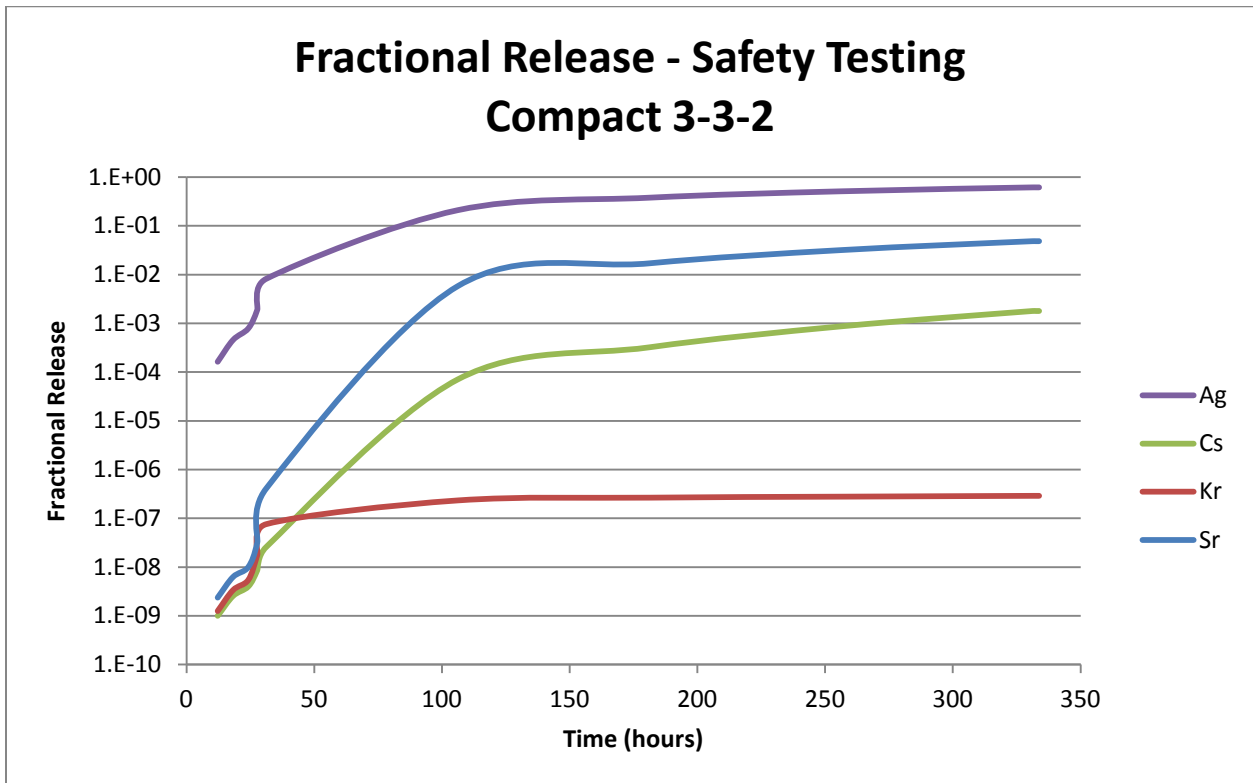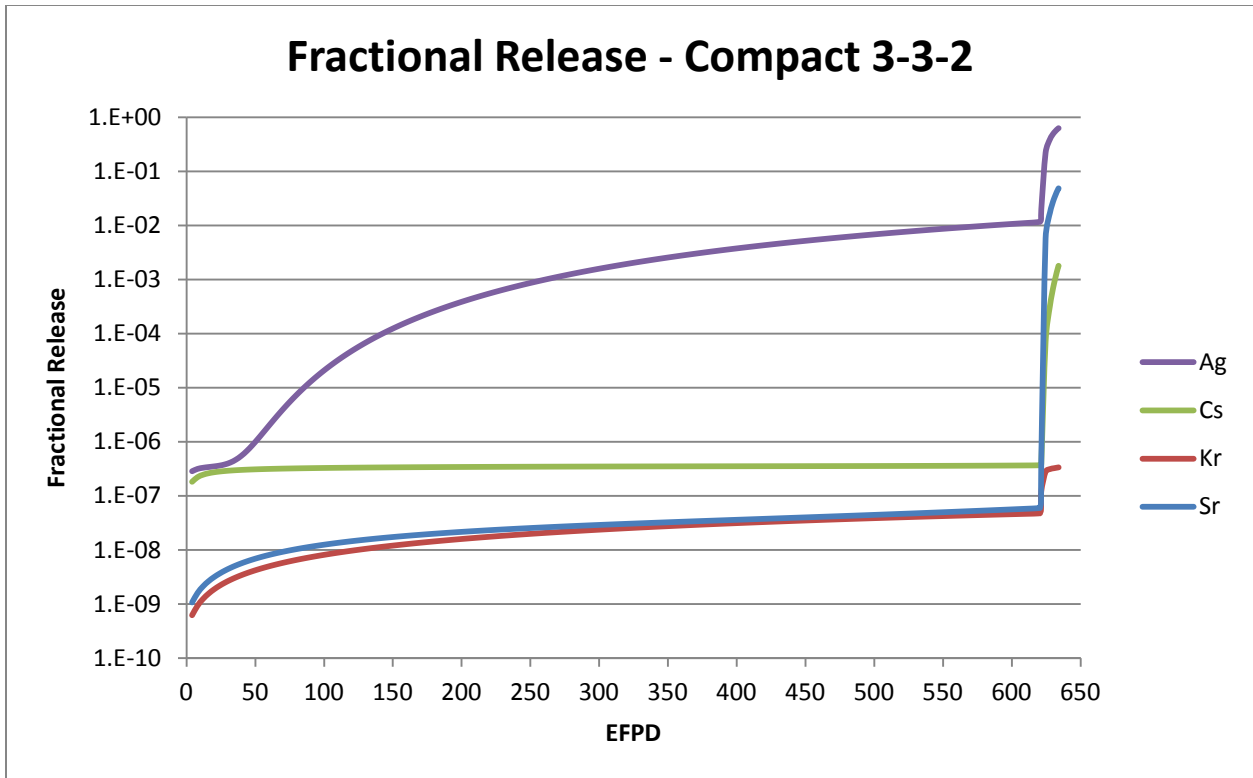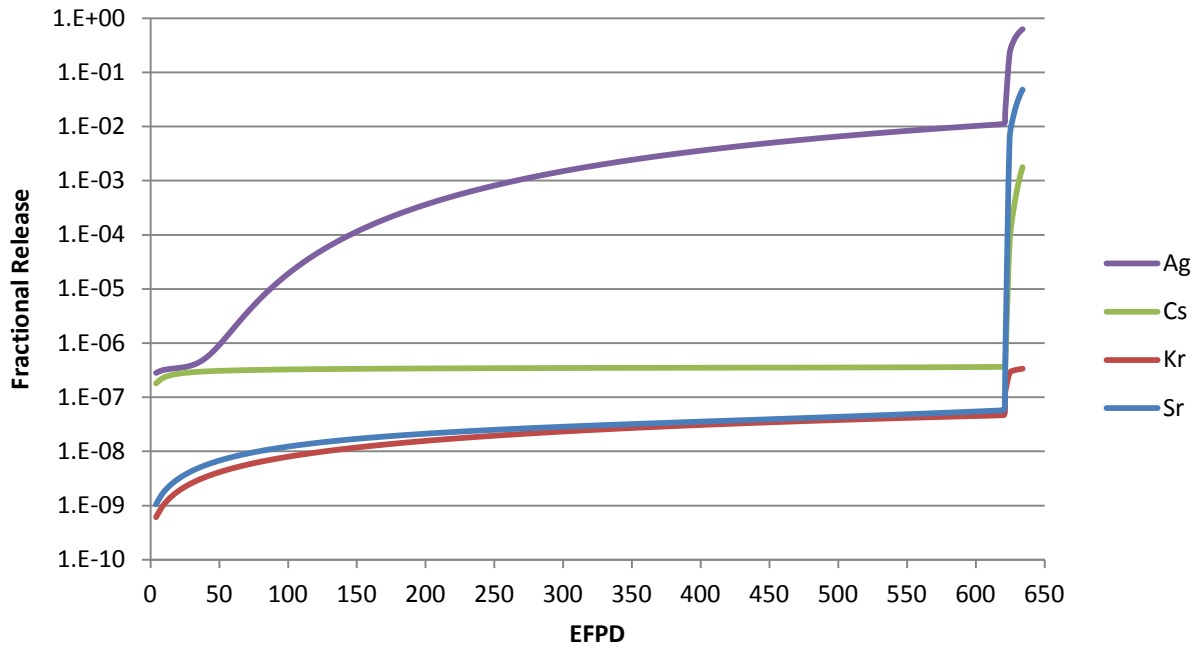

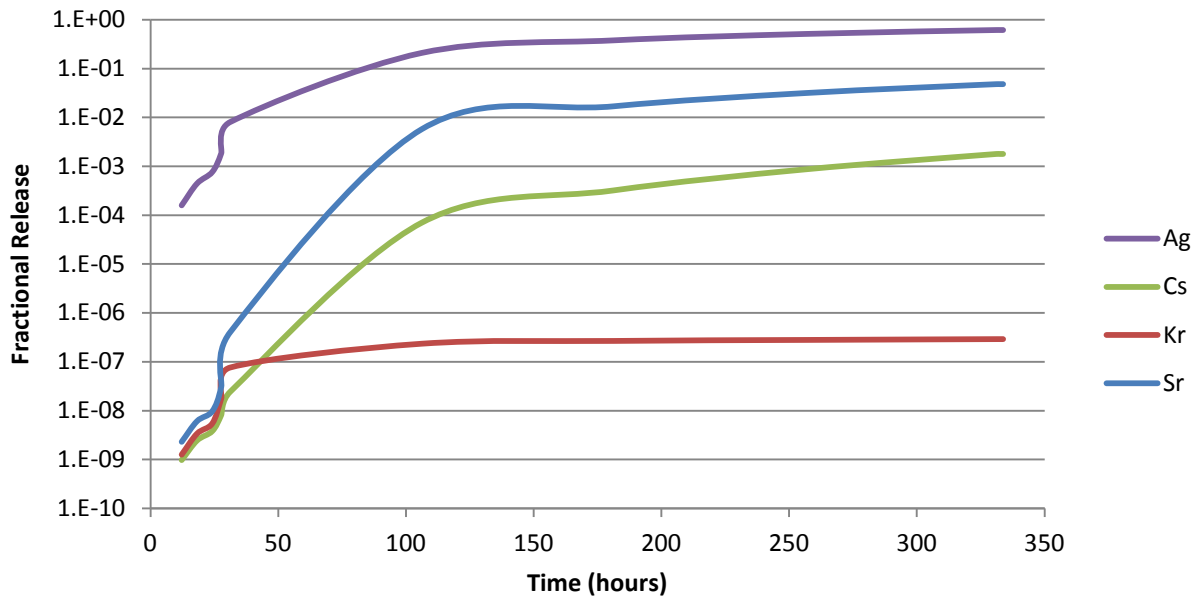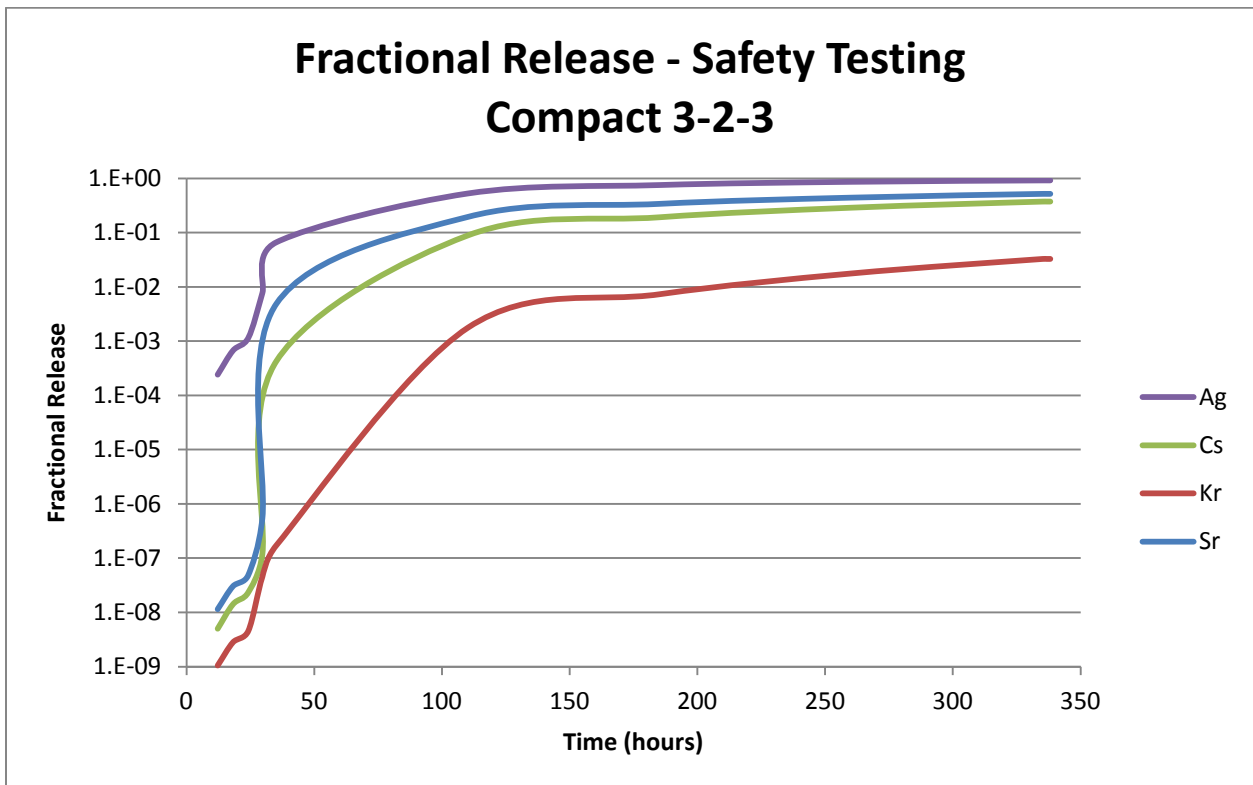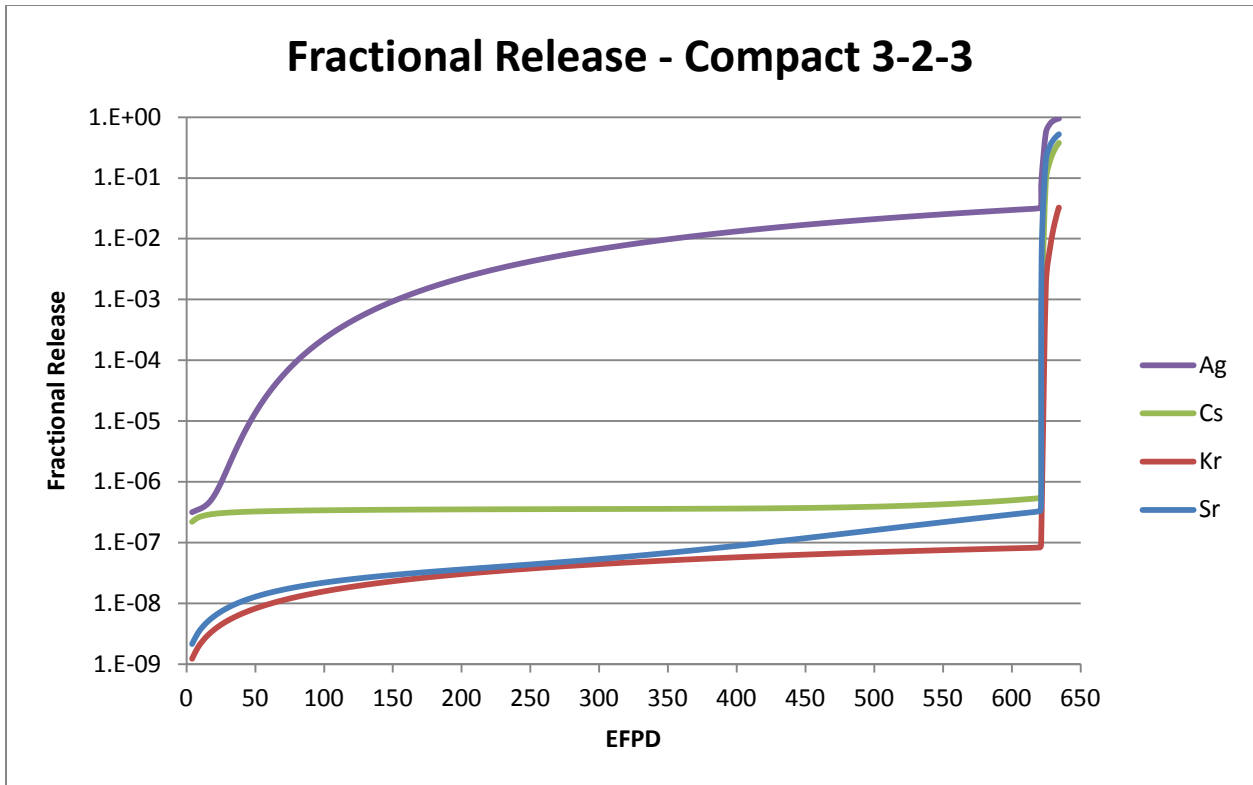Fractional Release - Safety Testing Compact 3-2-2

Fractional Release - Compact 3-2-3

Fractional Release - Safety Testing
Compact 3-2-3

APPENDIX E – PARFUME Input Deck

Highlighted values are specific to each fuel type (Baseline, Variant 1, and Variant 3).
Italic values are specific to each compact.
Italic Bold values are specific to the irradiation phase.
Bold values are specific to the safety testing phase.

NB: Card 201001 (fpspecie) is used for diffusion calculation with the Monte Carlo calculation scheme (pfss=0).

```
************** GENERAL OPTIONS (SOLVERS/MODELS) **************
*
* CARD 100001 (simulation name)
*
* title
*
100001        'AGR-1 Safety Test Predictions - Compact 6-4-1'
* Compact 6-4-1 -> Baseline @ 1873 K
*
* CARD 101001 (run parameters)
*
* pfss ncases nburp sample dtf iseed
*
101001        2 0 1000 1 0 305
*101001       0 10000 1000 1 0 305
*
* CARD 101002 (models)
*
* idebondp ifacet rbvalue comodel fgmodel idebug
*
101002        0 1 2 1 2 0
*
*
******************** MATERIAL PROPERTIES ********************
*
* CARD 102001 (fuel characteristics)
*
* u235enr(%) ourat curat
*
102001        19.736 1.3613 0.3253
*
* CARD 103001 (kernel properties)
*
* kernd(g/cm^3) kernt(g/cm^3)
*
103001        10.924 11.64
*
* CARD 103002 (buffer properties)
*
* buffd(g/cm^3) bufft(g/cm^3)
*
103002        1.10 2.25
*
*
```

* CARD 103003 (IPyC properties)
*
* ipycdn(g/cm^3) ipycdvar(g/cm^3)
*
103003   1.904 0.
*
* CARD 103005 (OPyC properties)
*
* opycdn(g/cm^3) opycdvar(g/cm^3)
*
103005   1.907 0.
*
* CARD 103013 (IPyC Bacon anisotropic factor)
*
* ibafn ibafvar
*
103013   1.033 0.
*
* CARD 103015 (OPyC Bacon anisotropic factor)
*
* obafn obafvar
*
103015   1.033 0.
*
*
******************* FUEL PARTICLE GEOMETRY *******************
*
* CARD 104001 (kernel geometry)
*
* kerndia(e-6 m) kernvar(e-6 m)
*
104001   349.7 9.0
*
* CARD 104002 (buffer geometry)
*
* buffthk(e-6 m) buffvar(e-6 m)
*
104002   103.5 8.2
*
* CARD 104003 (IPyC geometry)
*
* ipycthk(e-6 m) ipycvar(e-6 m)
*
104003   39.4 2.3
*
* CARD 104004 (SiC geometry)
*
* sicthk(e-6 m) sicvar(e-6 m)
*
104004   35.3 1.3
*
* CARD 104005 (OPyC geometry)
*
* opycthk(e-6 m) opycvar(e-6 m)
*
104005   41.0 2.1

******************* FUEL ELEMENT DESCRIPTION *******************
*
* CARD 105001
*
105001 ATRCYLNDR
*
* CARD 105011
*
* partnum(particles/compact) ngnfm ngn
*
105011   4154. 17 20
*
* CARD 105021
*
* fuedia(m) fuecldtk(m)
*
105021   0.01236 0.000001
*
* CARD 105031
*
* fmden(g/cm^3)
*
105031   1.297
*
* CARD 105041
*
* ucontam
*
105041   3.64E-7
*
*
******************* FUEL ELEMENT ENVIRONMENT *******************
*
* CARD 106001 (fuel temperature option)
*
* rtmpopt
*
106001   VOLAVGTMP
*
* CARD 201001 (fission product transport description)
*
* fpspecie
*
*201001 Ag
*201001 Cs
*201001 Kr
*201001 Sr
*
* CARD SERIES 301XXX (fluence v- time input)
*
* timeirr(days) flu(e25 n/m^2)
*
301001   0.   0.
301002   620.2   *2.43*
301003   620.2001   *2.43001*
301004   620.3285   *2.43002*

73

```
301005      620.4118    2.43003
301006      620.7069    2.43004
301007      621.2069    2.43005
301008      621.4986    2.43006
301009      633.9986    2.43007
301010      634.1076    2.43008
*
* CARD SERIES 302XXX (burnup v- fluence input)
*
* flu(e25 n/m^2) bup(%fima)
*
302001      0.          0.
302002      2.43        13.22
302003      2.43008     13.22
*
* CARD SERIES 303XXX (external pressure v- fluence input)
*
* external pressure v- fluence input
*
* flu(e25 n/m^2) pamb(MPa)
*
303001      0.          0.1
*
* CARD SERIES 304XXX (boundary temperature v- fluence input)
*
* flu(e25 n/m^2) btemp(k)
*
304001      0.          1314.0
304002      2.43        1314.0
304003      2.43001     303.0
304004      2.43002     673.0
304005      2.43003     673.0
304006      2.43004     1523.0
304007      2.43005     1523.0
304008      2.43006     1873.0
304009      2.43007     1873.0
304010      2.43008     303.0
*
* CARD SERIES 306XXX (time heatup starts and irradiation ends)
*
* thus(days)
*
306001 620.2
*
*
************* CORRELATION PARAMETERS AND COEFFICIENTS *************
*
* CARD SERIES 402XXX (asphericity)
*
* siga0(mpa) um(mpa) delum(mpa) aration aratvar
*
402001  1951.665  456.300  321.800  1.040  0.000
*
*


.
```